INSTITUTE OF PLASMA PHYSICS
OF THE CZECH ACADEMY OF SCIENCES

INTRODUCTION TO ENERGY PRINCIPLE, INTERNAL KINK & SAWTOOTH RECONNECTION THEORY AND MODELLING

FABIEN JAULMES

Institute of Plasma Physics of the CAS, Prague, Czech Republic

MINISTRY OF EDUCATION,
YOUTH AND SPORTS

Overview of this lecture

- Safety factor profile in tokamaks
- Introduction to the internal kink and the sawtooth crash
- Energy principle and derivation of linear growth rate of internal kink
- Reconnecting magnetic flux based on ideal MHD for poloidal mapping
- Computationally efficient poloidal mapping of the flux and the electric potential

Toroidal device

Resistivity of plasma

$$\eta \sim \frac{Z}{T_e^{3/2}}$$

Current diffusion time (**transport**)

$$\tau_\eta = \mu_0 L^2/\eta$$

- **A purely toroidal device yields charge separation: need for poloidal field:** current can be driven externally in the plasma to achieve this
- The field lines are thus twisted and **achieve m poloidal turn for n poloidal turns before they loop to the same 3D point**

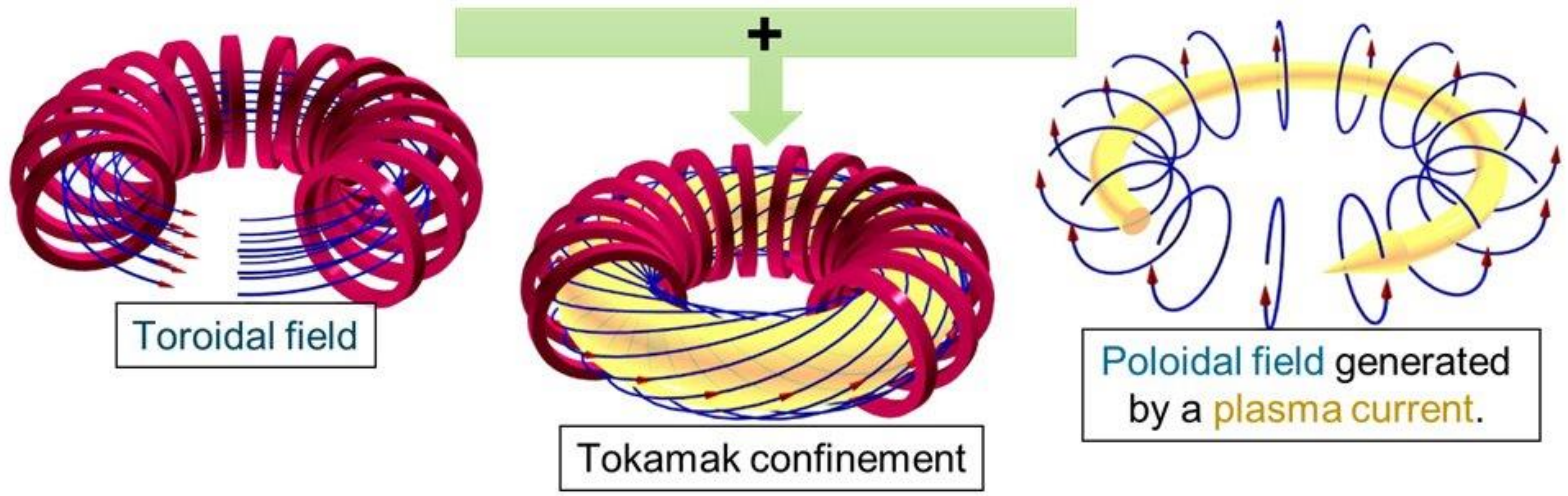

Helicity of the line: safety factor **$q=m/n \sim B/I_p$**

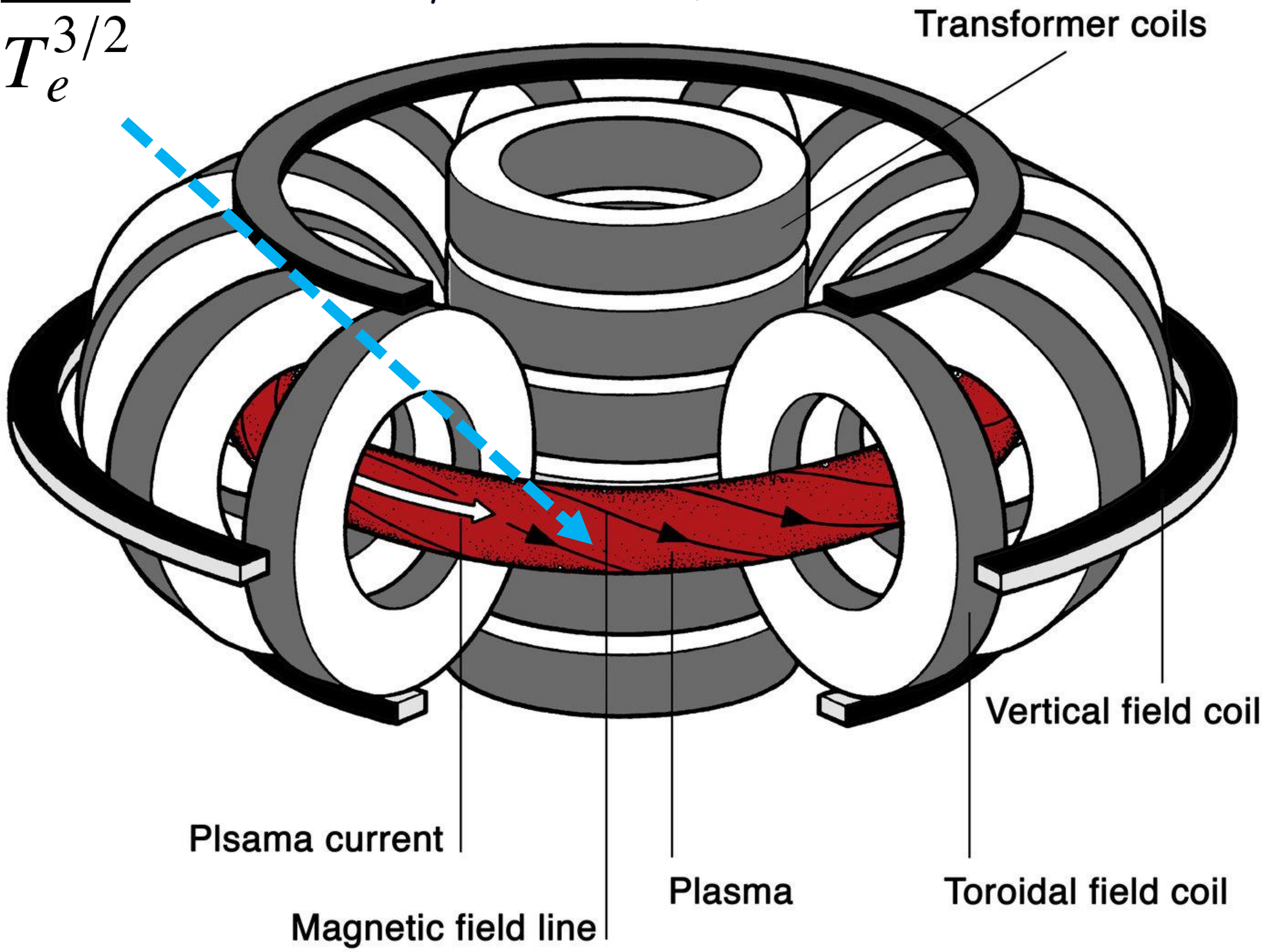

Safety factor profile

- The poloidal field of a toroidally symmetric device can be described by the angular poloidal flux map:

Ψ = Ψ(R,Z), so that we express the equilibrium field as:

$$\mathbf{B_0} = \nabla\varphi\times\nabla\psi_0+\frac{1}{R}B_t(R,Z)\nabla\varphi$$

- Angular toroidal flux χ can be expressed as:

$$2\pi\chi = \int\!\!\int B_t\,dR\,dZ = \int d\psi_0 \oint_{\Psi_0} \frac{B_t}{|\nabla\psi_0|}dL,$$

- We define the local helicity of the field line as:

$$q = \frac{m}{n} = \frac{d\varphi}{d\theta} = \frac{d\chi}{d\psi}$$

Tokamak cylindrical coordinates (R,Z,φ)

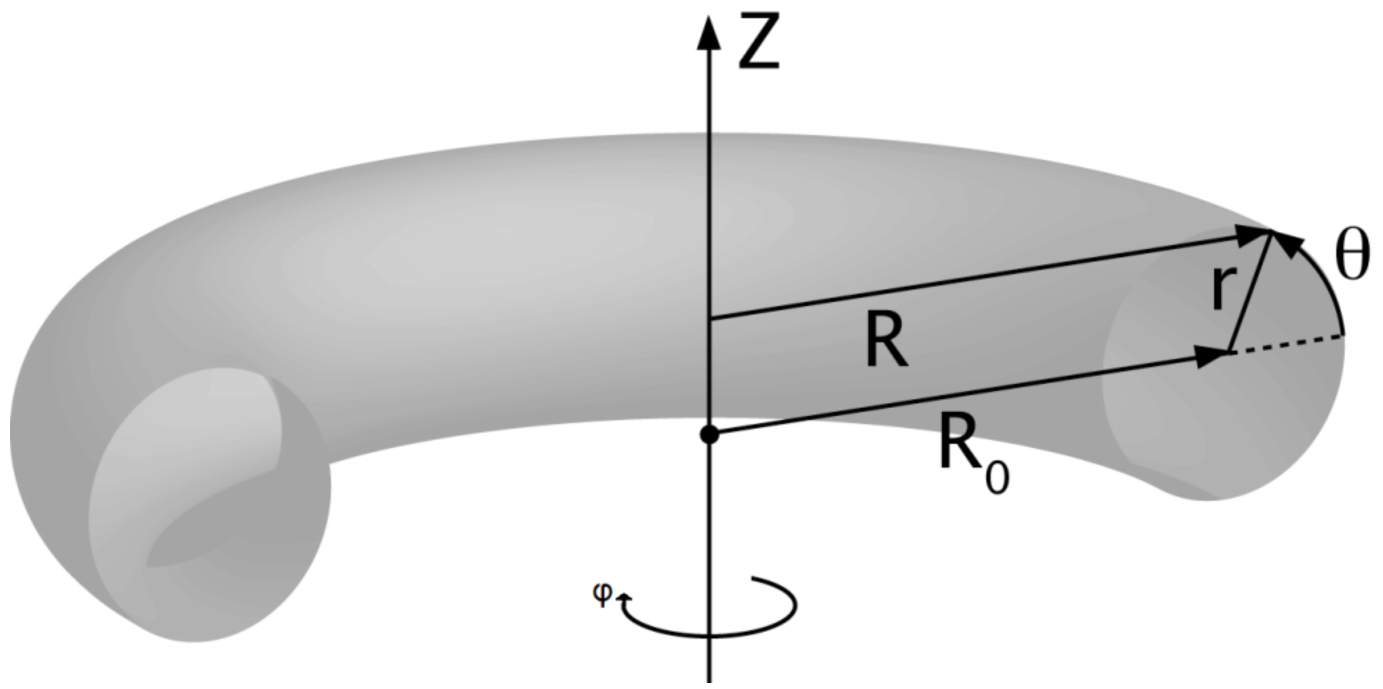

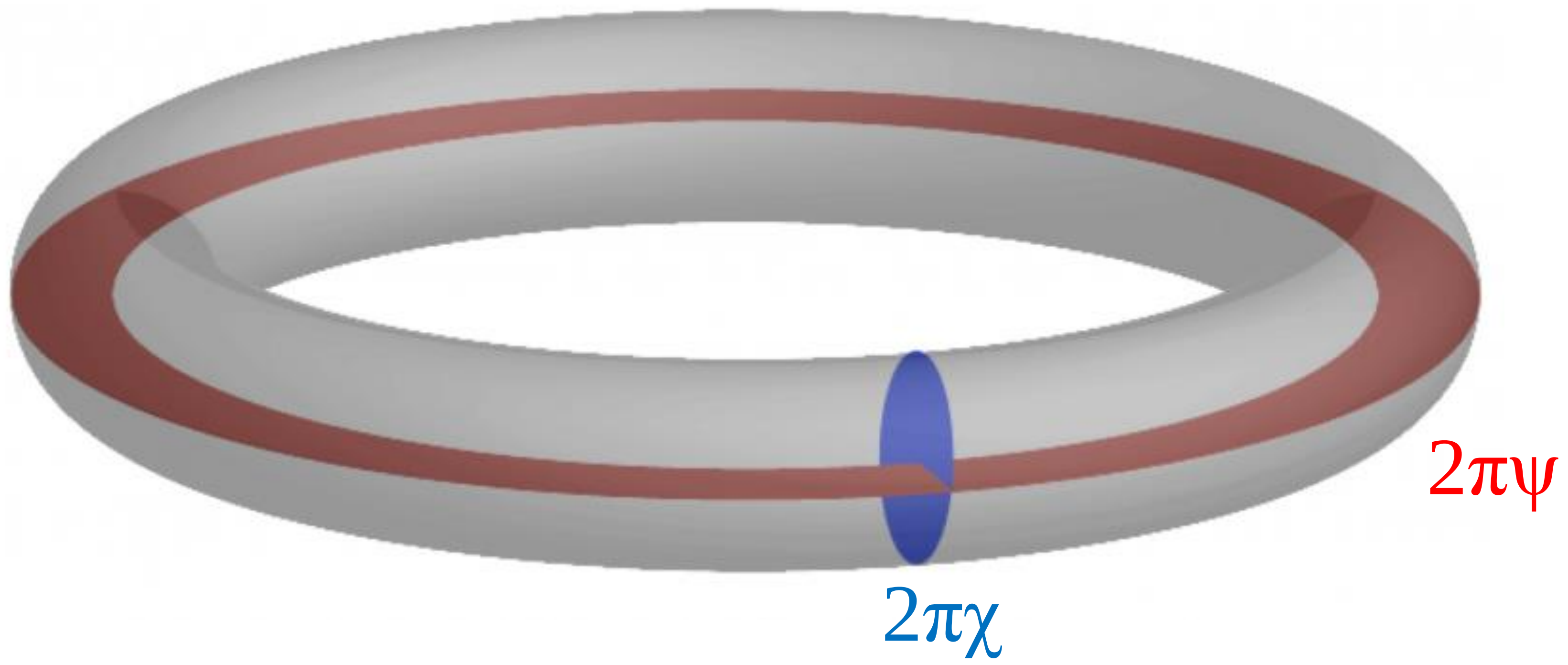

Straight field line angle: $\theta = \int_{\varphi} \frac{B_t}{|\nabla\chi|}dL$

Safety factor profile

There are several basic values which can be measured in the experiment and characterize MHD instability in tokamaks:

- growth rate of the mode (γ),
- mode numbers (m, n),
- mode frequency in the laboratory frame (ω),
- radial structure of the eigenfunction $\left(\hat{\xi}_r(\rho)\right)$, where ρ is the radial coordinate.

$$\xi(\rho, \theta, \phi, t) = \hat{\xi}_r(\rho) \cdot \cos(m\theta - n\phi + \omega t) \cdot e^{\gamma t}$$

$$\boldsymbol{\xi} = \boldsymbol{\xi}_0 \exp(i\omega t)$$

Overview of this lecture

- Safety factor profile in tokamaks
- Introduction to the internal kink and the sawtooth crash
- Energy principle and derivation of linear growth rate of internal kink
- Ideal MHD for poloidal mapping of the reconnecting magnetic flux based on
- Computationally efficient poloidal mapping of the reconnecting magnetic flux

Experimental patterns of kink and sawtooth

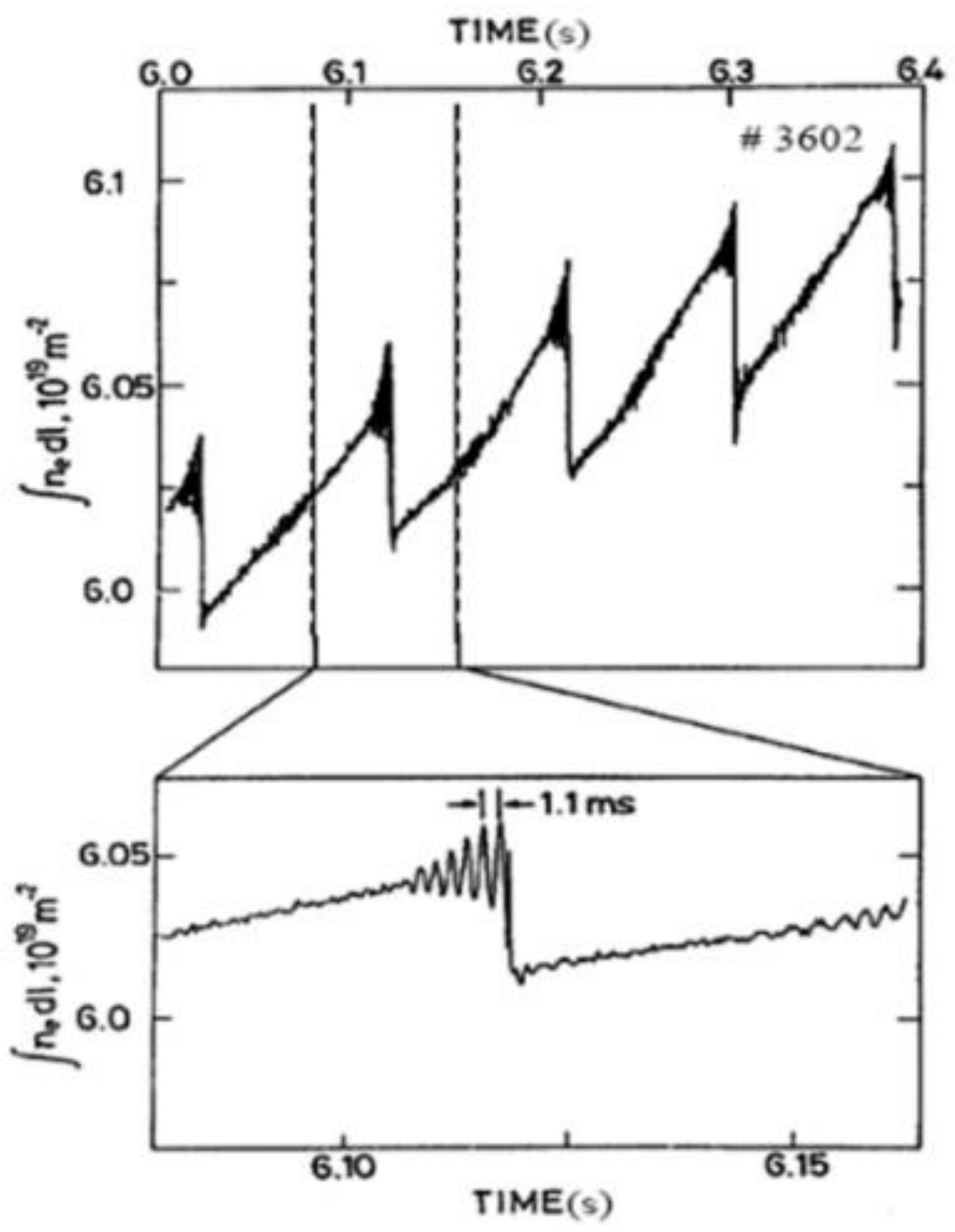

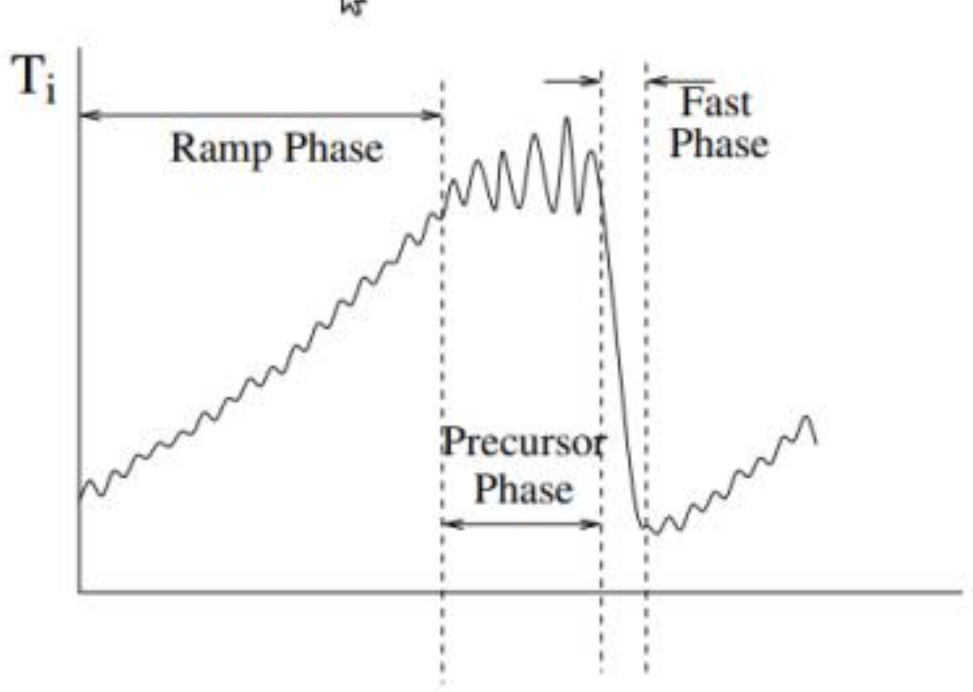

The line-integrated electron density of an early JET sawtoothing plasma. The sawtooth oscillation typically consists of a ramp phase, then a precursor oscillation followed by the fast collapse phase.

[1] I T Chapman 2011 Plasma Phys. Control. Fusion 53 013001

Experimental patterns of kink and sawtooth

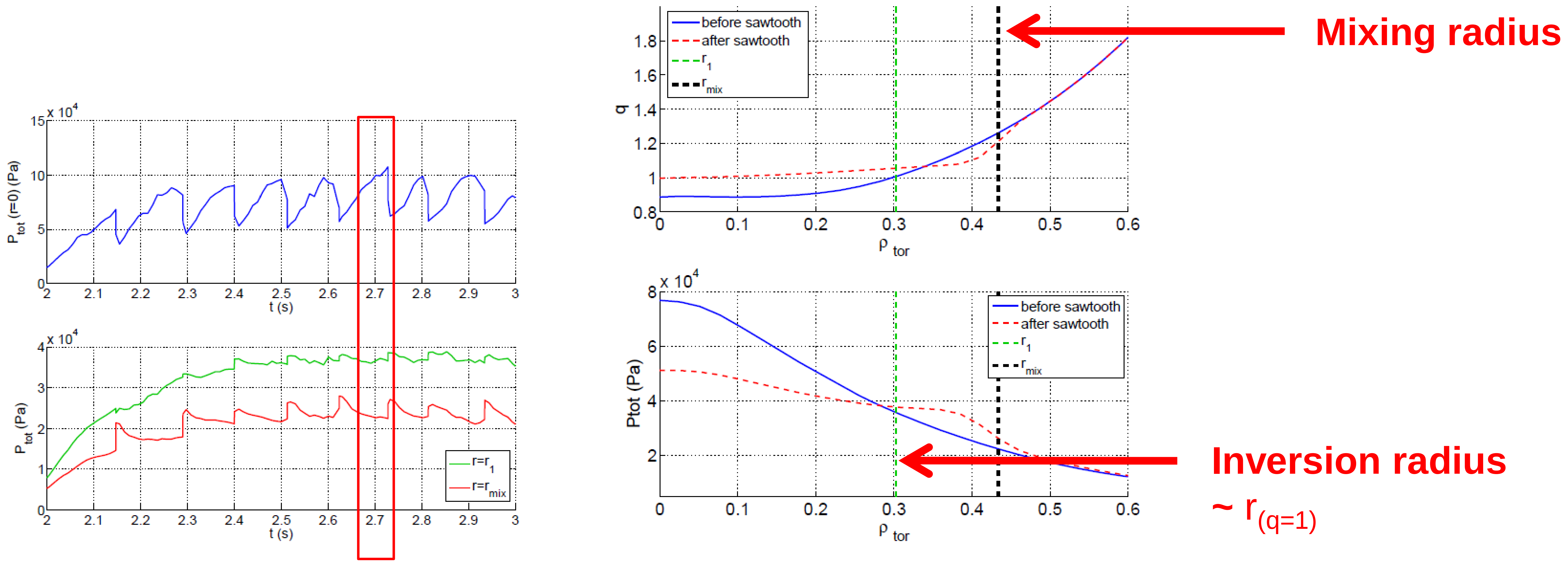

FIGURE 1.4: Left figure: Time evolution of the reconstructed total pressure in an ASDEX Upgrade experiment (discharge #30382). The evolution of the pressure is given at different radial position, displayed in the right figure. The characteristic shape of the evolution of the pressure in the core gave its name to the phenomenon. The radial position where the pressure is not modified by the crash (close to $q = 1$) is often called the 'inversion radius'. Right figure: evolution of the radial profiles of the safety factor corresponding to the sawtooth crash happening at 2.51s.

Physics of the (1,1) (q=1) mode

At large I_p, as current diffuses inward, it accumulates in the core and q eventually drops below 1. MHD modes appear:

- **Internal kink (aka, Long Lived Mode (LLM))**
- **Sawteeth (reconnection mode)**
- **Fishbones (fast particle mode)**

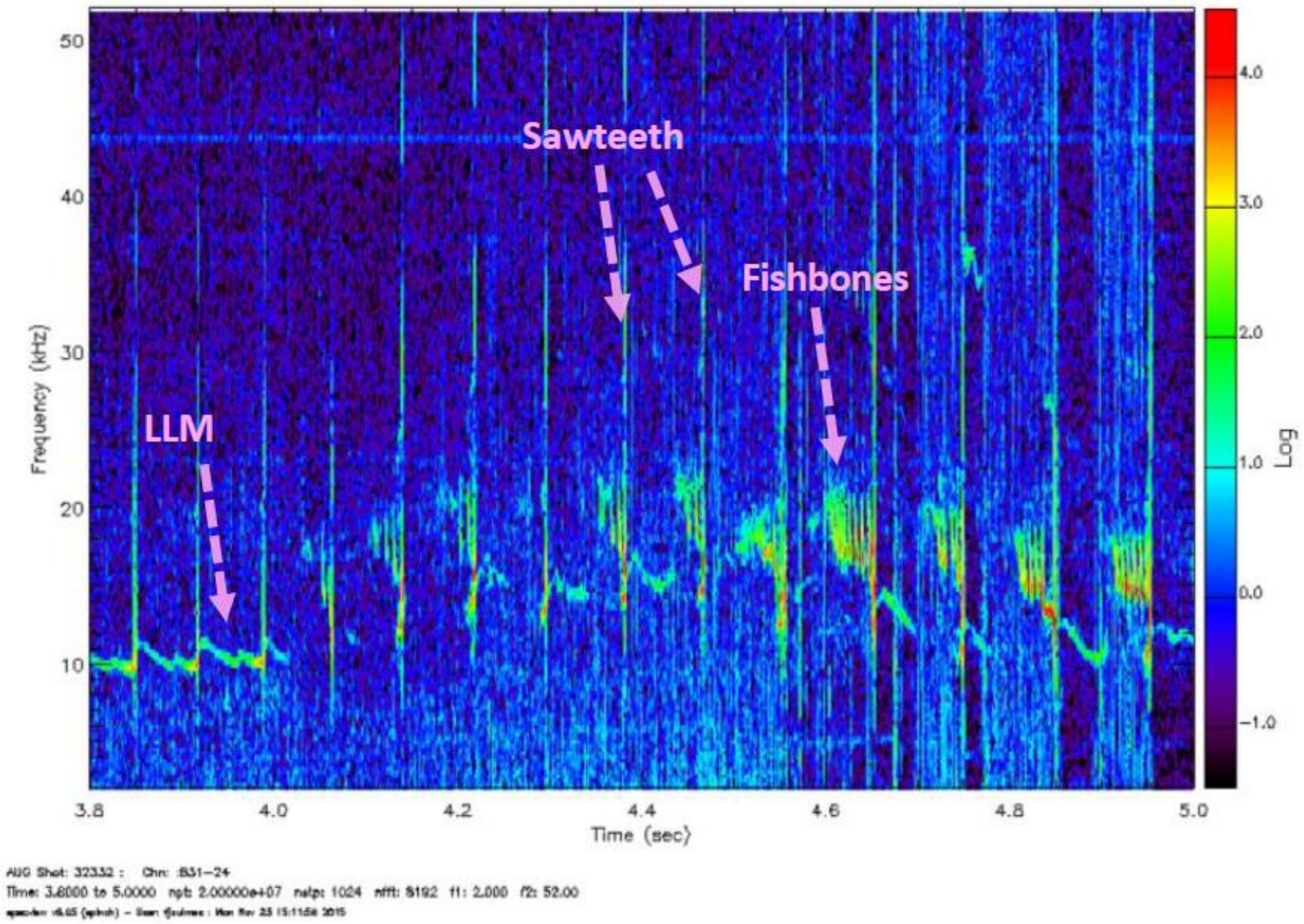

Experimental measurements with Soft X-ray (SXR) tomography of kink followed by sawtooth crash

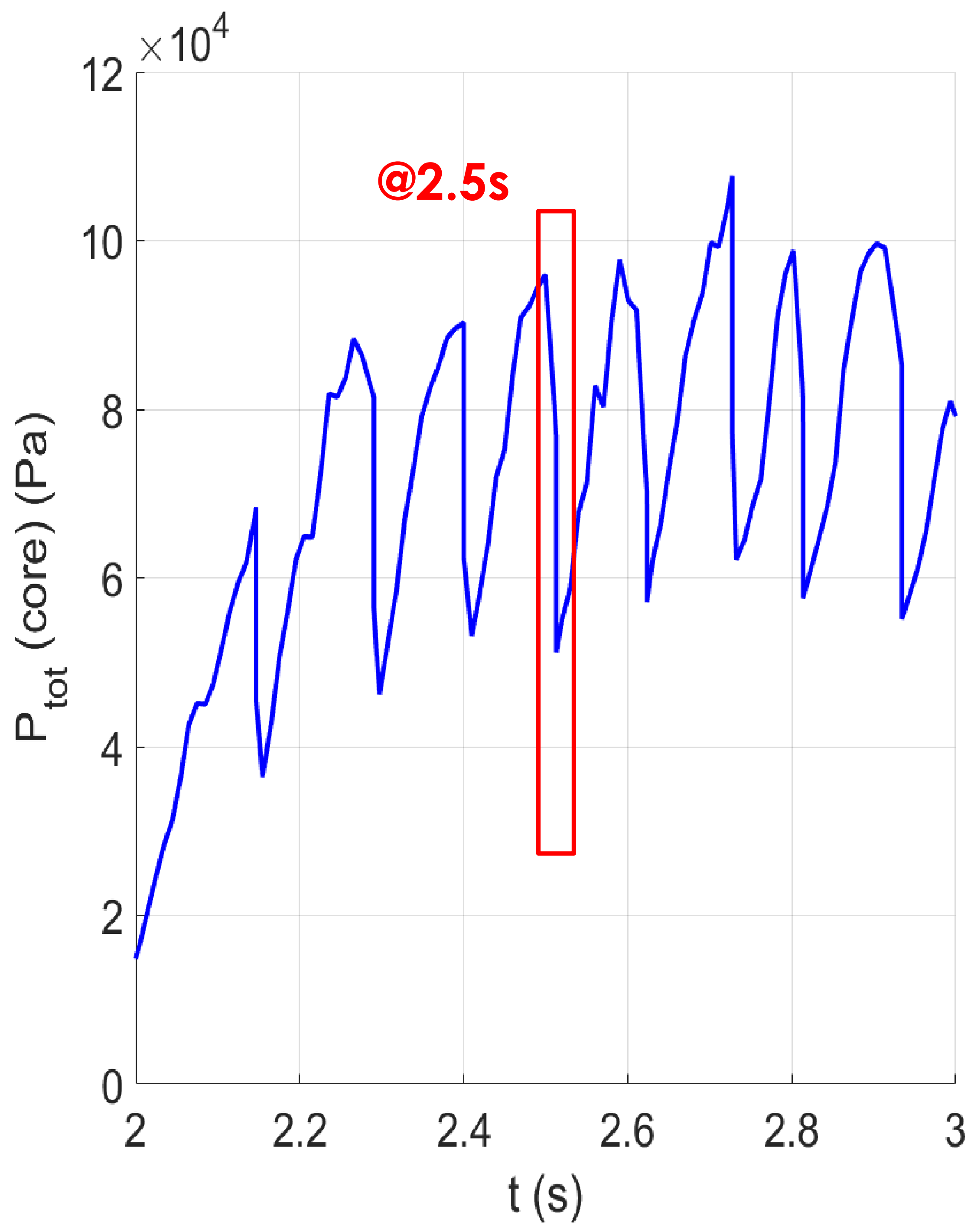

(AUG#30382@2.5s)

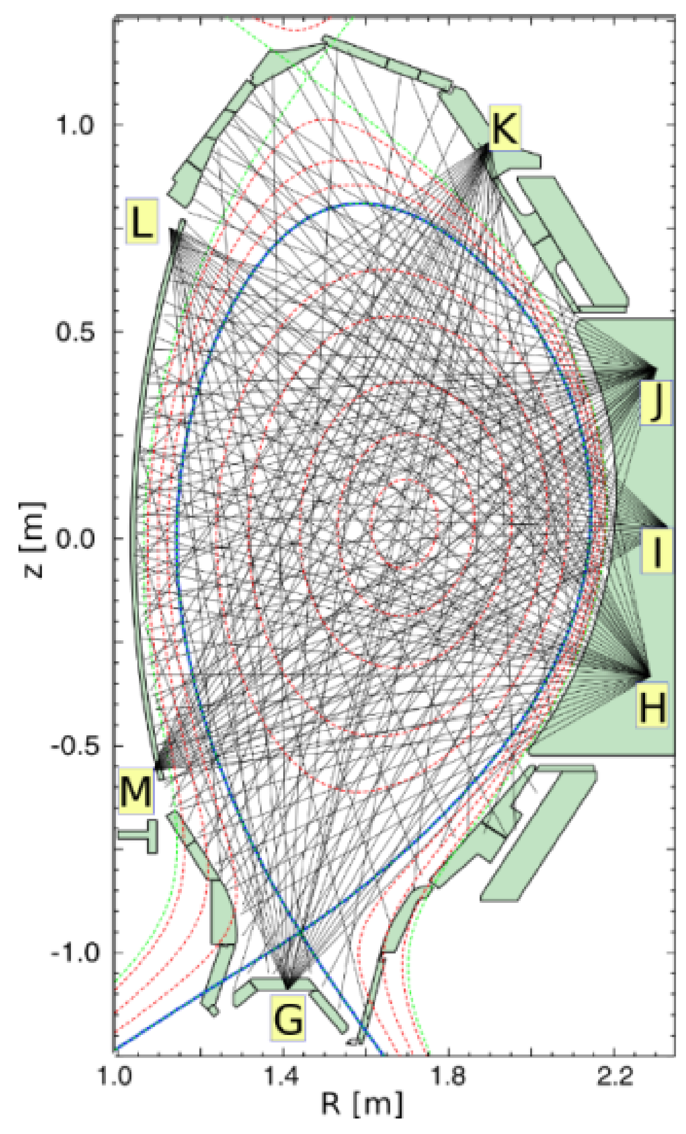

SXR array in ASDEX Upgrade

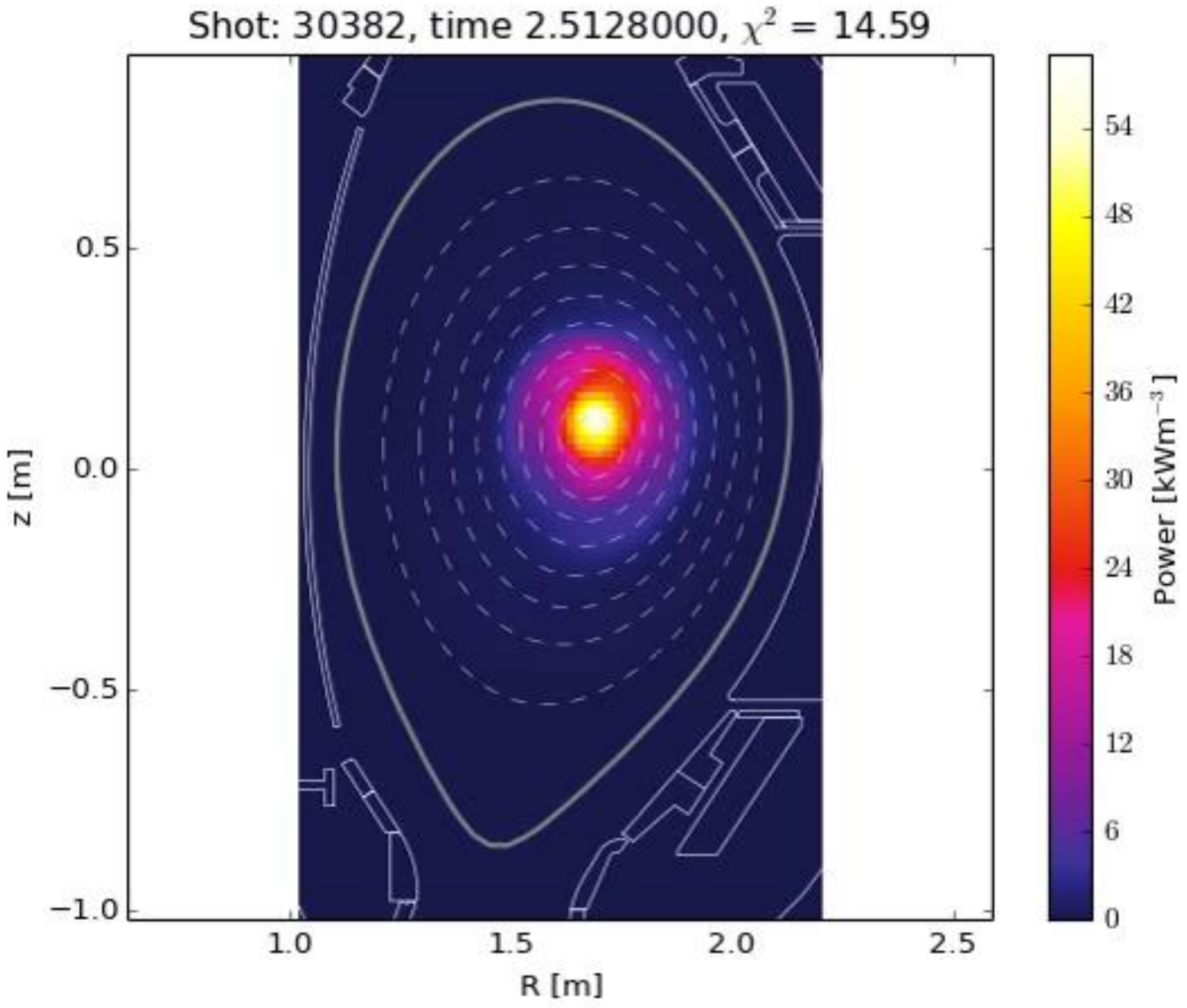

Patterns of ψ_*

$\Psi_*(r,\omega)$

$\omega=\theta-\varphi$

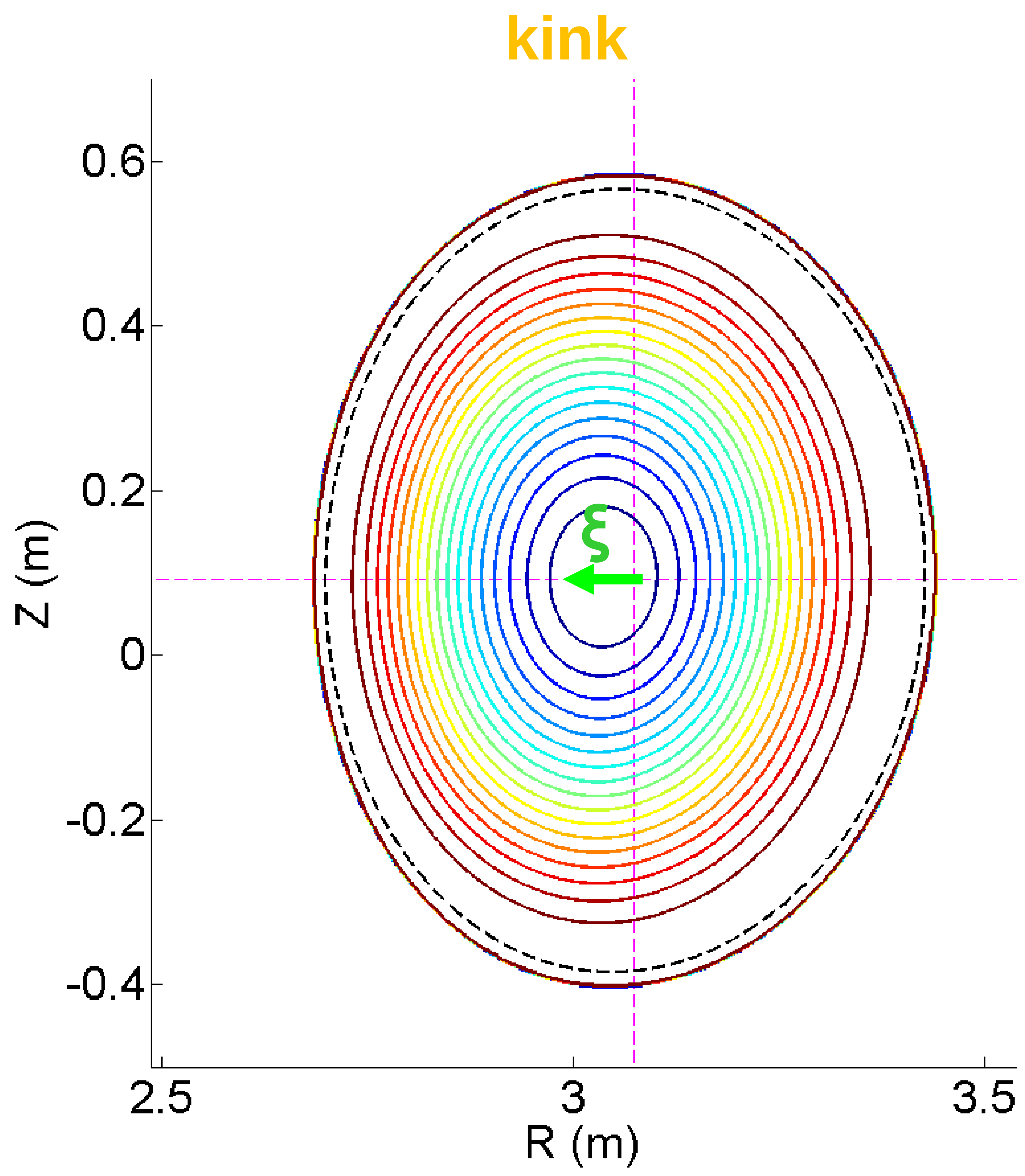

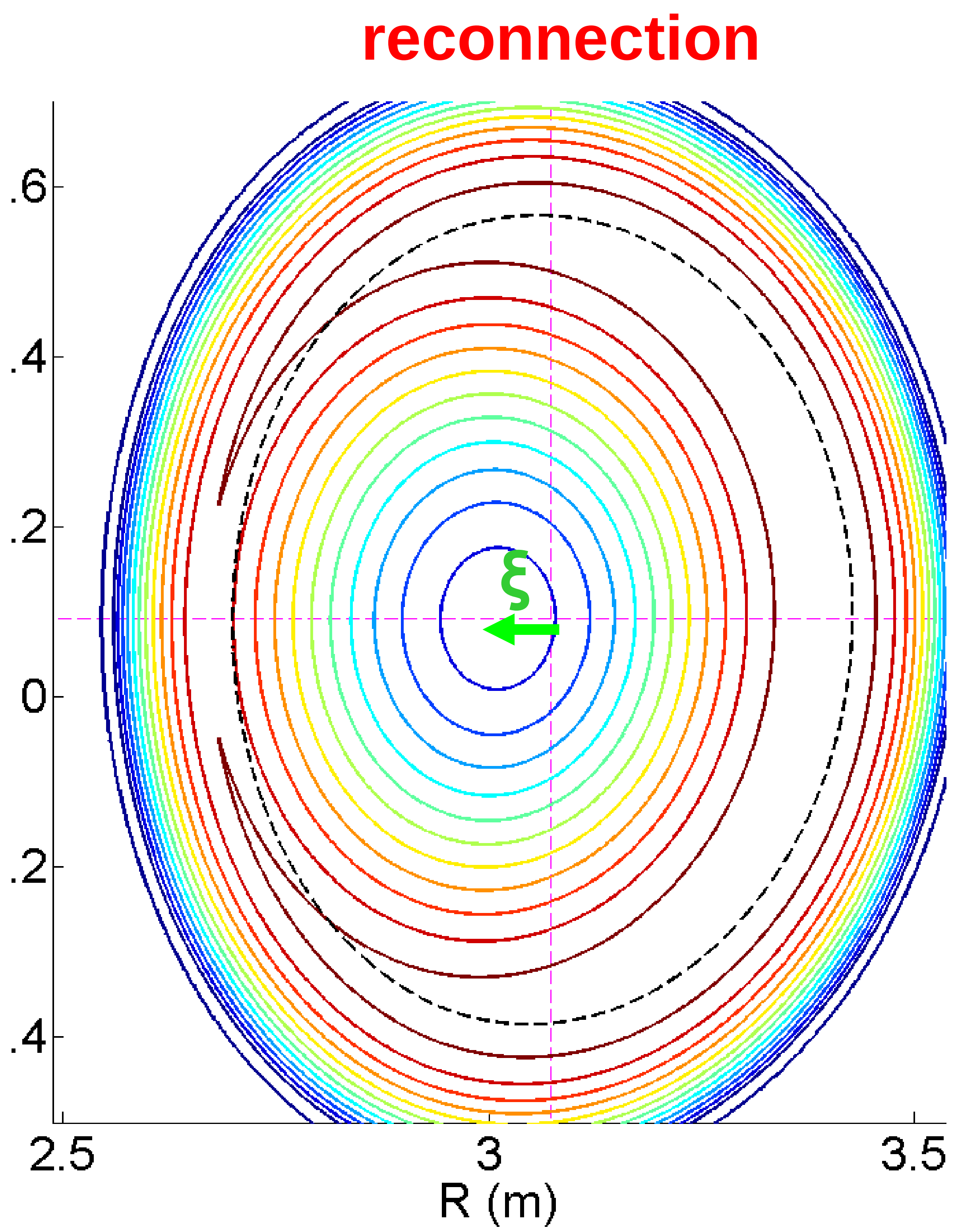

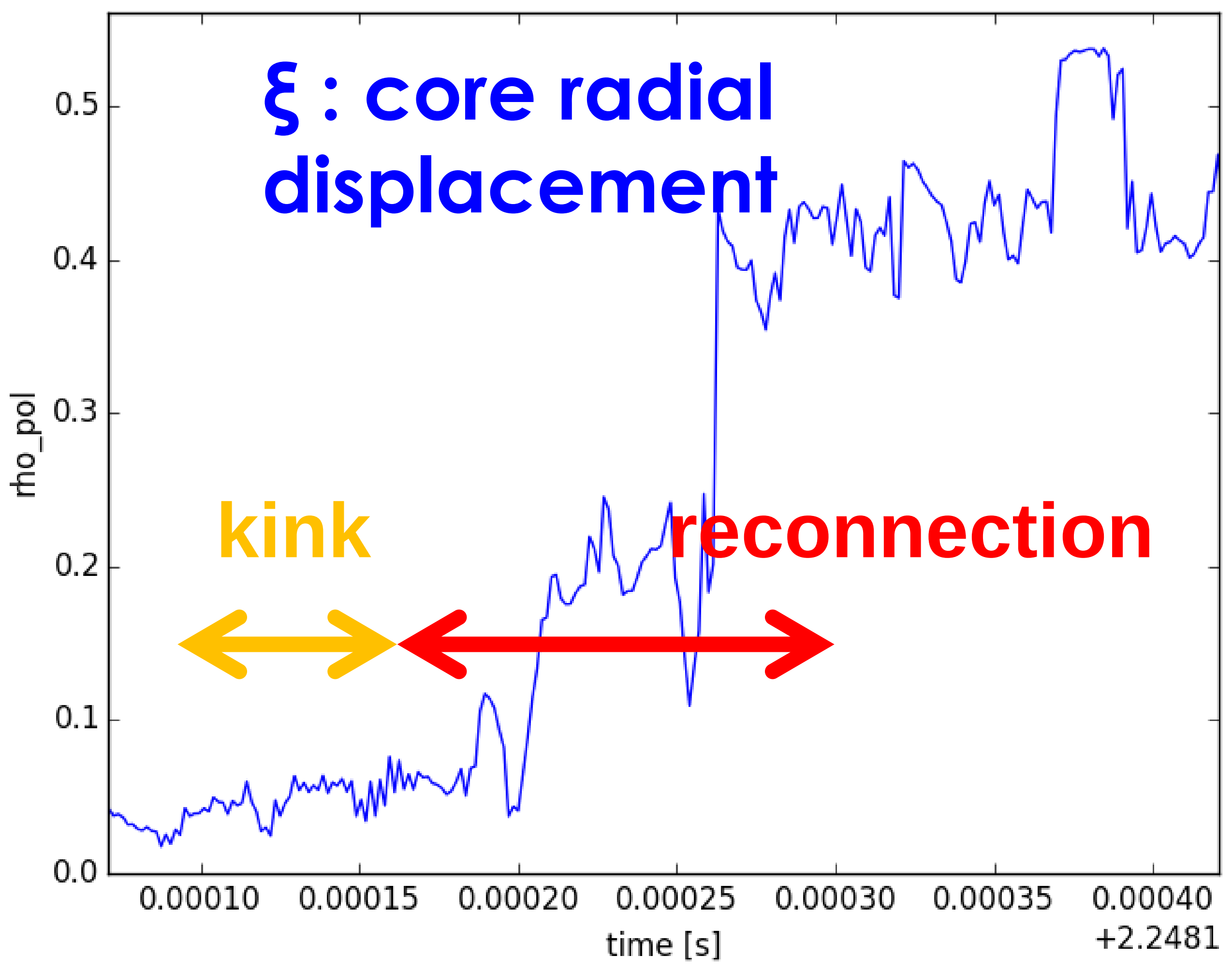

DIVERSITY OF SAWTEETH

AUG #30382

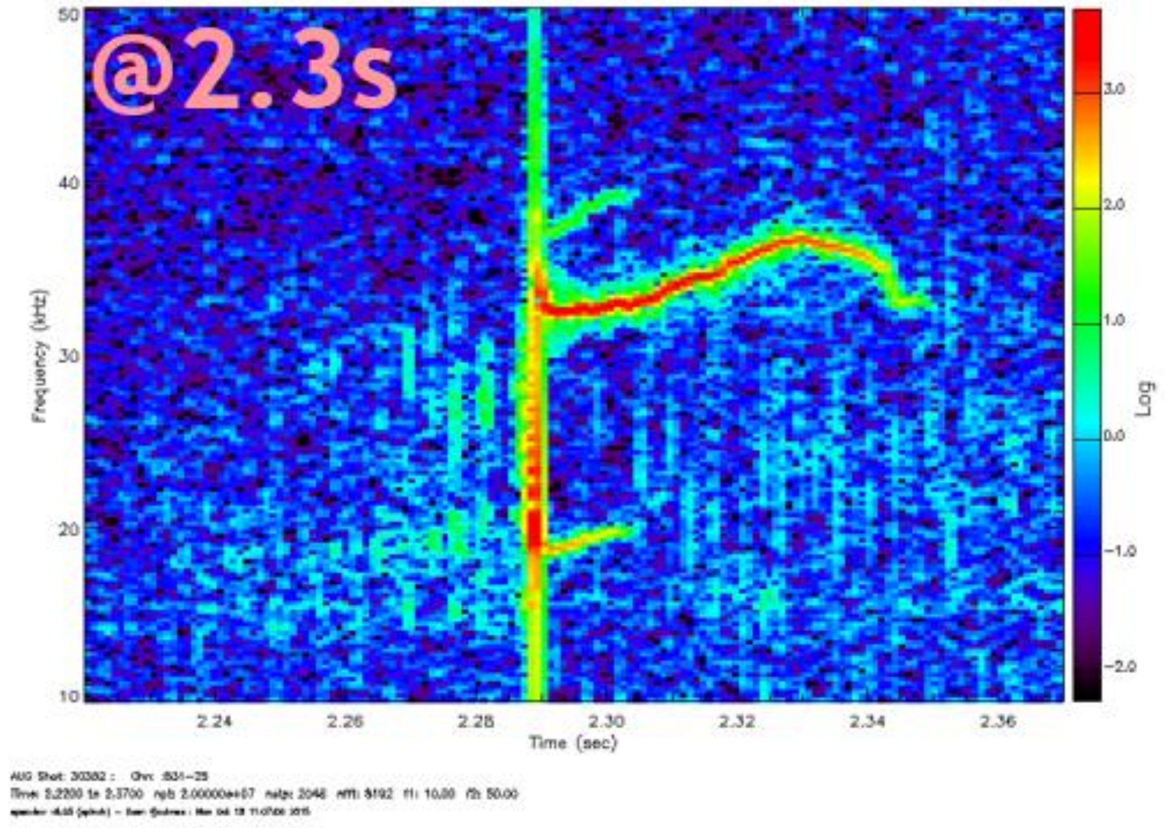

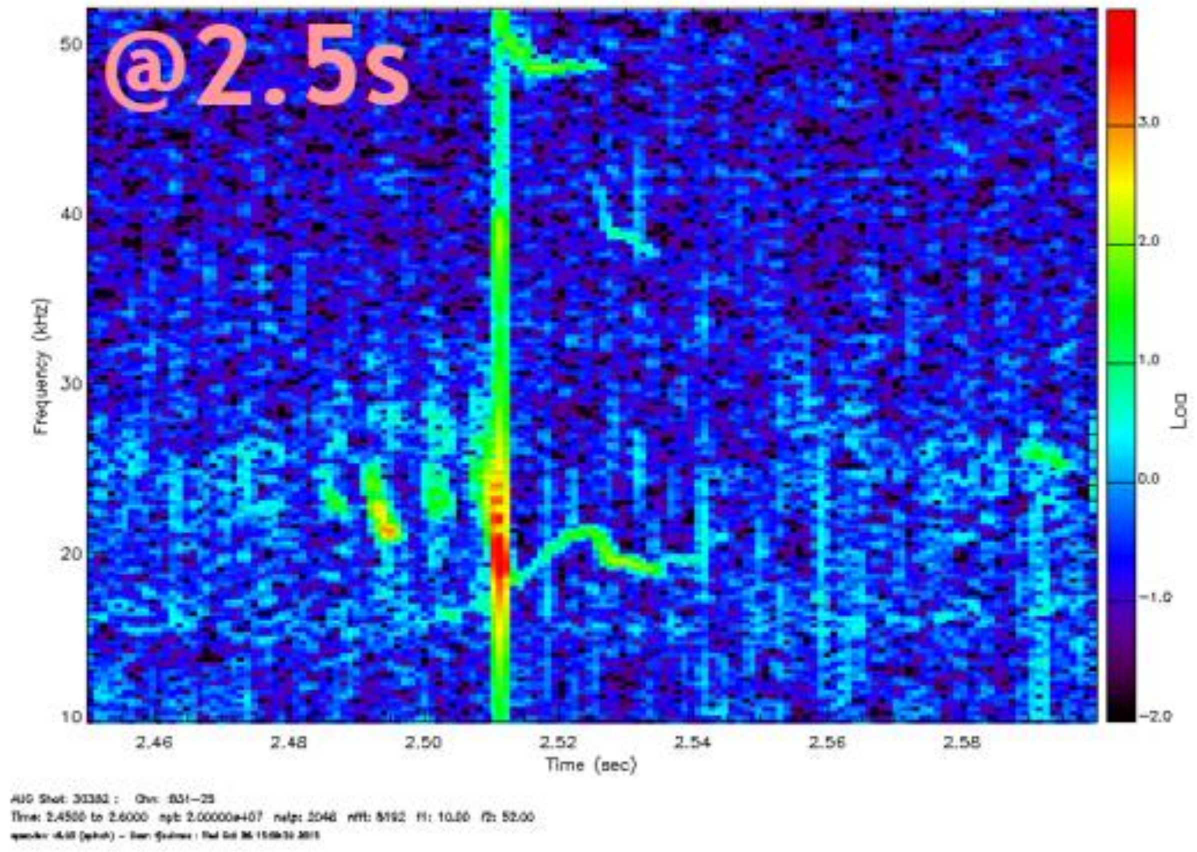

AUG #31557 @2.25s

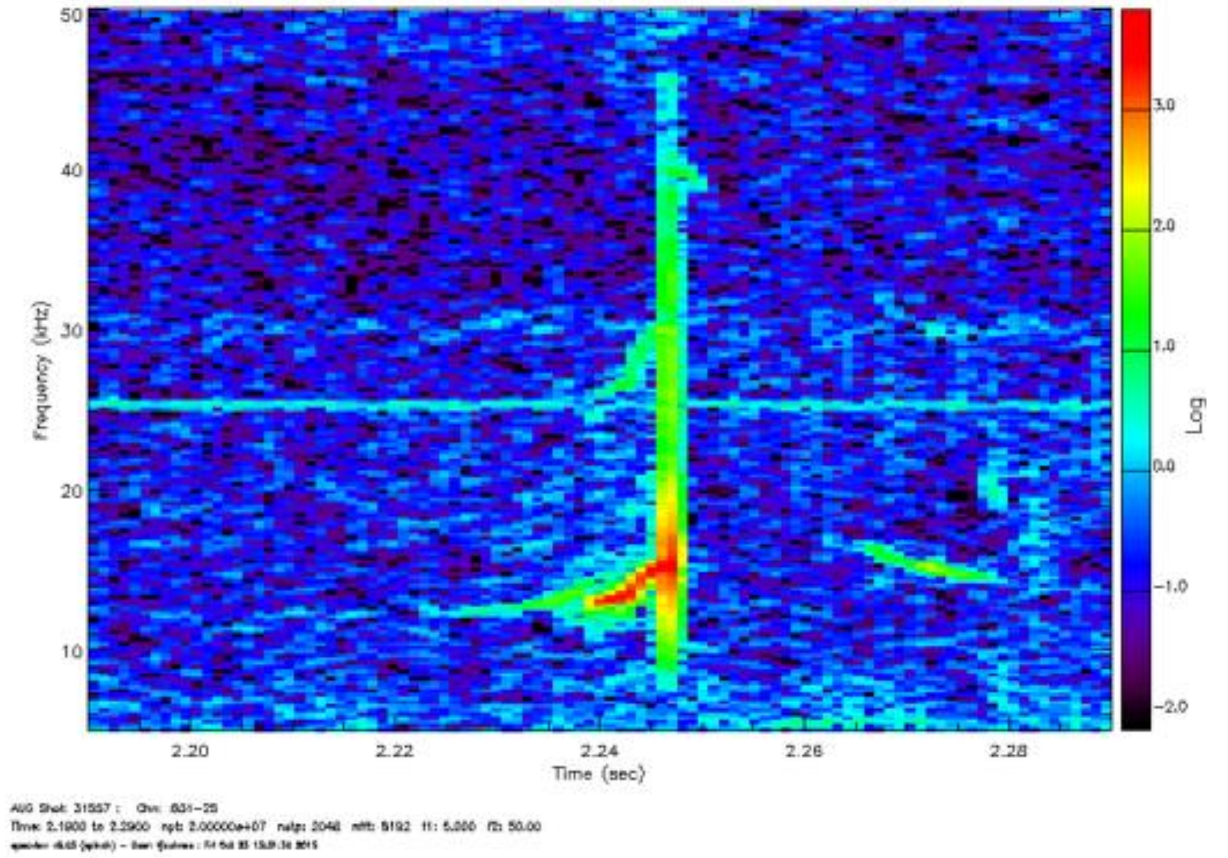

AUG #30815

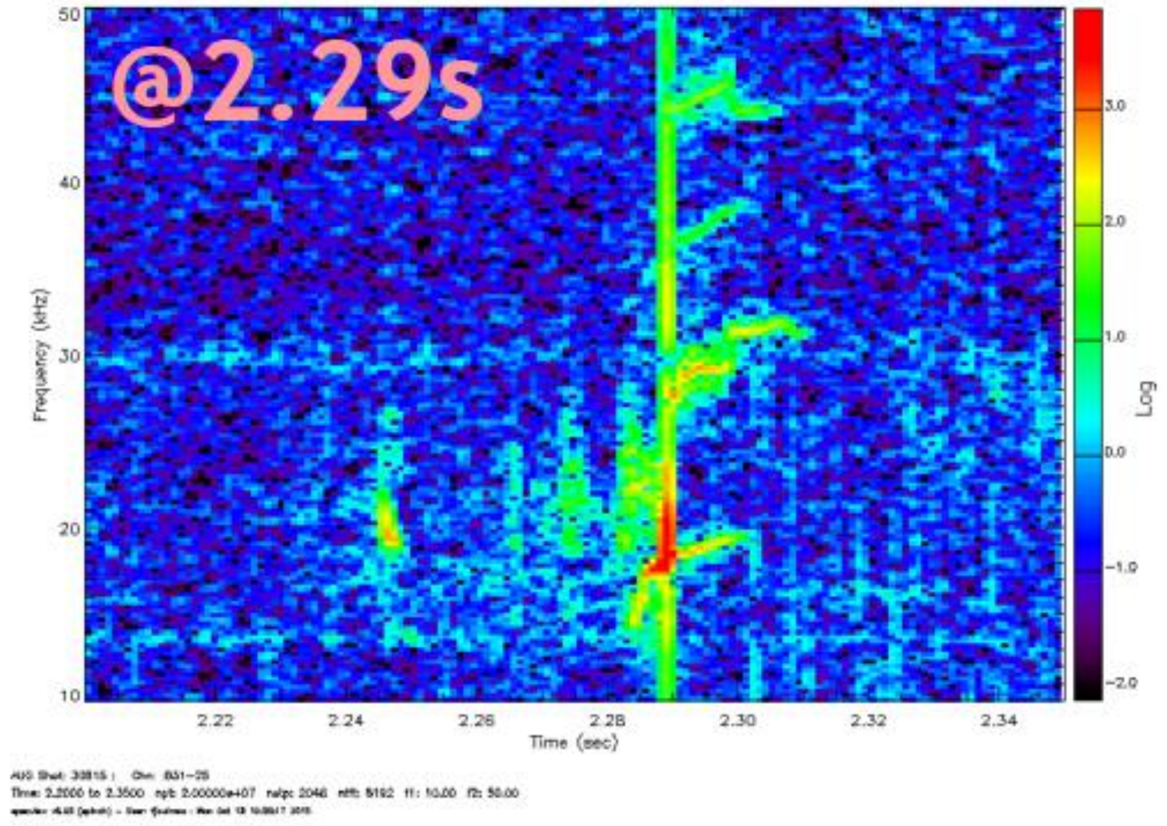

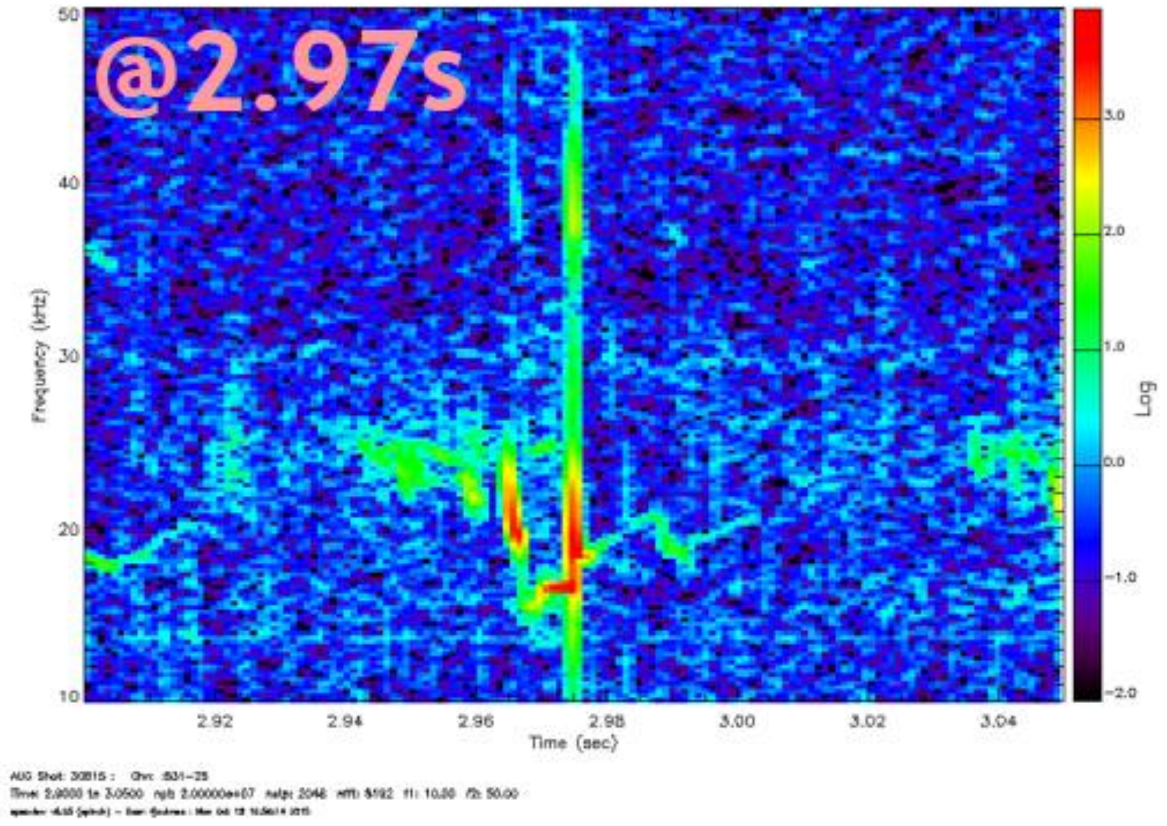

STRUCTURE OF PERTURBED HELICAL FLUX

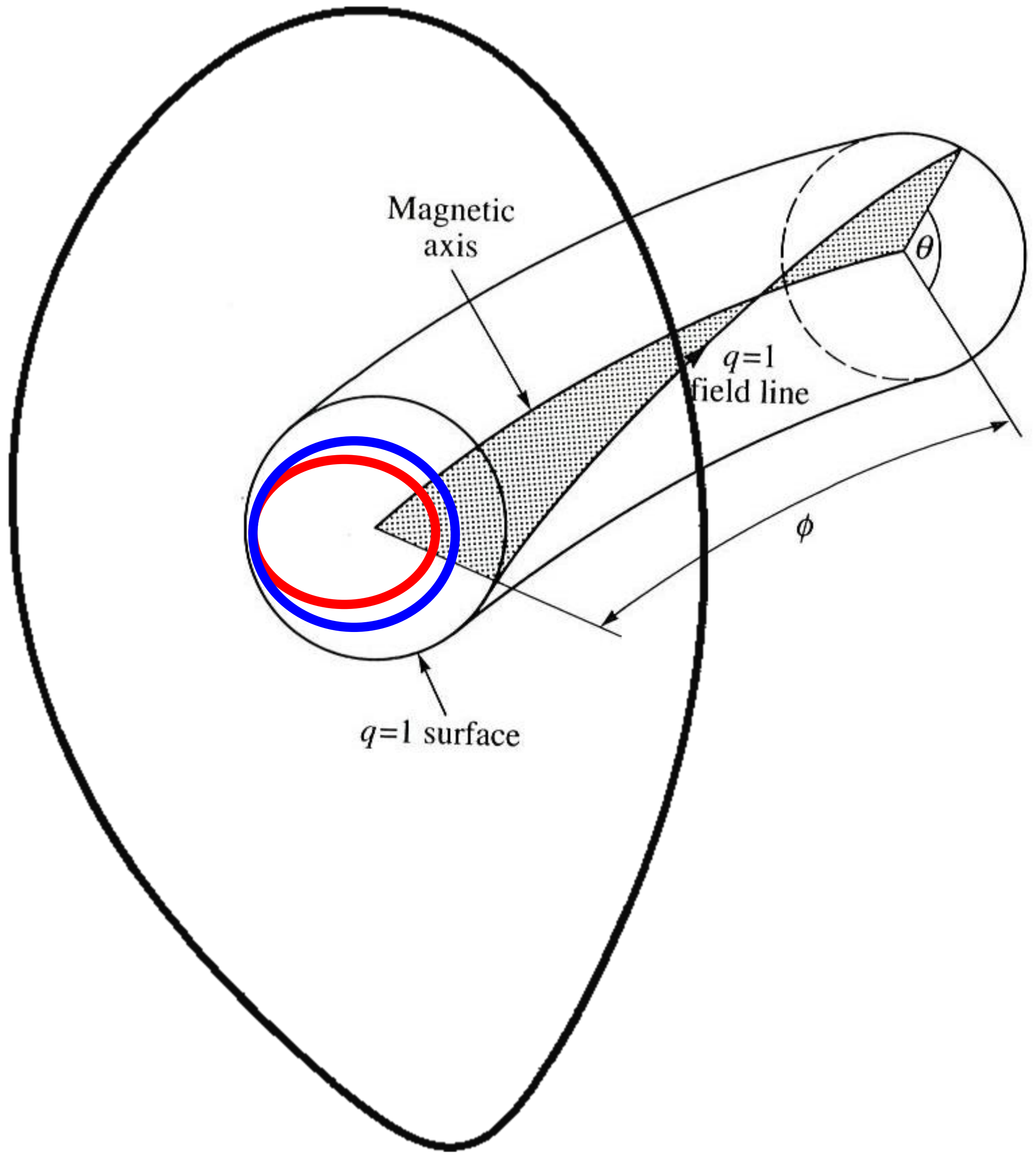

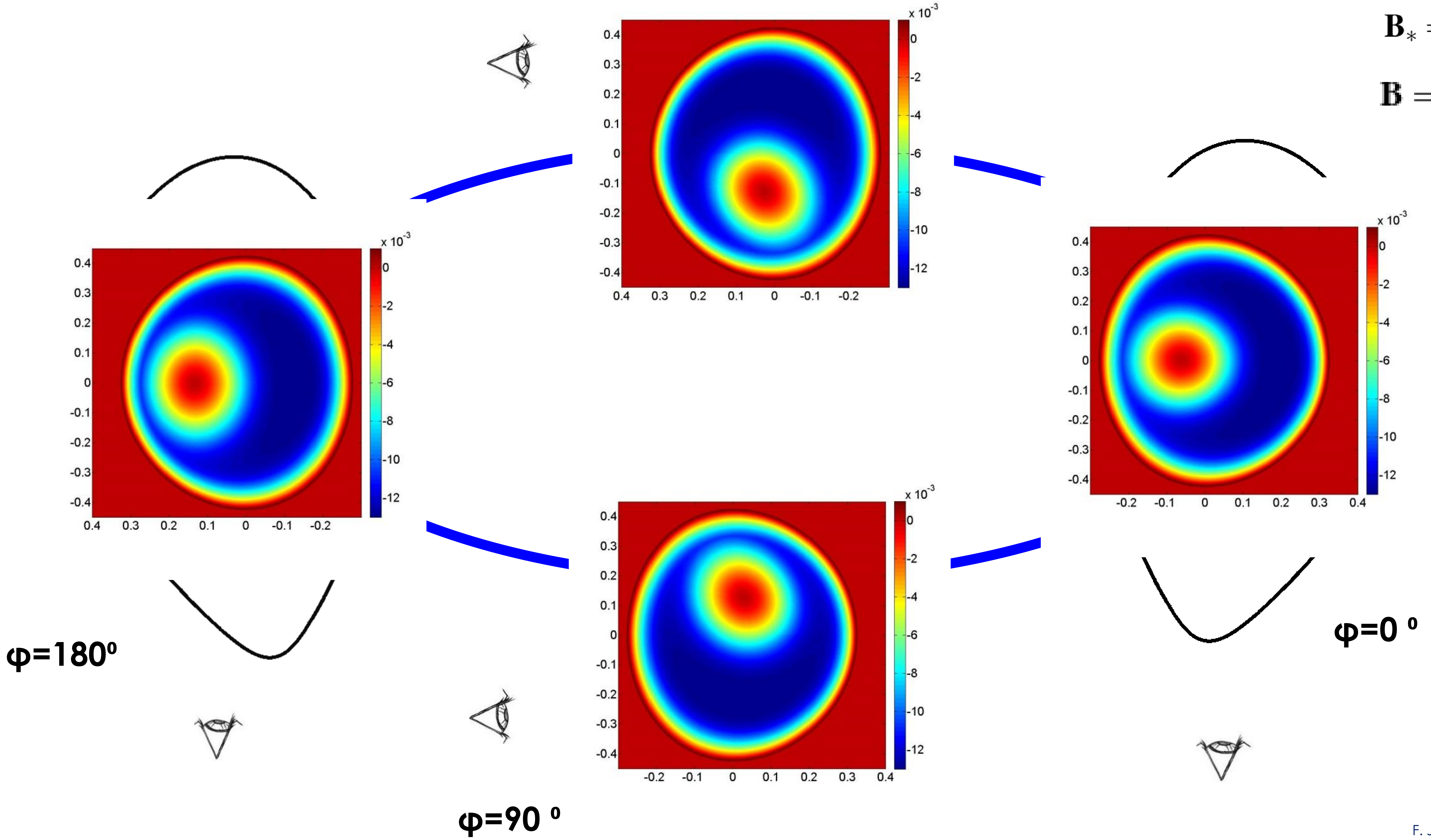

$$\mathbf{B}_* = \frac{1}{R}(\mathbf{e}_\varphi \times \nabla \psi_*)$$

$$\mathbf{B} = \mathbf{B_H} + \mathbf{B}_*$$

$\omega = \theta - \varphi$

$\psi_*(r, \omega)$

F. Jaulmes et. al. 2014 Nucl. Fusion **54** 104013

Overview of this lecture

- Safety factor profile in tokamaks
- Introduction to the internal kink and the sawtooth crash
- **Energy principle and derivation of linear growth rate of internal kink**
- **Ideal MHD for poloidal mapping of the reconnecting magnetic flux**
- **Computationally efficient poloidal mapping of the reconnecting magnetic flux**

Thermonuclear plasma in a tokamak

MHD : fluid model of plasma

Momentum equation applied to a fluid element moving along the vector ξ with velocity –iξ from initial equilibrium:

$$\rho\frac{\partial \mathbf{u}}{\partial t} + \rho(\mathbf{u}\cdot\nabla)\mathbf{u} = \mathbf{F}(\boldsymbol{\xi}) = -\boldsymbol{\nabla}P + \mathbf{j}\times\mathbf{B} \qquad \mathbf{u} = \mathrm{d}\boldsymbol{\xi}/\mathrm{d}t$$

This corresponds to the change of potential energy:

$$\delta W = -\frac{1}{2}\int (\mathbf{F}(\boldsymbol{\xi})\cdot\boldsymbol{\xi}^*)\,\mathrm{d}\mathcal{V}$$

$\boldsymbol{\xi}^*$ denotes the conjugate of the complex displacement vector $\boldsymbol{\xi}$.

Thermonuclear plasma in a tokamak

MHD : fluid model of plasma

Momentum equation applied to a fluid element moving along the vector ξ with velocity –iξ from initial equilibrium:

$$\rho\frac{\partial \mathbf{u}}{\partial t} + \rho(\mathbf{u}\cdot\nabla)\mathbf{u} = \mathbf{F}(\boldsymbol{\xi}) = -\boldsymbol{\nabla}P + \mathbf{j}\times\mathbf{B} \qquad \mathbf{u} = \mathrm{d}\boldsymbol{\xi}/\mathrm{d}t$$

This corresponds to the change of potential energy:

$$\delta W = -\frac{1}{2}\int(\mathbf{F}(\boldsymbol{\xi})\cdot\boldsymbol{\xi}^*)\,\mathrm{d}\mathcal{V}$$

$\boldsymbol{\xi}^*$ denotes the conjugate of the complex displacement vector $\boldsymbol{\xi}$.

$$\dot{\xi} = \frac{\mathbf{E}\times\mathbf{B}}{B^2}$$

Conservation of the total energy of the plasma yields:

$$\delta W + \delta K = \delta W + \frac{1}{2}\int \rho_i|\dot{\boldsymbol{\xi}}|^2\mathrm{d}\mathcal{V} = 0 \longrightarrow \omega^2 = \frac{2\delta W}{\int \rho_i|\boldsymbol{\xi}_0|^2\mathrm{d}\mathcal{V}}$$

δW<0 yields destabilization

Thermonuclear plasma in a tokamak

MHD : fluid model of plasma

Momentum equation applied to a fluid element moving along the vector ξ with velocity –iξ from initial equilibrium:

$$\rho\frac{\partial \mathbf{u}}{\partial t} + \rho(\mathbf{u}\cdot\nabla)\mathbf{u} = \mathbf{F}(\boldsymbol{\xi}) = -\boldsymbol{\nabla} P + \mathbf{j}\times\mathbf{B} \qquad \mathbf{u} = \mathrm{d}\boldsymbol{\xi}/\mathrm{d}t$$

This corresponds to the change of potential energy:

$$\delta W = -\frac{1}{2}\int (\mathbf{F}(\boldsymbol{\xi})\cdot\boldsymbol{\xi}^*)\,\mathrm{d}\mathcal{V}$$

$\boldsymbol{\xi}^*$ denotes the conjugate of the complex displacement vector $\boldsymbol{\xi}$.

Expressing as a function of perturbed magnetic field: $\mathbf{B_1} = \nabla\times(\boldsymbol{\xi}_\perp\times\mathbf{B})$ $\qquad \mu_0\mathbf{j} = \nabla\times\mathbf{B}$

$$\delta W = \frac{1}{2}\int_{\mathcal{V}}\Big[\frac{B_1^2}{\mu_0} + \frac{B^2}{\mu_0}|\boldsymbol{\nabla}\cdot\boldsymbol{\xi}_\perp + 2\boldsymbol{\xi}_\perp\cdot\boldsymbol{\kappa}|^2 - 2(\boldsymbol{\xi}_\perp\cdot\boldsymbol{\nabla}P)(\boldsymbol{\kappa}\cdot\boldsymbol{\xi}_\perp^*) - \mathbf{B_1}\cdot(\boldsymbol{\xi}_\perp\times\mathbf{b})j_\| + \gamma_{\mathrm{thermo}}P(\boldsymbol{\nabla}\cdot\boldsymbol{\xi})^2\Big]\,\mathrm{d}\mathcal{V}$$

Plasma only!

Discussion on plasma stability term in energy principle

Stabilizing terms > 0

$$\delta W_{plasma} = \frac{1}{2}\int_{plasma} \left\{ \frac{\left|\vec{B}_{1,\perp}\right|^2}{\mu_0} + \frac{B_0^2}{\mu_0}\left|\nabla\cdot\vec{\xi}_\perp + 2\vec{\xi}_\perp\cdot\vec{\kappa}\right|^2 + \Gamma p_0\left|\nabla\cdot\vec{\xi}\right|^2 - 2\left(\vec{\xi}_\perp\cdot\nabla p_0\right)\left(\vec{\kappa}\cdot\vec{\xi}_\perp^*\right) - J_{\|}\left(\vec{\xi}_\perp^* \times \vec{b}\right)\cdot\vec{B}_{1,\perp} \right\} dV$$

Possibly destabilizing term

Possibly destabilizing term

Thorough study needs to include also vacuum region and stabilizing effect of the conductive wall….

Book: Active Control of Magnetohydrodynamic Instabilities in Hot Plasmas - Valentin Igochine

Thermonuclear plasma in a tokamak

Change of potential energy:

$$\delta W = \frac{1}{2}\int_{\mathcal{V}}\left[\frac{B_1^2}{\mu_0} + \frac{B^2}{\mu_0}|\boldsymbol{\nabla}\cdot\boldsymbol{\xi}_\perp + 2\boldsymbol{\xi}_\perp\cdot\boldsymbol{\kappa}|^2 - 2(\boldsymbol{\xi}_\perp\cdot\boldsymbol{\nabla}P)(\boldsymbol{\kappa}\cdot\boldsymbol{\xi}_\perp^*) - \mathbf{B_1}\cdot(\boldsymbol{\xi}_\perp\times\mathbf{b})j_\parallel + \gamma_{\text{thermo}}P(\boldsymbol{\nabla}\cdot\boldsymbol{\xi})^2\right]\mathrm{d}\mathcal{V}$$

$$\mathbf{B_1} = \nabla\times(\boldsymbol{\xi}_\perp\times\mathbf{B})$$

$$\omega^2 = \frac{2\delta W}{\int\rho_i|\boldsymbol{\xi}_0|^2\mathrm{d}\mathcal{V}}$$

$$\gamma_I^2 = -\omega^2$$

Considering an approximate circular geometry (neglecting toroidal displacement):

$$\delta W_m(\xi) = \frac{2\pi^2}{\mu_0}\frac{B_{0\varphi}^2}{R_0}\int_0^a\left(\left((m^2-1)\xi_r^2 + \left(r\frac{\mathrm{d}}{\mathrm{d}r}\xi_r\right)^2\right)\left(\frac{n}{m}-\frac{1}{q}\right)^2\right)r\mathrm{d}r$$

always stabilizing for $m \geq 2$ modes

$$\delta W_{m=1} = \pi^2\frac{B_0^2}{R_0}\int_0^a r^3|\xi_r'|^2\left(1-\frac{1}{q}\right)^2 dr$$

Plugging in the observed radial shape of the displacement function………..

……..

…….and doing lots of tedious algebra……………

………..

$$\xi_{in} = \xi_0\left[1-\frac{2}{\pi}\arctan\left(x\frac{B_{0\varphi}}{\sqrt{3\rho\mu_0}R_0}\frac{s_1}{\gamma_I}\right)\right] \quad \text{with} \quad x = 1-\frac{r}{r_1}\ .$$

Thermonuclear plasma in a tokamak

Change of potential energy:

$$\delta W = \frac{1}{2}\int_{\mathcal{V}} \left[\frac{B_1^2}{\mu_0} + \frac{B^2}{\mu_0}|\boldsymbol{\nabla}\cdot\boldsymbol{\xi}_\perp + 2\boldsymbol{\xi}_\perp\cdot\boldsymbol{\kappa}|^2 - 2(\boldsymbol{\xi}_\perp\cdot\boldsymbol{\nabla}P)(\boldsymbol{\kappa}\cdot\boldsymbol{\xi}_\perp^*) - \mathbf{B_1}\cdot(\boldsymbol{\xi}_\perp\times\mathbf{b})j_\parallel + \gamma_{\text{thermo}}P(\boldsymbol{\nabla}\cdot\boldsymbol{\xi})^2 \right] \mathrm{d}\mathcal{V}$$

$$\mathbf{B_1} = \nabla\times(\boldsymbol{\xi}_\perp\times\mathbf{B})$$

$$\omega^2 = \frac{2\delta W}{\int \rho_i|\boldsymbol{\xi}_0|^2\mathrm{d}\mathcal{V}}$$

$$\gamma_I^2 = -\omega^2$$

We find an ideal stability criteria mostly based on the poloidal beta inside q=1

$$\beta_p(r_1) \equiv -2\frac{R_0^2q^2}{B_0^2r_1^4}\int_0^{r_1} p' r^2 dr\,.$$

This quantity represents the total available kinetic energy within $r = r_1$. A simple form for δW can be obtained if we consider a parabolic current profile $j_\phi(r)$, and if we assume that $q(r)$ in the centre does not differ very much from unity,

$$|1-q(0)| \ll 1\,, \qquad q(0) < 1\,.$$

Then, the $m = 1$ internal kink mode is mainly pressure driven and the potential energy is approximately [18]

$$\delta W \approx 6\pi^2\frac{B_0^2r_1^4}{R_0^3}|\xi_r(0)|^2\left[1-q(0)\right]\left[\beta_{\text{crit}}^2 - \beta_p^2(r_1)\right]\,, \qquad (27)$$

where $\beta_{\text{crit}}^2 = \frac{13}{144}$. One sees that instability, $\delta W < 0$, occurs if the driving force β_p exceeds the threshold value $\beta_{\text{crit}} \approx 0.3$.

18. M.N. Bussac, R. Pellat, D. Edery, and J.L. Soule, "Internal kink modes in toroidal plasma with circular cross-section," *Phys. Rev. Lett.* **35**, 1638 (1975).

Illustration of the energy principle to explain experimental effect of stabilization of kink by NBI particles

$$\delta W = \frac{1}{2}\int_{\mathcal{V}} \Bigg[\frac{B_1^2}{\mu_0} + \frac{B^2}{\mu_0}|\nabla\cdot\boldsymbol{\xi}_\perp + 2\boldsymbol{\xi}_\perp\cdot\boldsymbol{\kappa}|^2 - 2(\boldsymbol{\xi}_\perp\cdot\nabla P)(\boldsymbol{\kappa}\cdot\boldsymbol{\xi}_\perp^*) - \mathbf{B_1}\cdot(\boldsymbol{\xi}_\perp\times\mathbf{b})j_\| + \gamma_{\mathrm{thermo}} P(\nabla\cdot\boldsymbol{\xi})^2 \Bigg] \mathrm{d}\mathcal{V}$$

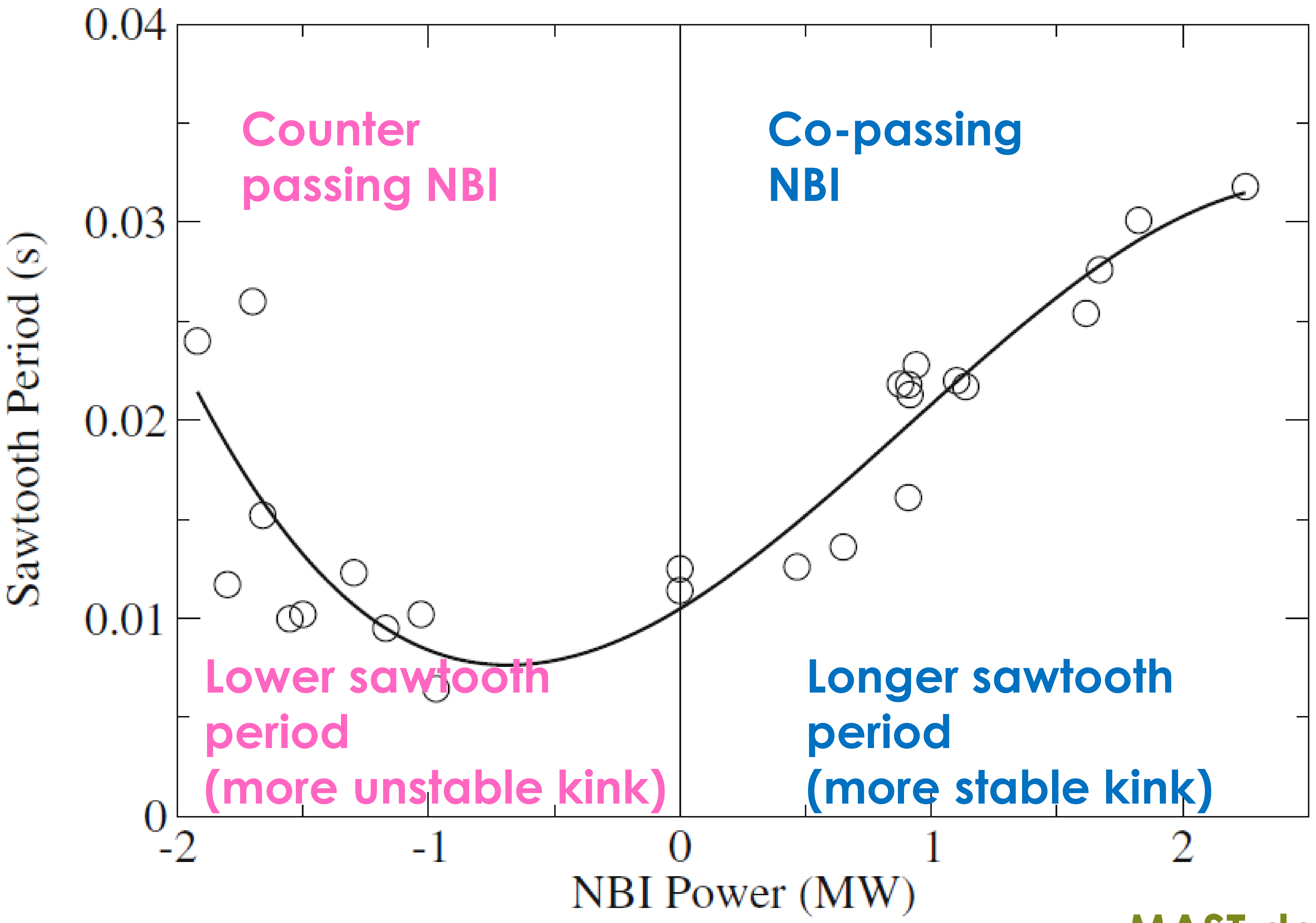

MAST data

Illustration of the energy principle to explain experimental effect of stabilization of kink by NBI particles

$$\delta W = \frac{1}{2}\int_{\mathcal{V}} \Big[\frac{B_1^2}{\mu_0} + \frac{B^2}{\mu_0}|\nabla\cdot\boldsymbol{\xi}_\perp + 2\boldsymbol{\xi}_\perp\cdot\boldsymbol{\kappa}|^2 - 2(\boldsymbol{\xi}_\perp\cdot\nabla P)(\boldsymbol{\kappa}\cdot\boldsymbol{\xi}_\perp^*) - \mathbf{B_1}\cdot(\boldsymbol{\xi}_\perp\times\mathbf{b})j_\parallel + \gamma_{\mathrm{thermo}}P(\nabla\cdot\boldsymbol{\xi})^2\Big]\,\mathrm{d}\mathcal{V}$$

$$\boldsymbol{\xi} = \int \dot{\boldsymbol{\xi}}\mathrm{d}t \simeq \mathbf{v_E}\ \mathrm{d}t\ .$$

$$\delta W_{\mathrm{fast}} = -\int_0^{r_1} (\boldsymbol{\xi}\cdot\nabla P_{\mathrm{fast}})\,(\boldsymbol{\xi}\cdot\boldsymbol{\kappa})\,\mathrm{d}\mathcal{V}$$

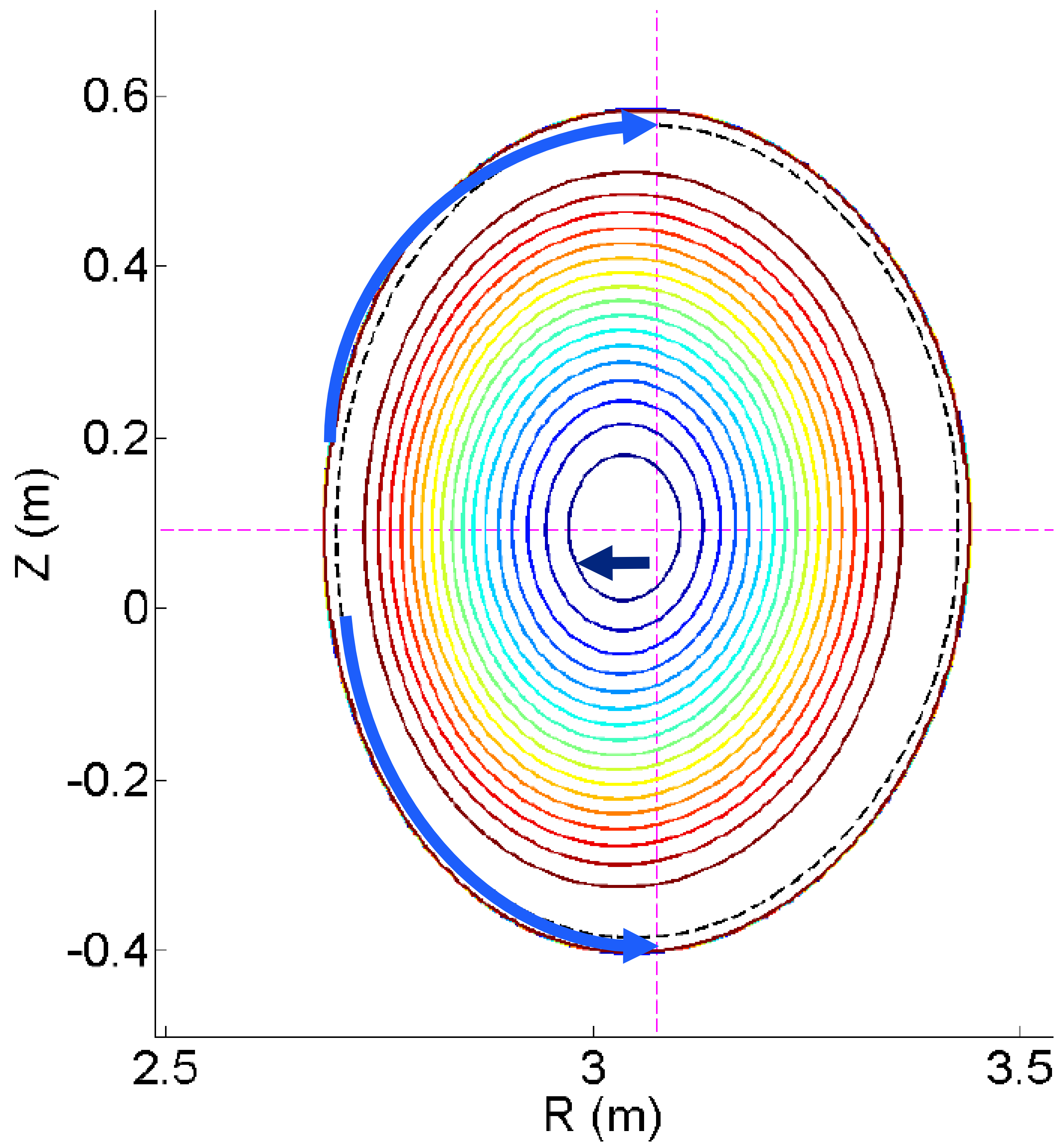

The backflow of plasma is always tangential to the q=1 contour!
(at any toroidal location)

Illustration of the energy principle to explain experimental effect of stabilization of kink by NBI particles

$$\delta W_{\mathrm{fast}} = -\int_0^{r_1} (\boldsymbol{\xi}\cdot\nabla P_{\mathrm{fast}})\,(\boldsymbol{\xi}\cdot\boldsymbol{\kappa})\,\mathrm{d}\mathcal{V}$$

$$P_{\mathrm{fast}} = (2/3) n_{\mathrm{fast}} \langle \mathcal{E}_{\mathrm{fast}} \rangle$$

$$\boldsymbol{\kappa_{pol}} = \frac{\mu_0}{B^2}\boldsymbol{\nabla}\left(P + \frac{B^2}{2\mu_0}\right) \;;$$

$$\kappa_\varphi = \left(\frac{(\mathbf{B}\times\boldsymbol{\nabla}B)\times\mathbf{B}}{B^3}\right)_\varphi \,.$$

$$\boldsymbol{\xi} = \int \dot{\boldsymbol{\xi}}\,\mathrm{d}t \simeq \mathbf{v_E}\;\mathrm{d}t \;.$$

Kink stabilization by energetic NBI (co-current)

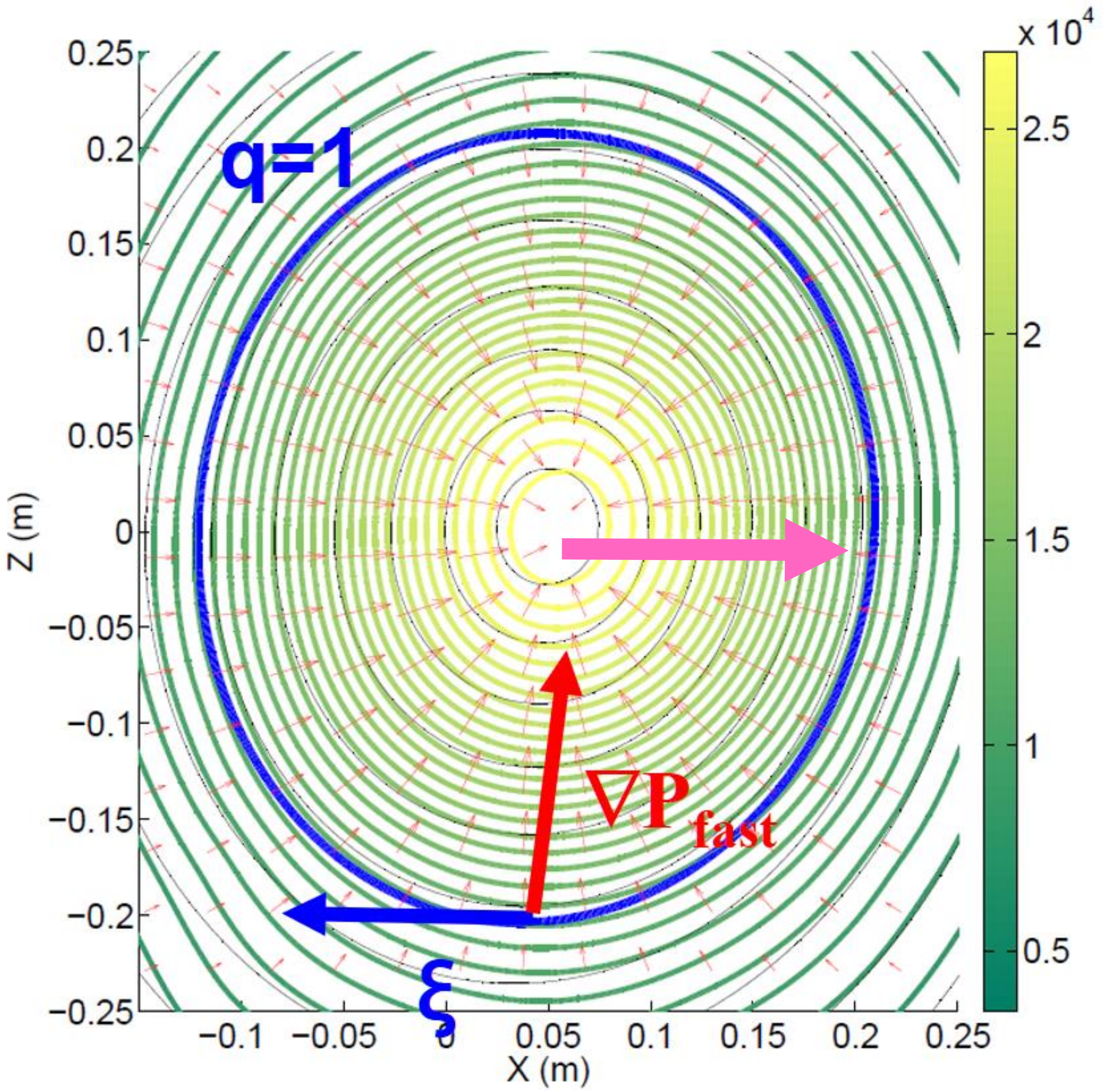

$$\delta W_{\mathrm{fast}} = -\int_0^{r_1} (\boldsymbol{\xi}\cdot\nabla P_{\mathrm{fast}})\,(\boldsymbol{\xi}\cdot\boldsymbol{\kappa})\,\mathrm{d}\mathcal{V}$$

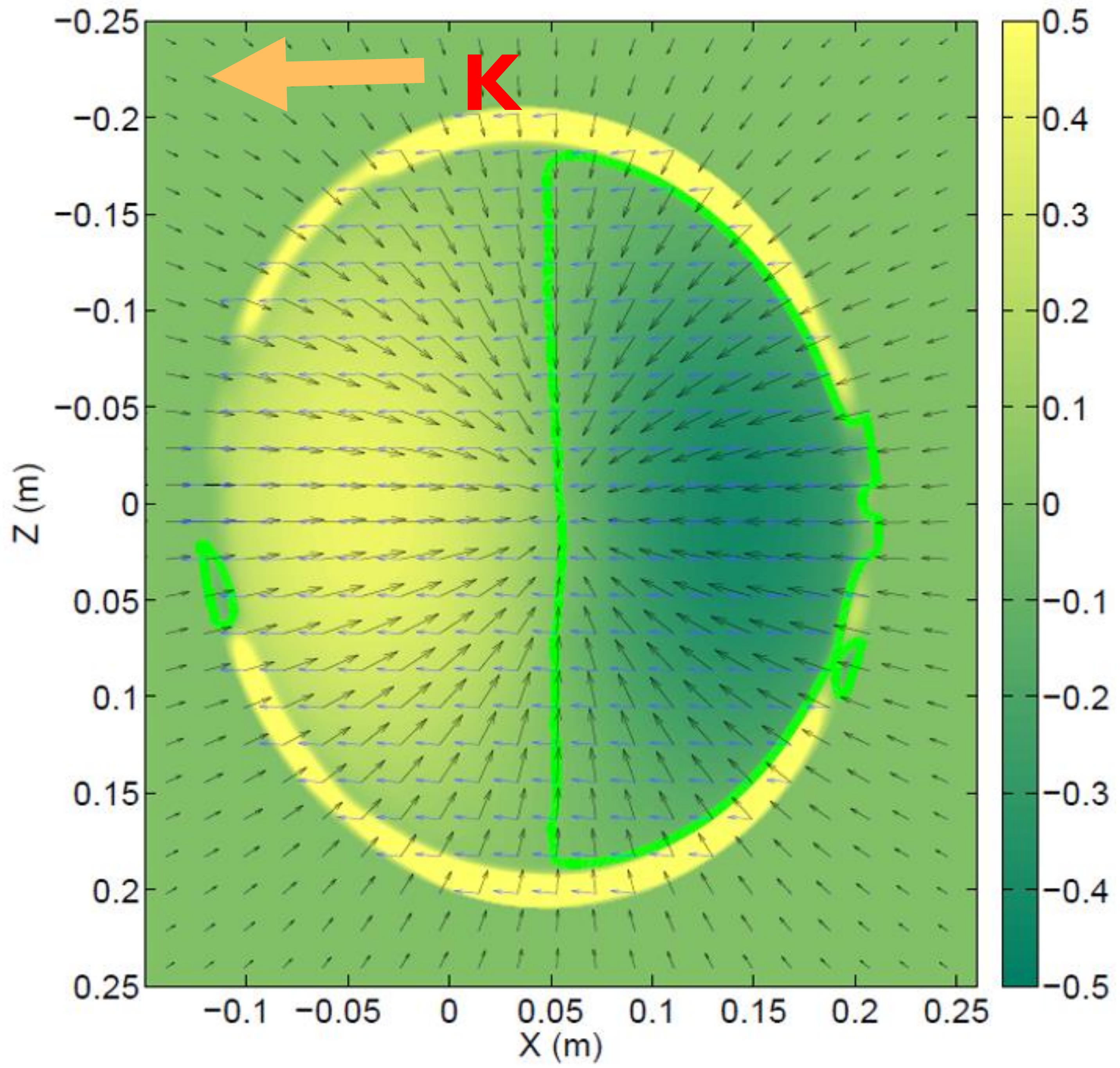

Illustration of the energy principle to explain experimental effect of stabilization of kink by NBI particles

Kink destabilization by energetic NBI (counter-current)

$$\delta W = \frac{1}{2}\int_{\mathcal{V}} \left[\frac{B_1^2}{\mu_0} + \frac{B^2}{\mu_0}|\nabla\cdot\boldsymbol{\xi}_\perp + 2\boldsymbol{\xi}_\perp\cdot\boldsymbol{\kappa}|^2 - 2(\boldsymbol{\xi}_\perp\cdot\nabla P)(\boldsymbol{\kappa}\cdot\boldsymbol{\xi}_\perp^*) - \mathbf{B_1}\cdot(\boldsymbol{\xi}_\perp\times\mathbf{b})j_\parallel + \gamma_{\mathrm{thermo}} P(\nabla\cdot\boldsymbol{\xi})^2 \right] d\mathcal{V}$$

$$P_{\mathrm{fast}} = (2/3) n_{\mathrm{fast}} \langle \mathcal{E}_{\mathrm{fast}} \rangle$$

$$\boldsymbol{\kappa_{pol}} = \frac{\mu_0}{B^2}\nabla\left(P + \frac{B^2}{2\mu_0}\right) ;$$

$$\kappa_\varphi = \left(\frac{(\mathbf{B}\times\nabla B)\times\mathbf{B}}{B^3}\right)_\varphi .$$

$$\boldsymbol{\xi} = \int \dot{\boldsymbol{\xi}}\, dt \simeq \mathbf{v_E}\ dt .$$

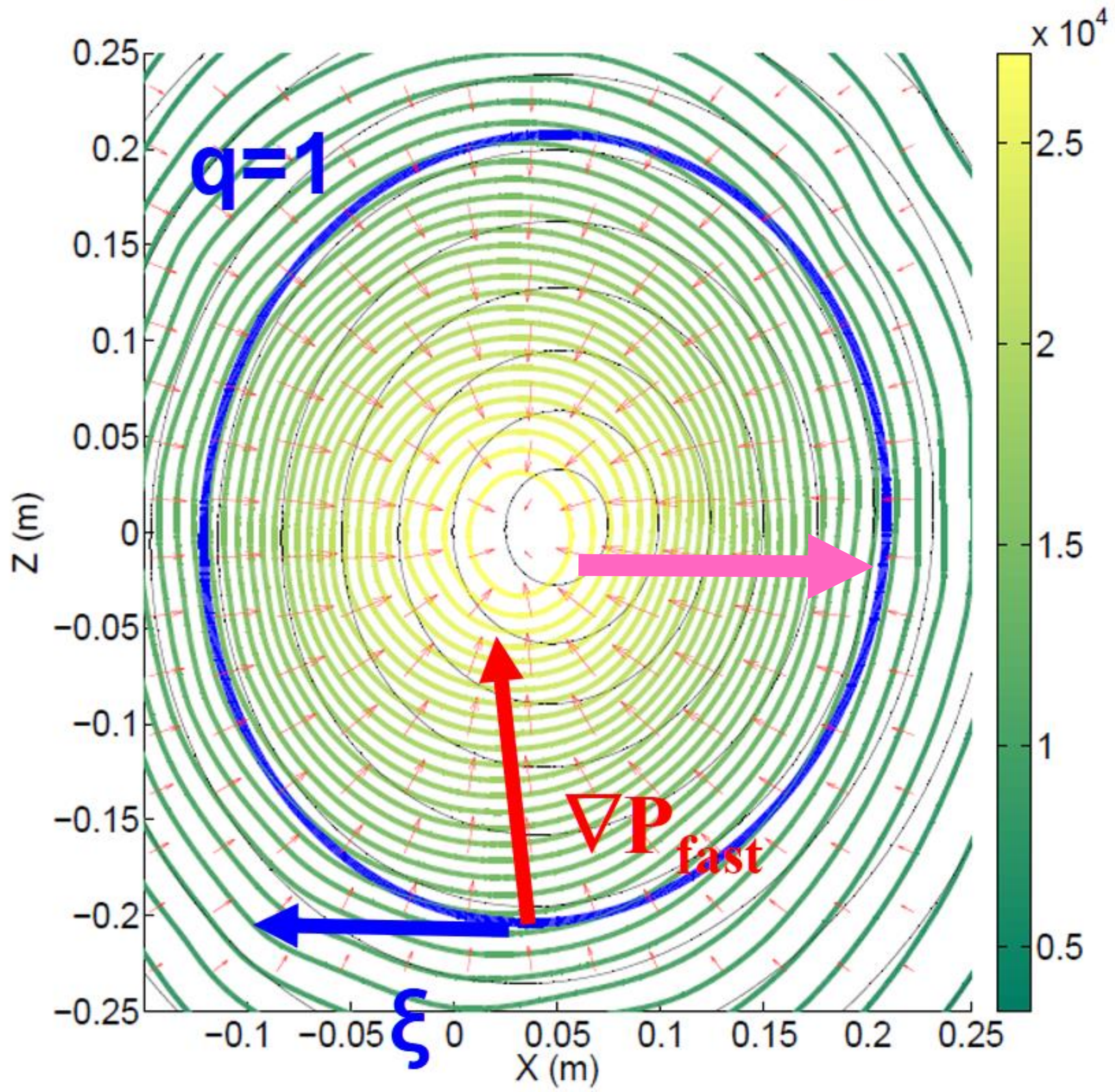

$$\delta W_{\mathrm{fast}} = -\int_0^{r_1} (\boldsymbol{\xi}\cdot\nabla P_{\mathrm{fast}})(\boldsymbol{\xi}\cdot\boldsymbol{\kappa})\, d\mathcal{V}$$

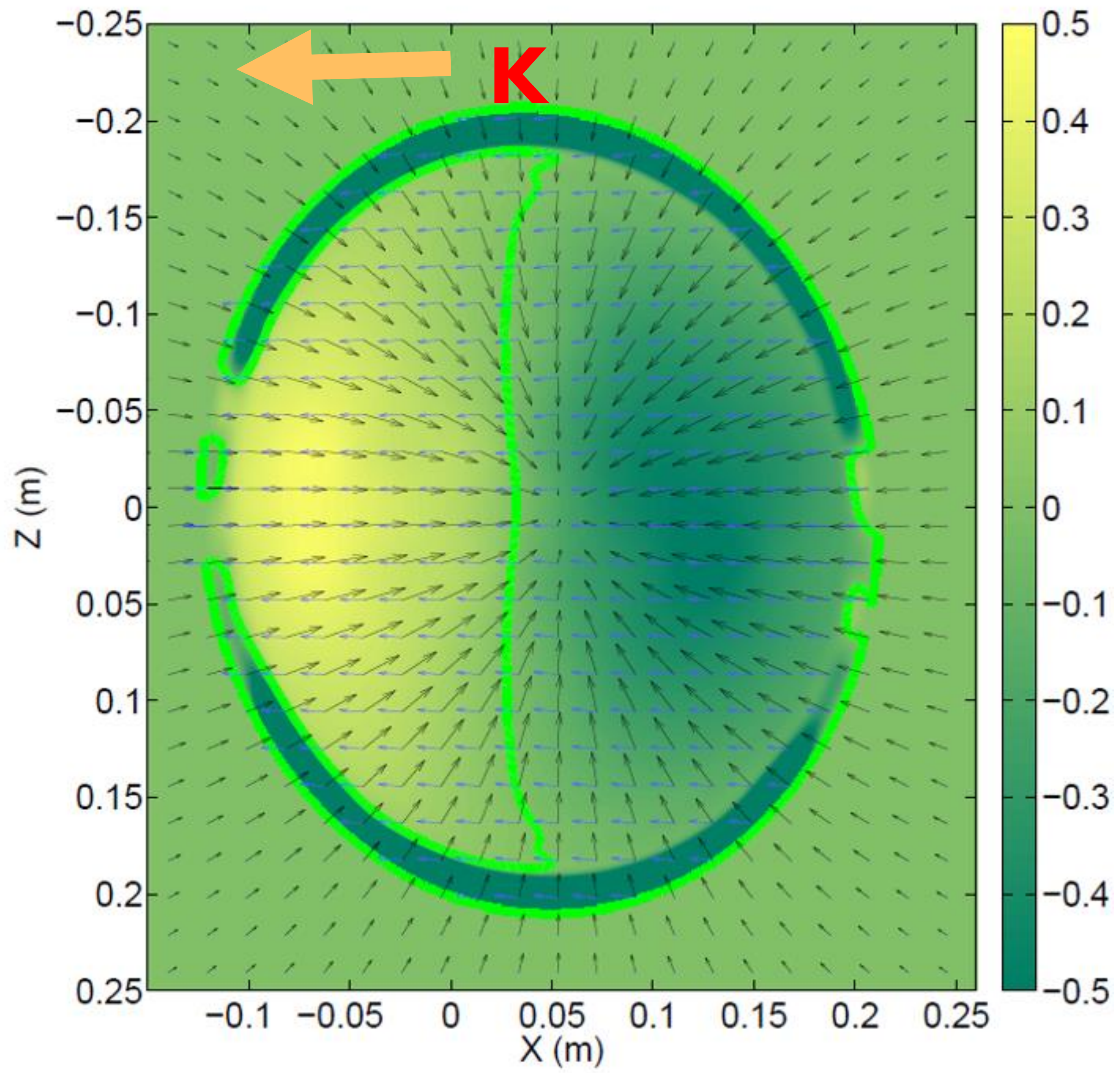

Overview of this lecture

- Safety factor profile in tokamaks
- Introduction to the internal kink and the sawtooth crash
- Energy principle and derivation of linear growth rate of internal kink
- **Ideal MHD for poloidal mapping of the reconnecting magnetic flux**
- **Computationally efficient poloidal mapping of the reconnecting magnetic flux**

Poloidal flux contour of the internal kink and sawtooth reconnection

Kink
(contained within q=1)

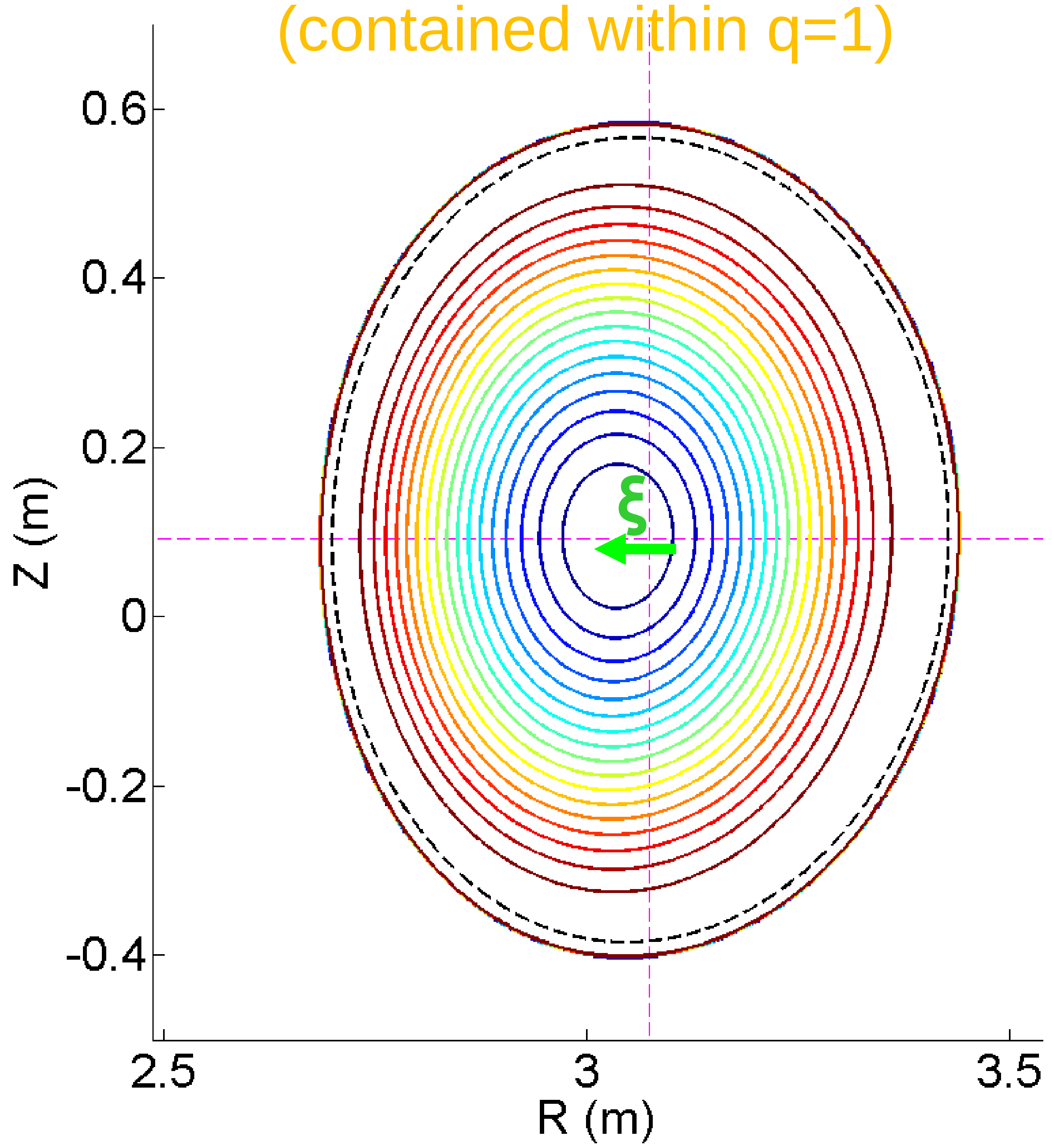

Reconnection
(extending to the mixing radius, beyond q=1)

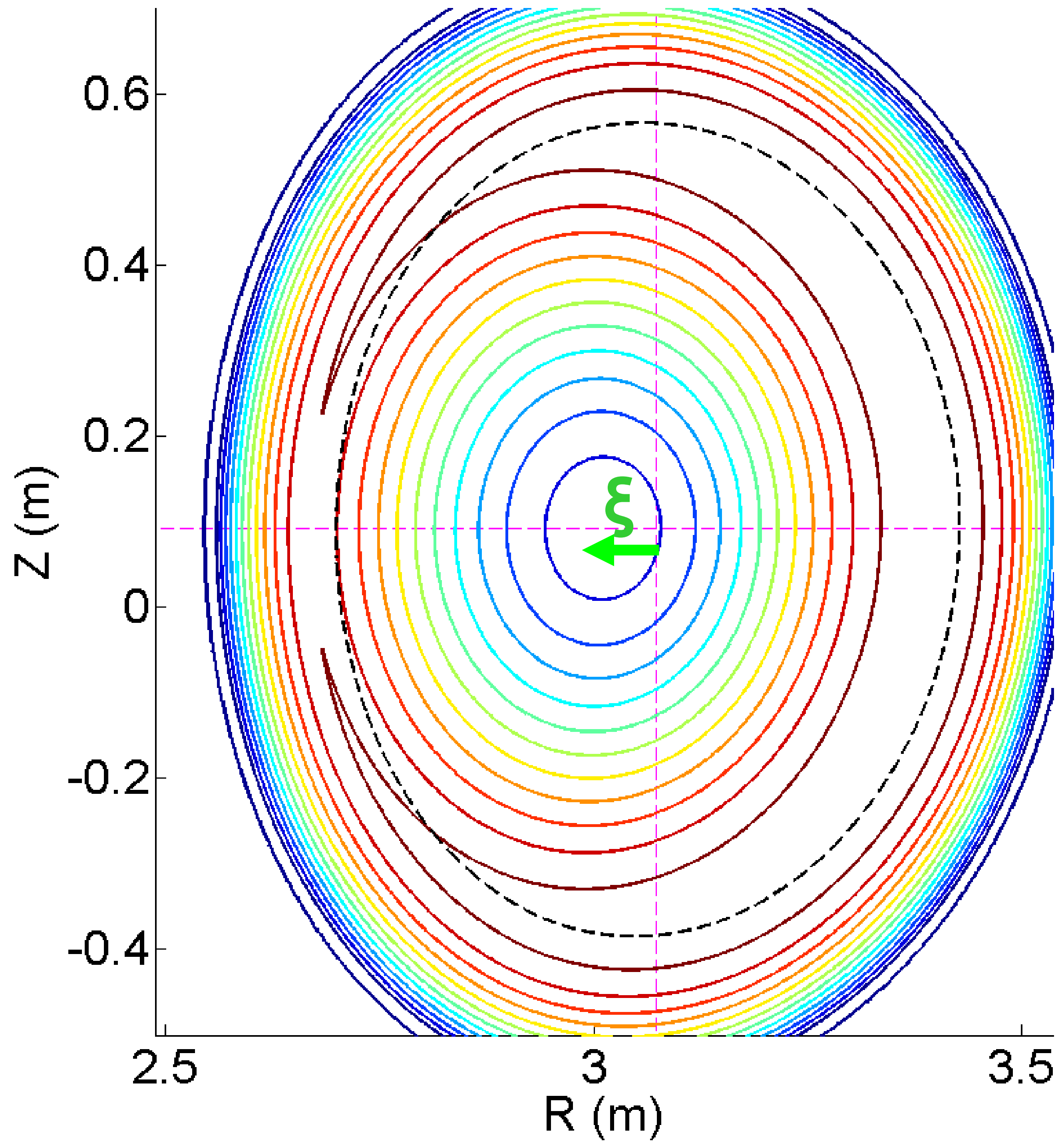

The perturbed helical flux

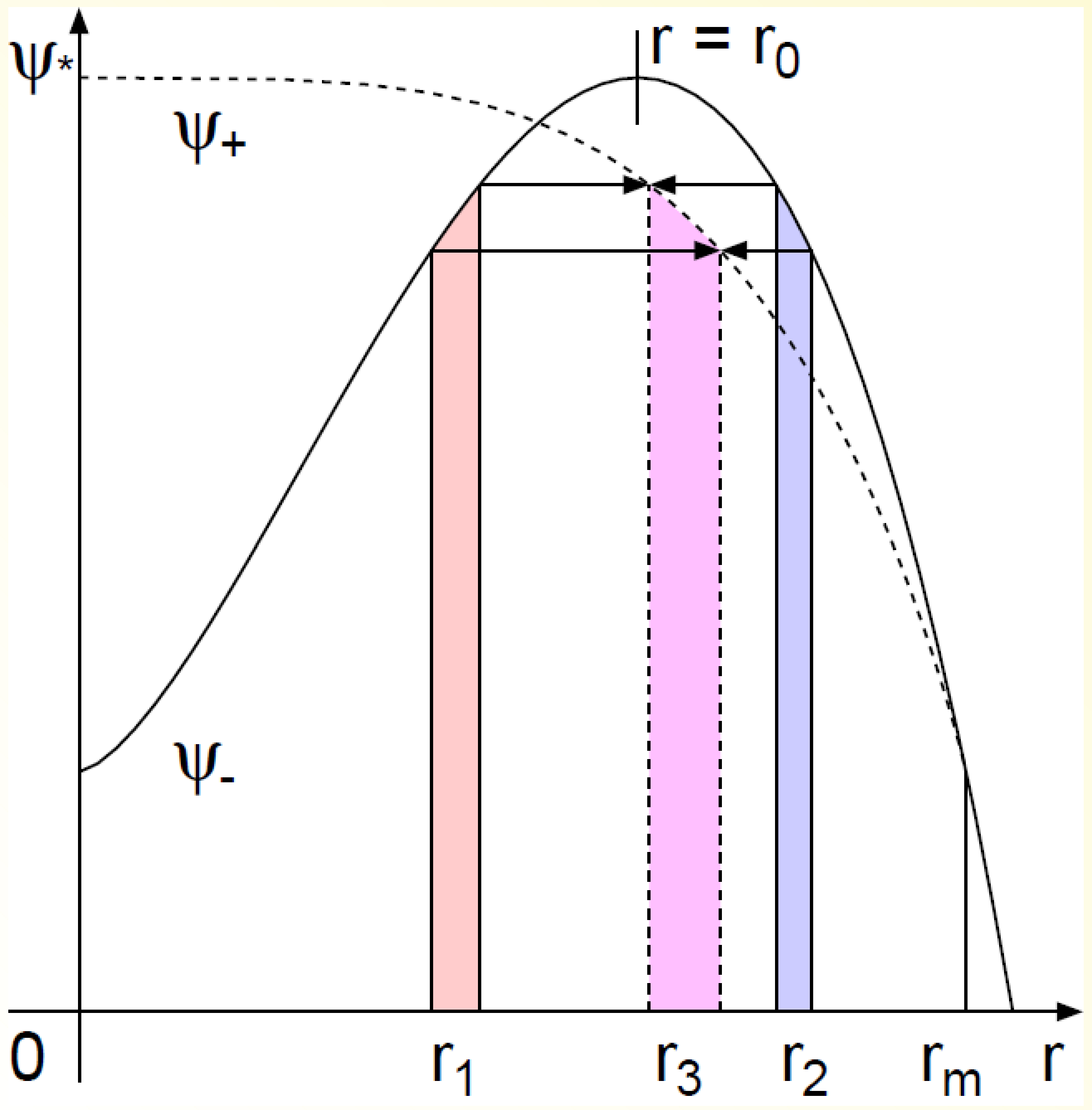

Initial (ψ_-) and final (ψ_+) helical flux profiles as a function of r. The arrows indicate the conservation of helical flux during reconnection, while conservation of toroidal flux is given by $r_2^2 - r_1^2 = r_3^2$.

$\Psi_*(r,\omega)$

$\omega=\theta-\varphi$

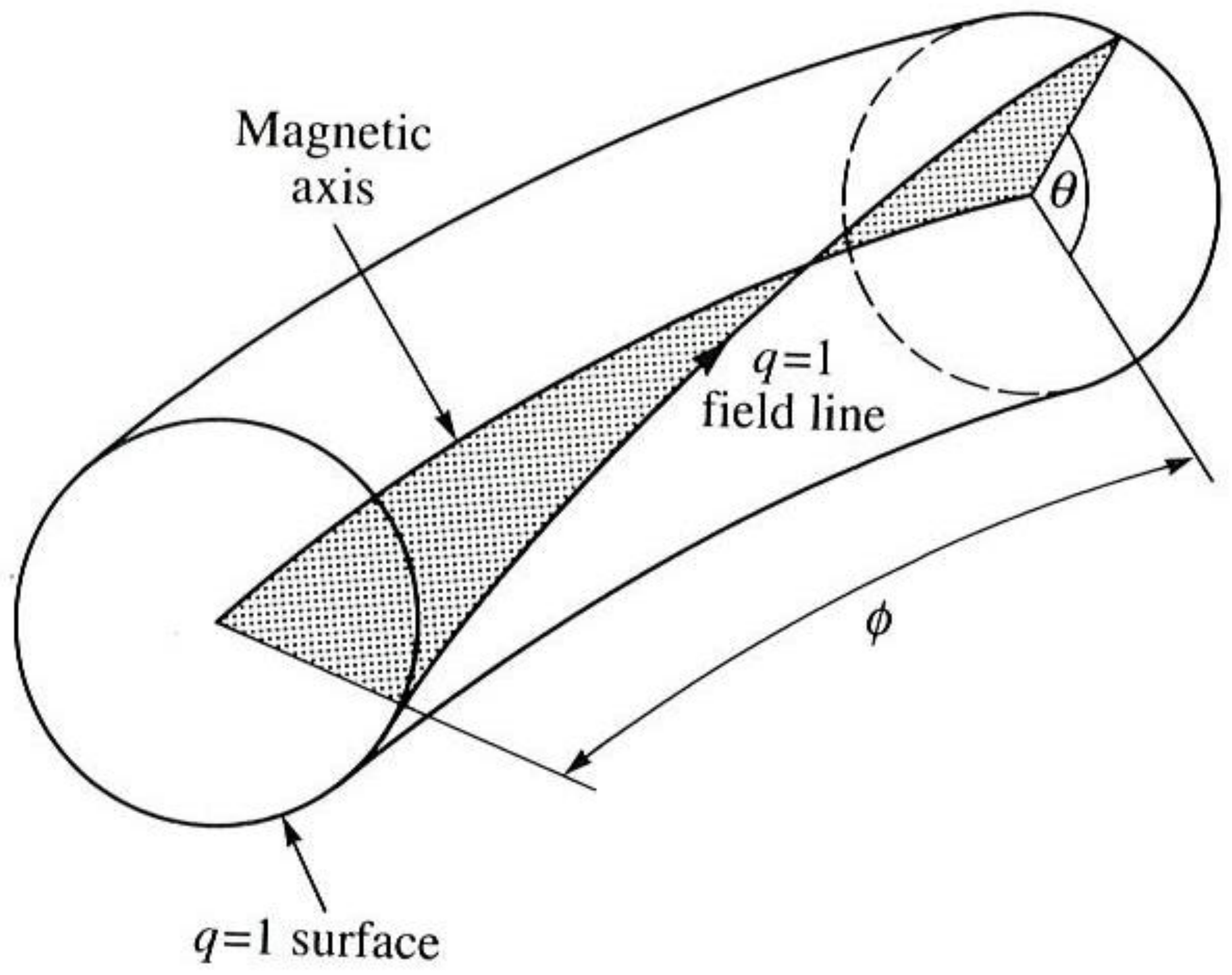

$$\mathbf{B_H} = \mathbf{B}_\varphi + q\mathbf{B}_{\mathbf{pol}}$$

$$\mathbf{B}_* = \frac{1}{R}(\mathbf{e}_\varphi \times \nabla \psi_*)$$

$$\mathbf{B} = \mathbf{B_H} + \mathbf{B}_*$$

The perturbed helical flux

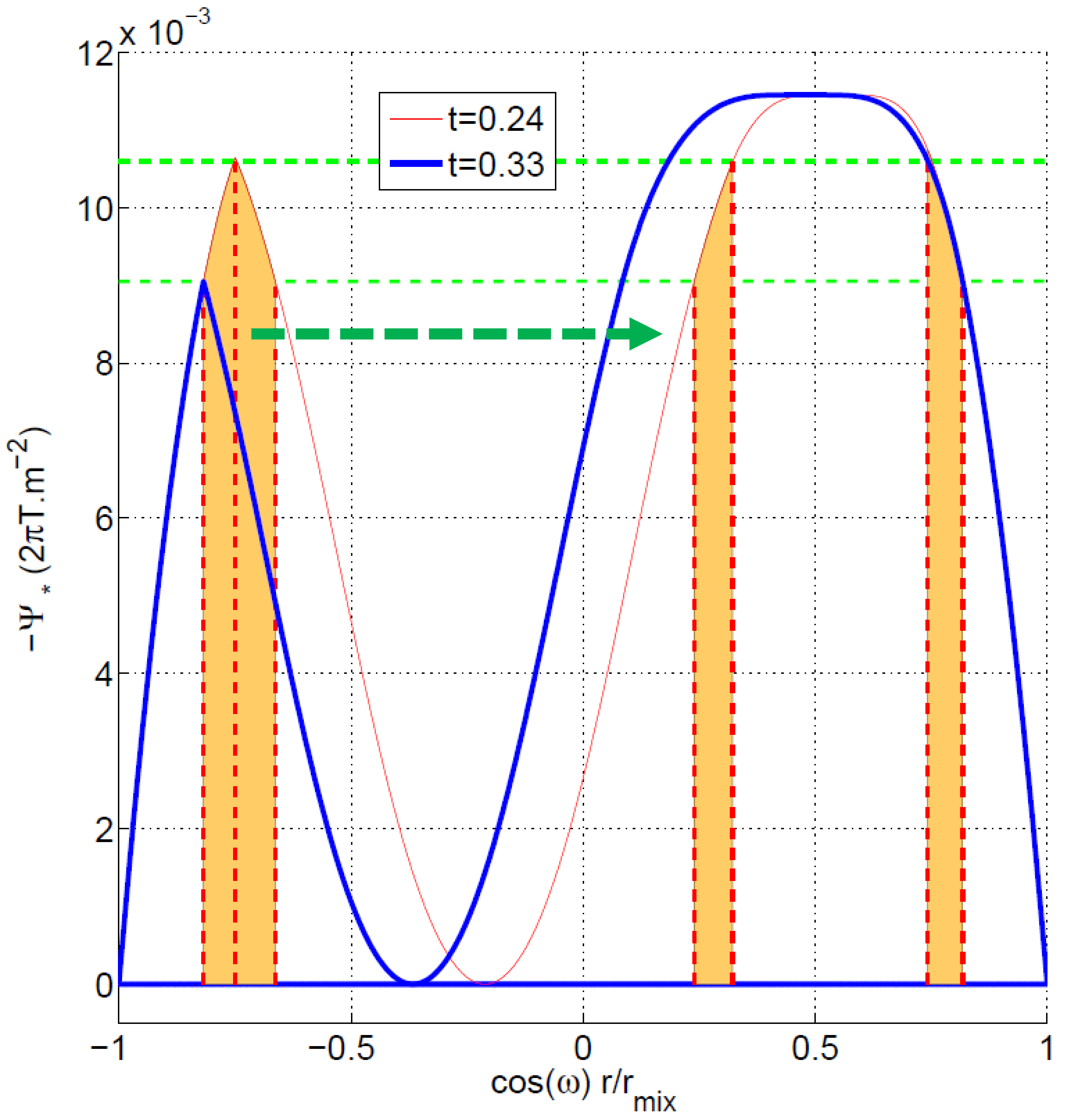

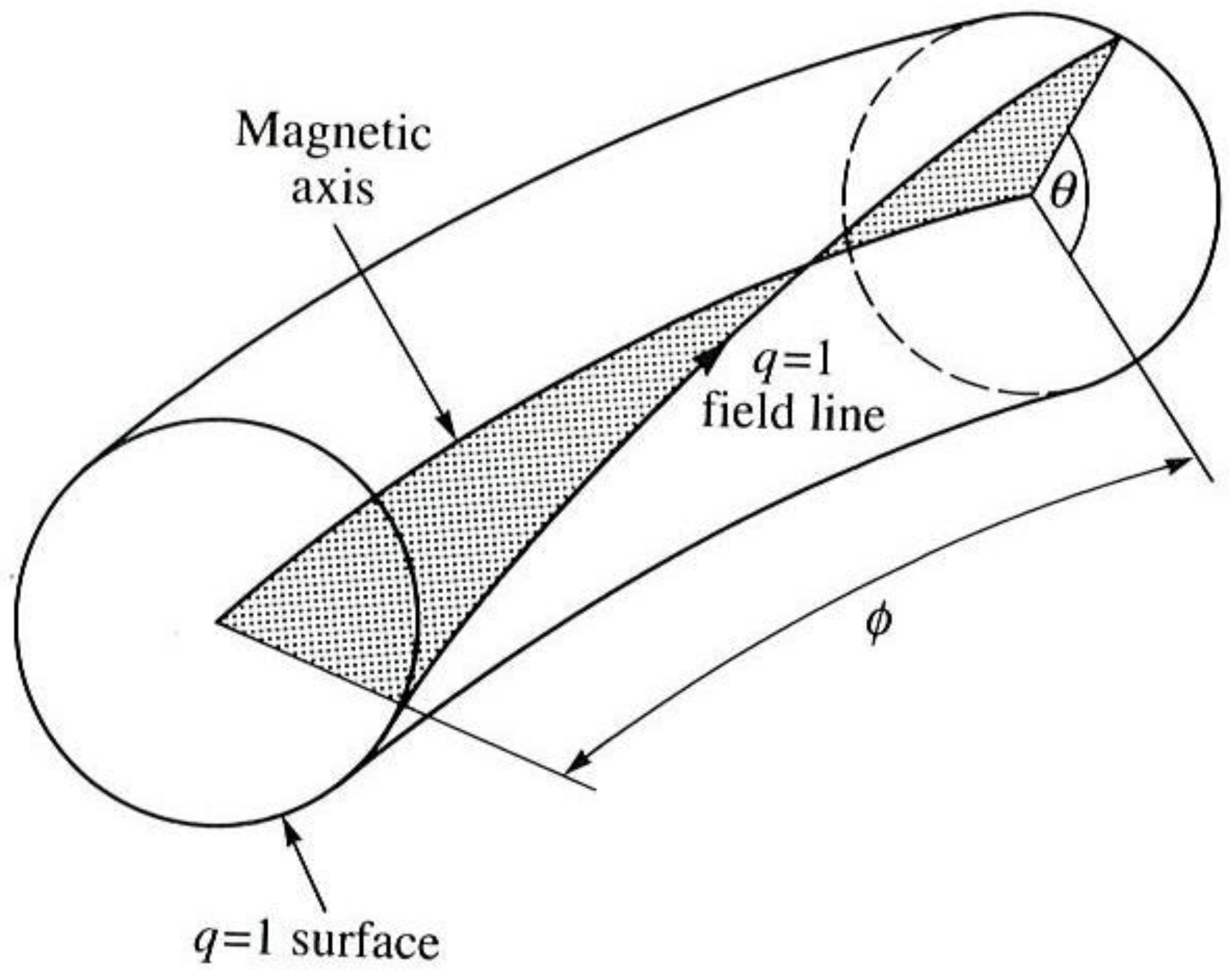

$\Psi_*(r,\omega)$

$\omega=\theta-\varphi$

$$\mathbf{B_H} = \mathbf{B}_\varphi + q\mathbf{B}_{\mathbf{pol}}$$

$$\mathbf{B}_* = \frac{1}{R}(\mathbf{e}_\varphi \times \nabla\psi_*)$$

$$\mathbf{B} = \mathbf{B_H} + \mathbf{B}_*$$

MHD model

Ideal MHD : fluid model of plasma

The mass continuity equation is

$$\frac{\partial \rho}{\partial t} + \nabla \cdot (\rho \mathbf{v}) = 0.$$

The Cauchy momentum equation is

$$\rho \left(\frac{\partial}{\partial t} + \mathbf{v} \cdot \nabla \right) \mathbf{v} = \mathbf{J} \times \mathbf{B} - \nabla p.$$

The Lorentz force term $\mathbf{J} \times \mathbf{B}$ can be expanded using Ampère's law and the vector calculus identity

$$\tfrac{1}{2}\nabla(\mathbf{B} \cdot \mathbf{B}) = (\mathbf{B} \cdot \nabla)\mathbf{B} + \mathbf{B} \times (\nabla \times \mathbf{B})$$

to give

$$\mathbf{J} \times \mathbf{B} = \frac{(\mathbf{B} \cdot \nabla)\,\mathbf{B}}{\mu_0} - \nabla \left(\frac{B^2}{2\mu_0} \right),$$

where the first term on the right hand side is the magnetic tension force and the second term is the magnetic pressure force.

The ideal Ohm's law for a plasma is given by

$$\mathbf{E} + \mathbf{v} \times \mathbf{B} = 0.$$

Faraday's law is

$$\frac{\partial \mathbf{B}}{\partial t} = -\nabla \times \mathbf{E}.$$

→

$$\mathbf{E} = -\frac{\partial \mathbf{A}}{\partial t} - \boldsymbol{\nabla} \Phi$$

The low-frequency Ampère's law neglects displacement current and is given by

$$\mu_0 \mathbf{J} = \nabla \times \mathbf{B}.$$

The magnetic divergence constraint is

$$\nabla \cdot \mathbf{B} = 0.$$

The energy equation is given by

$$\frac{\mathrm{d}}{\mathrm{d}t} \left(\frac{p}{\rho^\gamma} \right) = 0,$$

Simplified poloidal flux modelling of the sawtooth crash

$$\mathbf{E} + \mathbf{u} \times \mathbf{B} = \eta \mathbf{j}$$

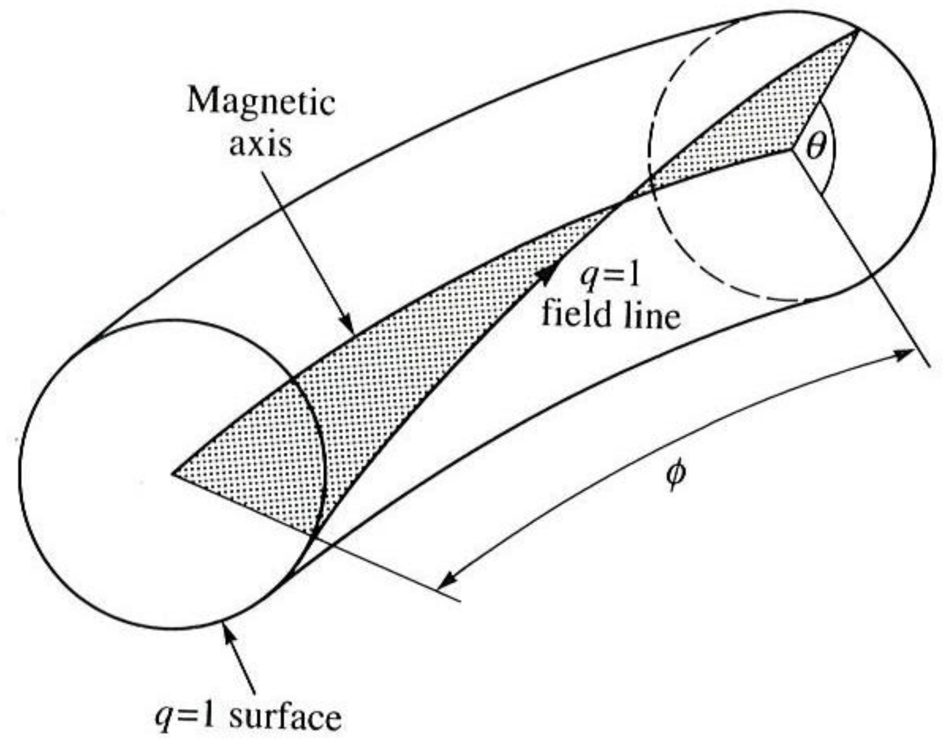

Ideal Ohm's law:

$$\mathbf{E} + \mathbf{u} \times \mathbf{B} = 0 \longrightarrow \mathbf{E} \cdot \mathbf{B} = 0$$

$$\left.\begin{aligned} \mathbf{E} &= \frac{\dot{\psi}_*}{R}\mathbf{e}_\varphi - \nabla\Phi \\ \mathbf{B} &= \mathbf{B_H} + \mathbf{B}_* \end{aligned}\right\} \xrightarrow{\mathbf{E} \cdot \mathbf{B} = 0} \nabla\Phi \cdot \mathbf{B}_* = \frac{B_\varphi \dot{\psi}_*}{R}$$

Simplified poloidal flux modelling of the sawtooth crash

Ya. I. Kolesnichenko et. Al Nucl. Fusion **36** 159 (1996)

$\mathbf{E} + \mathbf{u} \times \mathbf{B} = 0 \qquad \mathbf{E} \cdot \mathbf{B} = 0$

$$\mathbf{E} = \frac{\dot{\psi}_*}{R}\mathbf{e}_\varphi - \nabla\Phi, \qquad \mathbf{B} = \mathbf{B}_\mathrm{H} + \mathbf{B}_* \;\xrightarrow{\mathbf{E}\cdot\mathbf{B}=0}\; \nabla\Phi \cdot \mathbf{B}_* = \frac{B_\varphi \dot{\psi}_*}{R}$$

Method is computationally inefficient… It requires contour extraction!

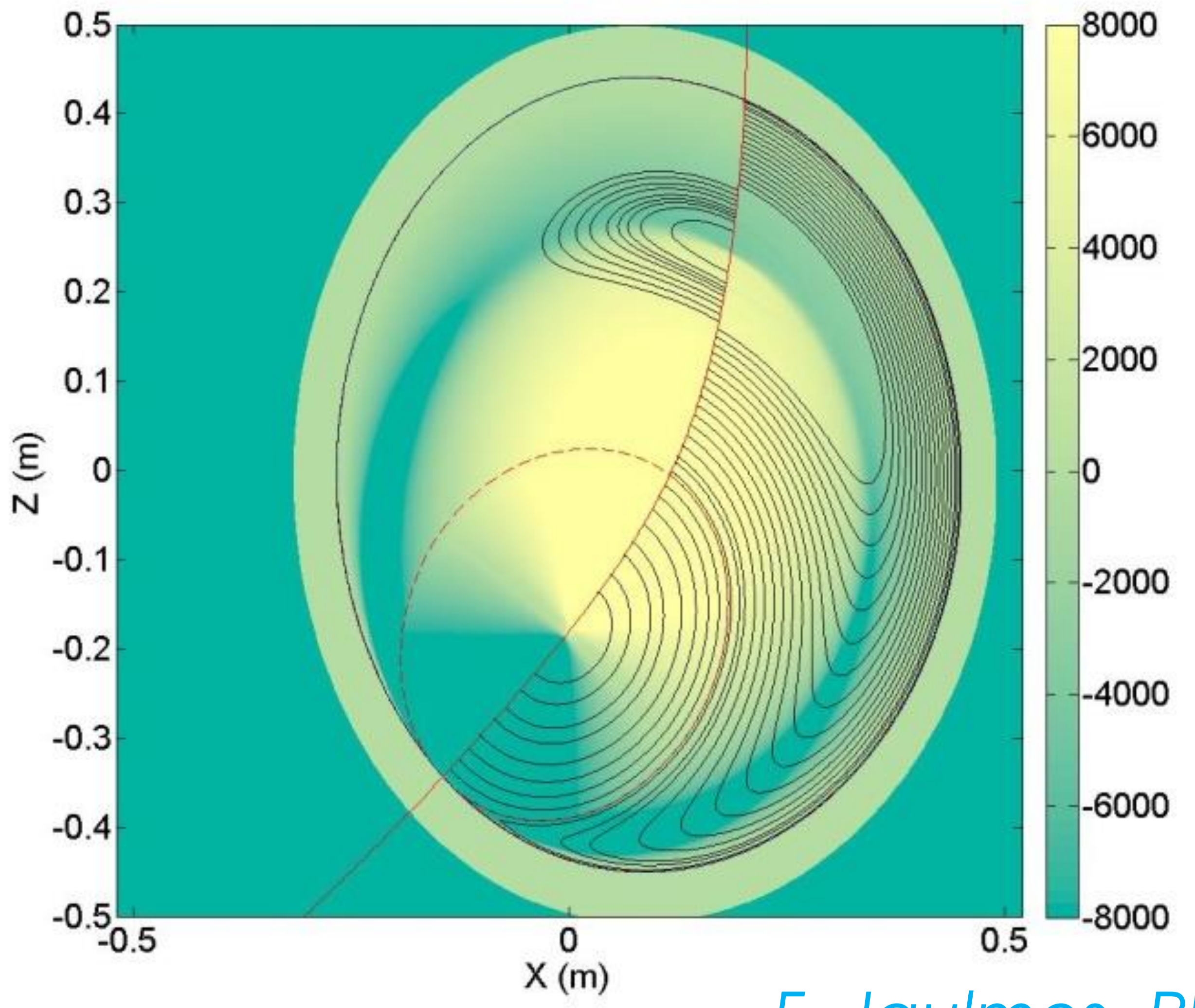

$$\Phi = \int_{\psi_* contour} \frac{B_\varphi \dot{\psi}_*}{R B_*} \mathrm{d}l_* + \Phi_0(\psi)$$

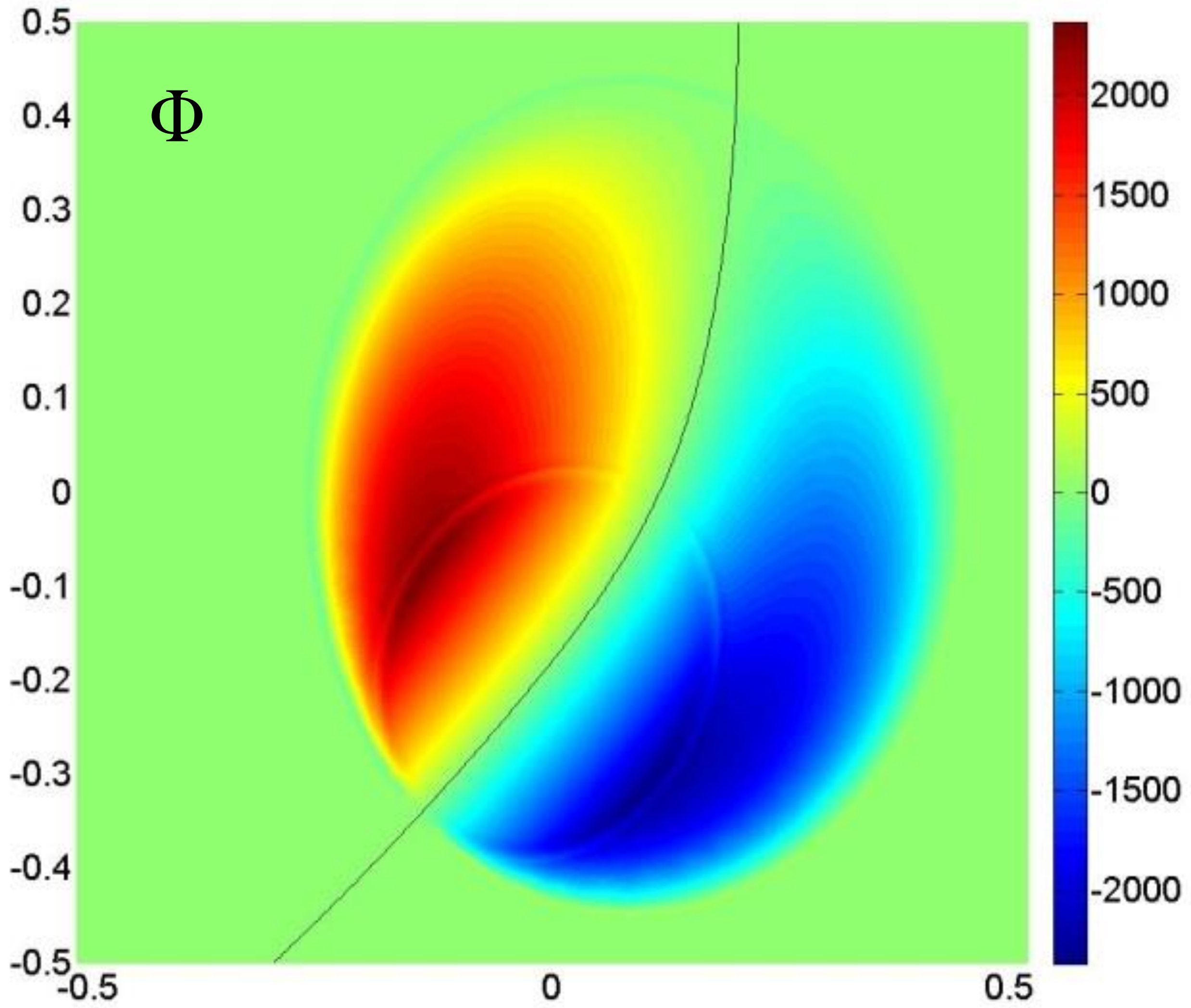

F. Jaulmes, PhD thesis, 2016

Overview of this lecture

- Safety factor profile in tokamaks
- Introduction to the internal kink and the sawtooth crash
- Energy principle and derivation of linear growth rate of internal kink
- Ideal MHD for poloidal mapping of the reconnecting magnetic flux
- **Computationally efficient poloidal mapping of the reconnecting magnetic flux**

How to improve the Electric potential calculation?

New coordinates to describe the build-up of the island

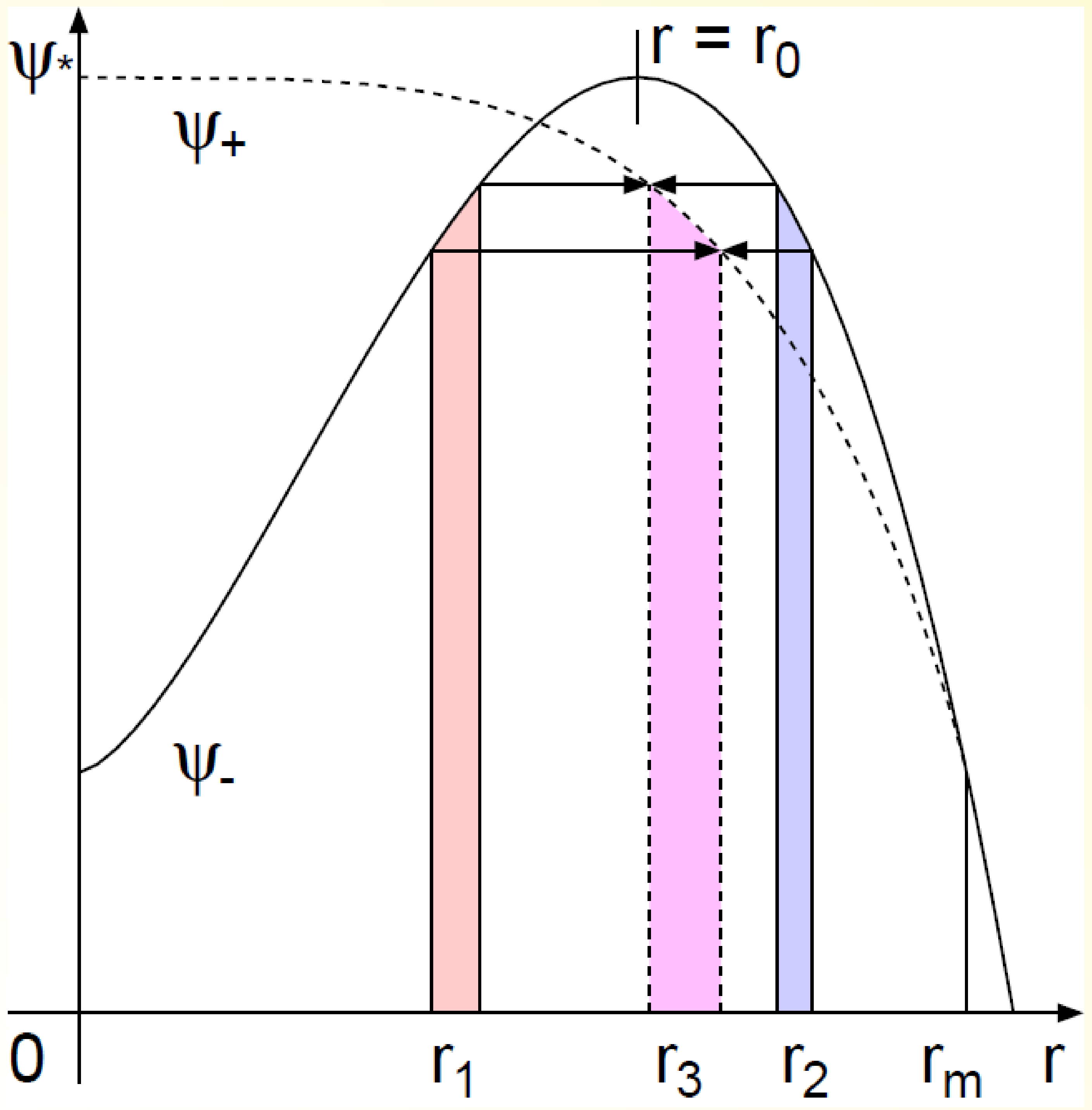

$$\psi_1' = q_2(1-q_1)r_1,$$
$$\psi_2' = q_1(1-q_2)r_2,$$

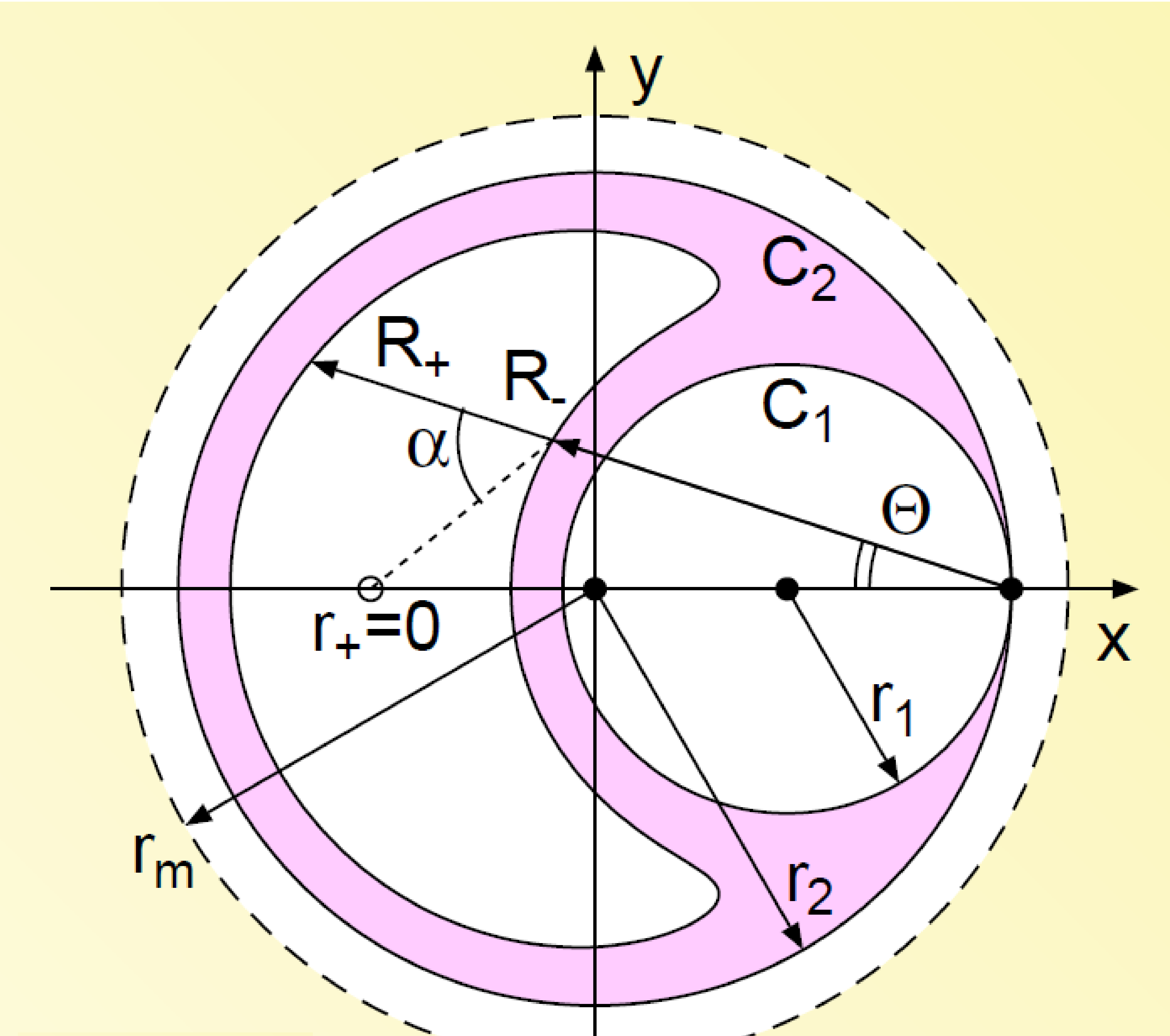

$$r = \sqrt{2\chi}$$

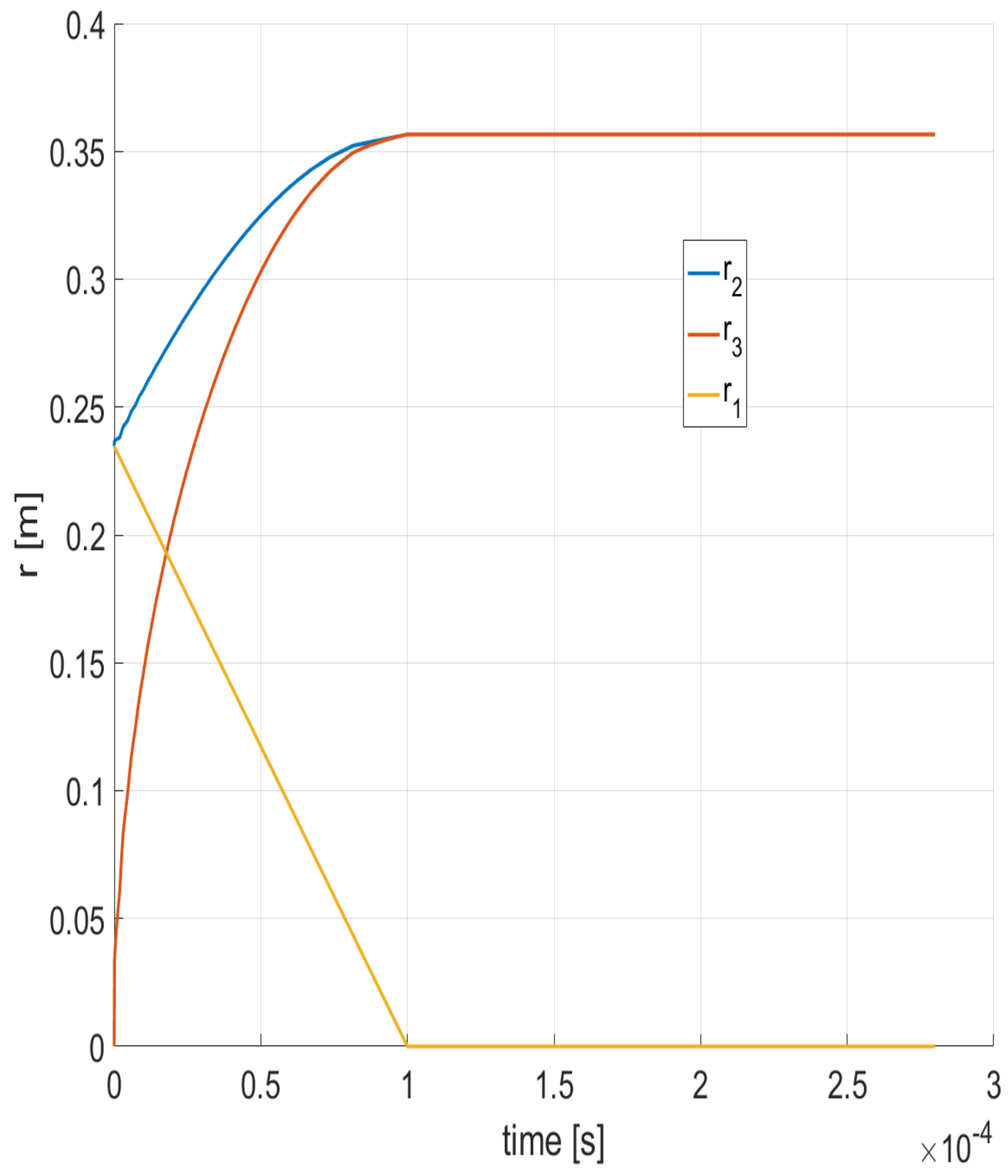

New coordinates to describe the build-up of the island

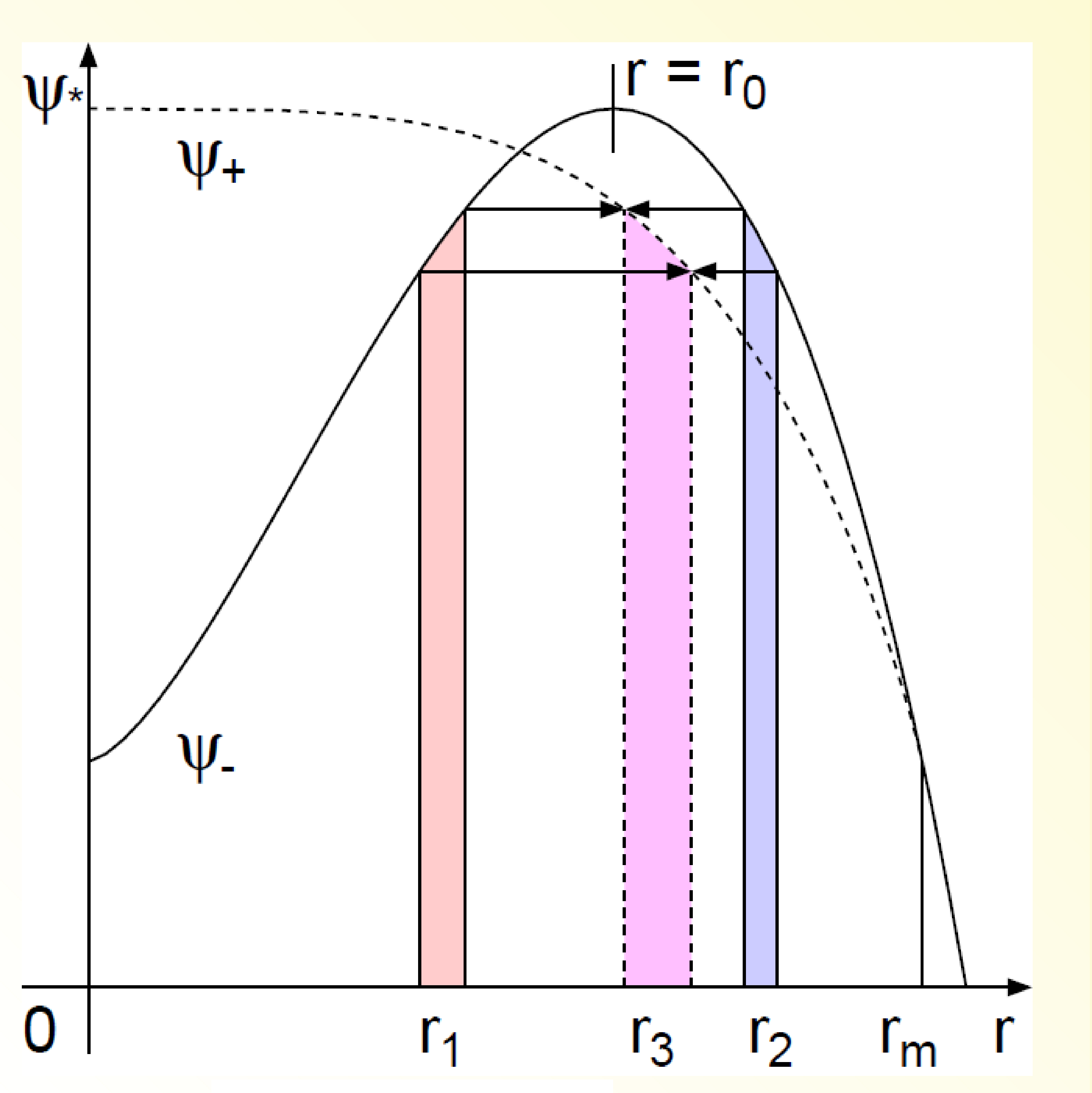

$$\psi_1' = q_2(1-q_1)r_1,$$
$$\psi_2' = q_1(1-q_2)r_2,$$

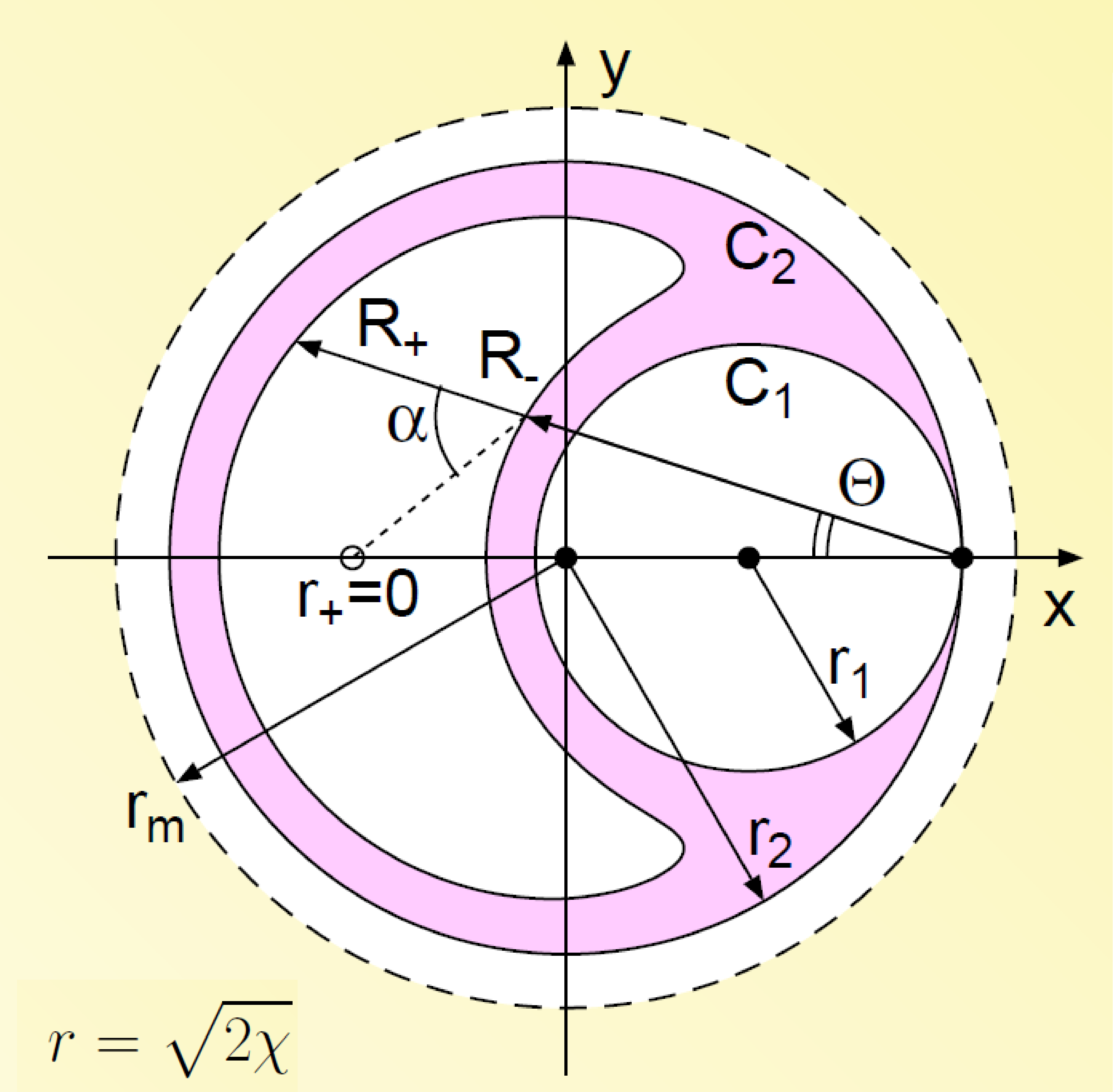

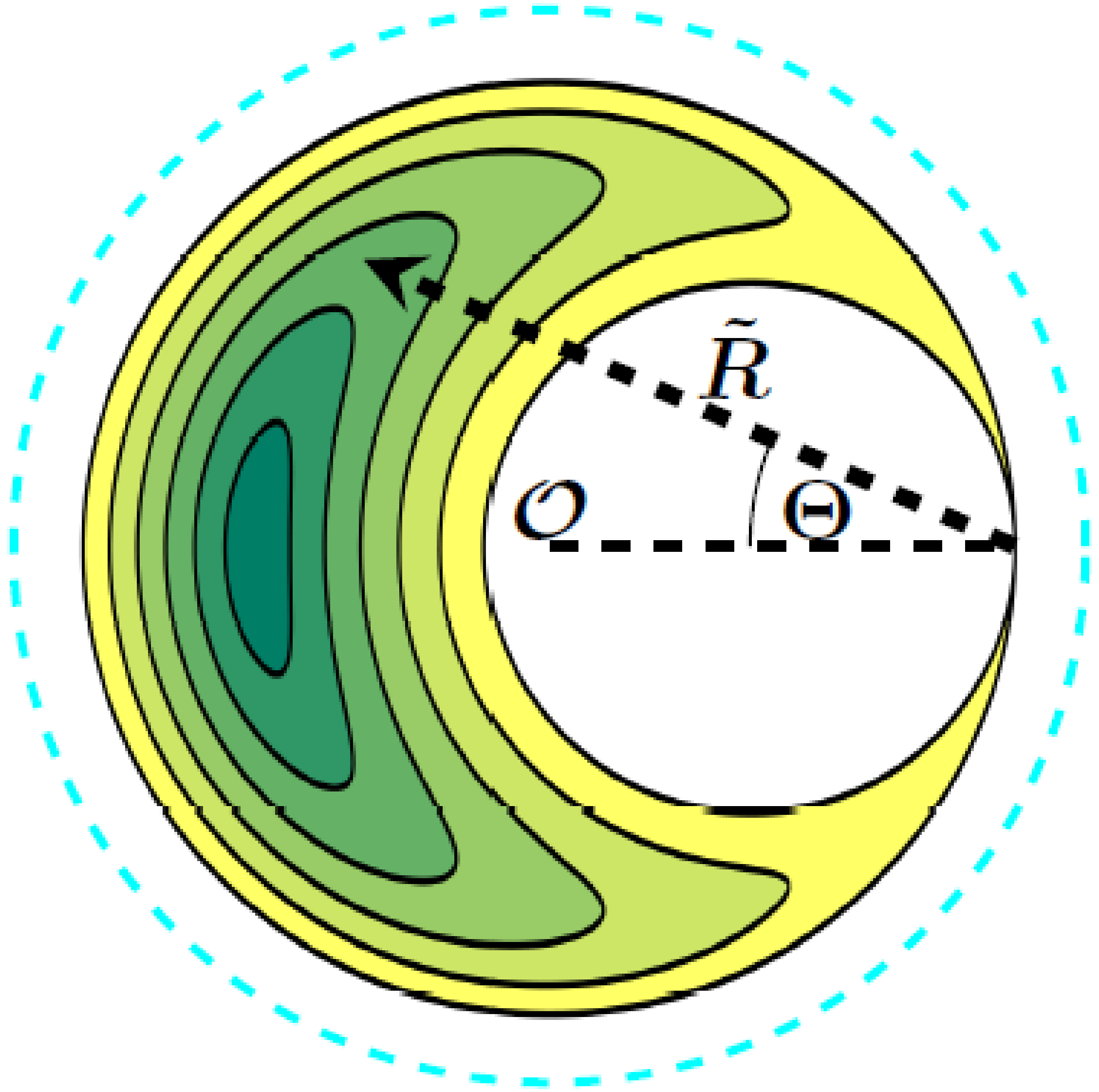

Coordinates $\tilde{R}, \Theta$ defined from the 'X'-point. Contours drawn here indicate surfaces of equal r_+ and enclose an area πr_+^2. Transformations in this model *preserve* this area, thus r_+ is the radial coordinate after the sawtooth.

New coordinates to describe the build-up of the island

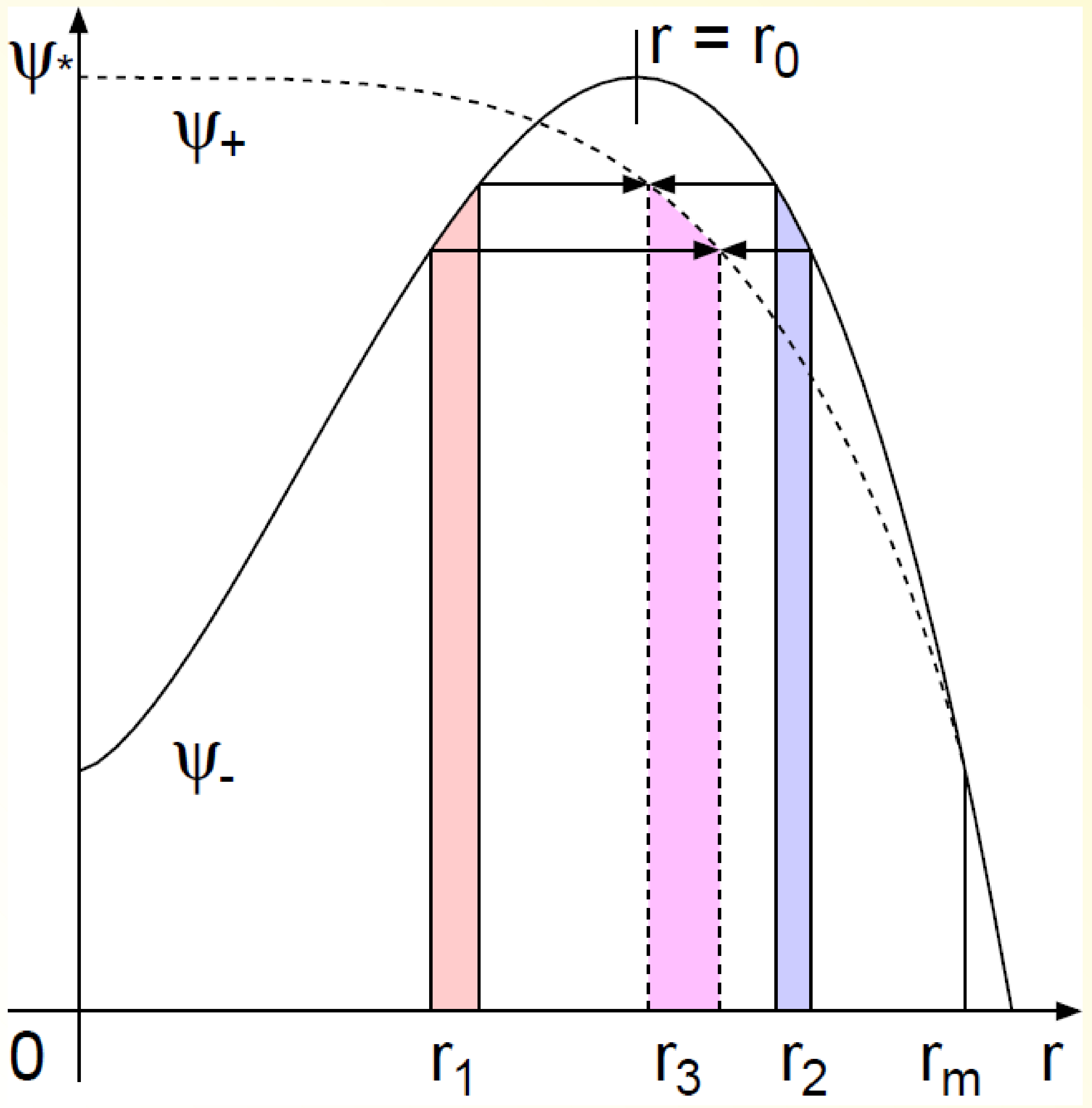

$$\psi_1' = q_2(1-q_1)r_1,$$
$$\psi_2' = q_1(1-q_2)r_2,$$

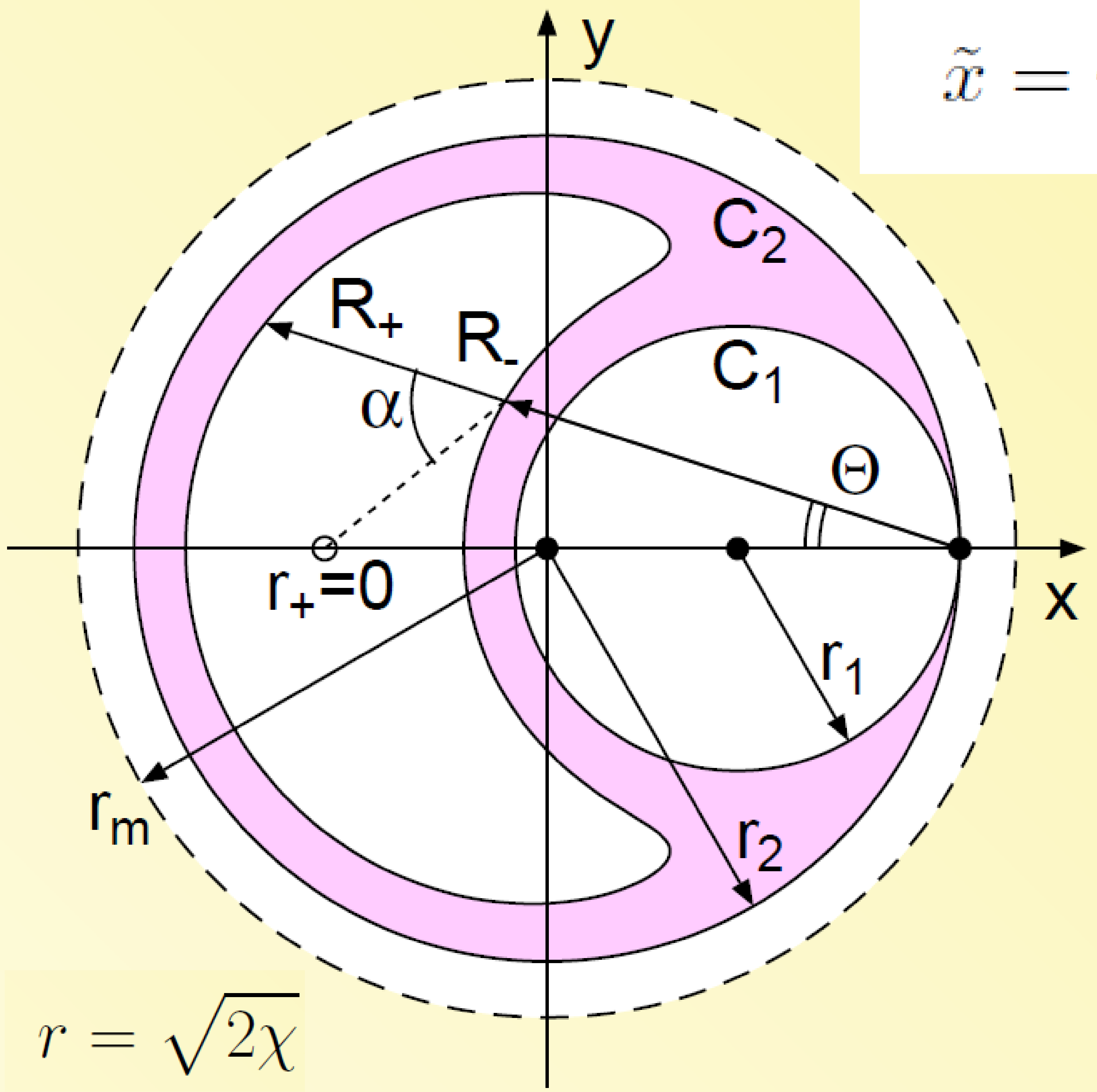

$$r = \sqrt{2\chi}$$

$$\tilde{x} = r\cos(\theta - \varphi) \qquad \tilde{y} = r\sin(\theta - \varphi),$$

Dimensions and time-dependent polar coordinate system (R, Θ) *during* $m = 1$ *reconnection of magnetic surfaces* C_1 *and* C_2*, shown in the* (x, y) *straight field-line coordinate space.*

New coordinates to describe the build-up of the island

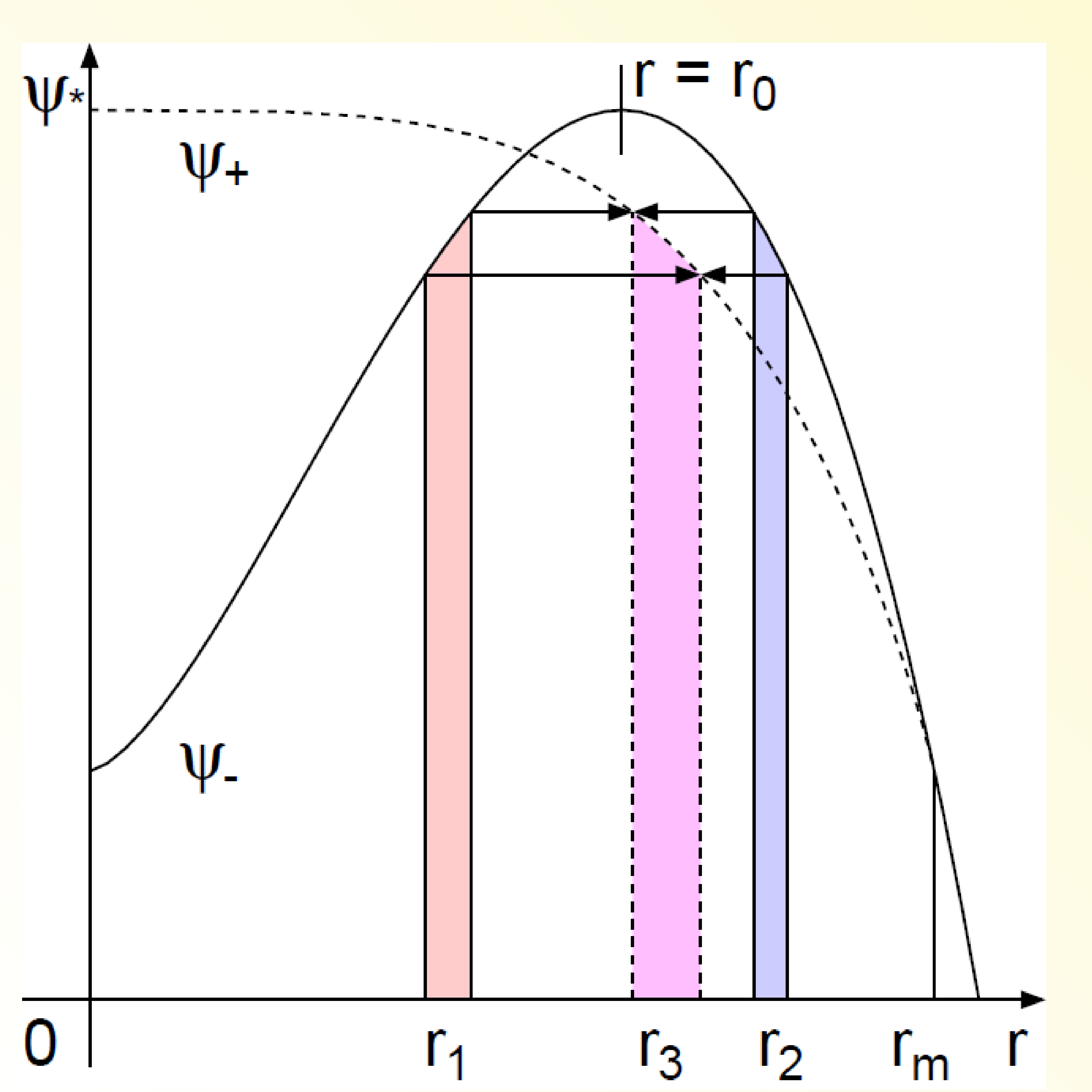

$$\psi_1' = q_2(1-q_1)r_1,$$
$$\psi_2' = q_1(1-q_2)r_2,$$

Mixing radius

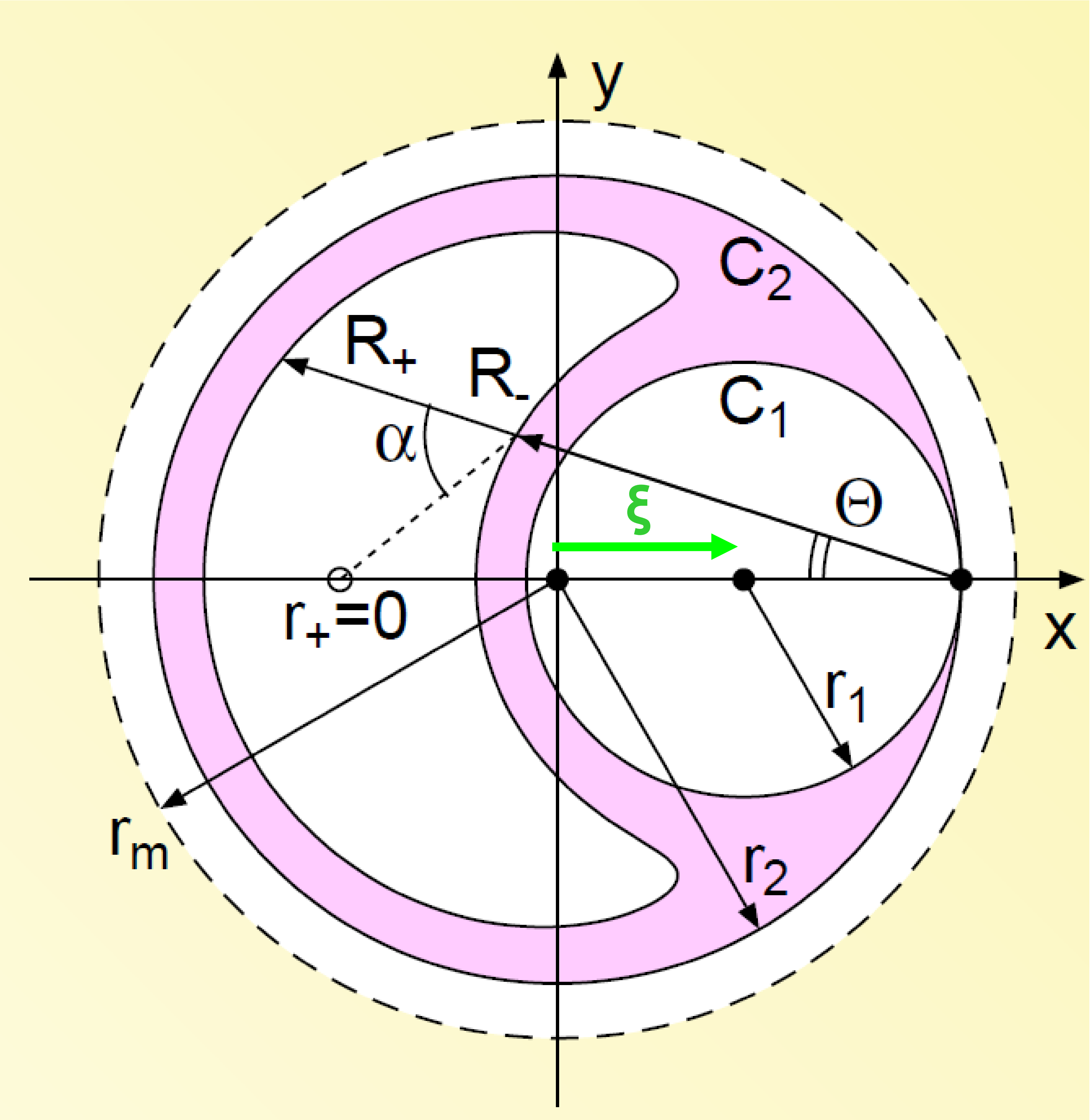

3 regions:

- Outer region ($r>r_2$) is still unperturbed.
- m=1 shifted, unconnected core of radius r_1. The displacement of the core is the helical displacement ξ .

$$\zeta = \sqrt{(\tilde{x}-\xi)^2+\tilde{y}^2}$$

- Reconnected (island) area, increasing from 0 to πr_m^2.

Defining the contour within the island

In the reconnected area, we define surfaces $r_+ =$ constant defined by

$$r_+ \equiv r_3\sqrt{\rho^2 + \sin^2\Theta},$$
$$\rho \equiv \frac{c\cos\Theta}{1+\sqrt{1+(\kappa-\kappa_r)c}},$$
$$c \equiv \kappa_r^{-1} + \kappa - \frac{R^2}{r_3^2\cos^2\Theta},$$
$$\kappa_r \equiv \frac{r_2 - r_1}{r_2 + r_1}.$$

$$\tilde{R} = \sqrt{(\tilde{x} - r_2)^2 + \tilde{y}^2)}$$

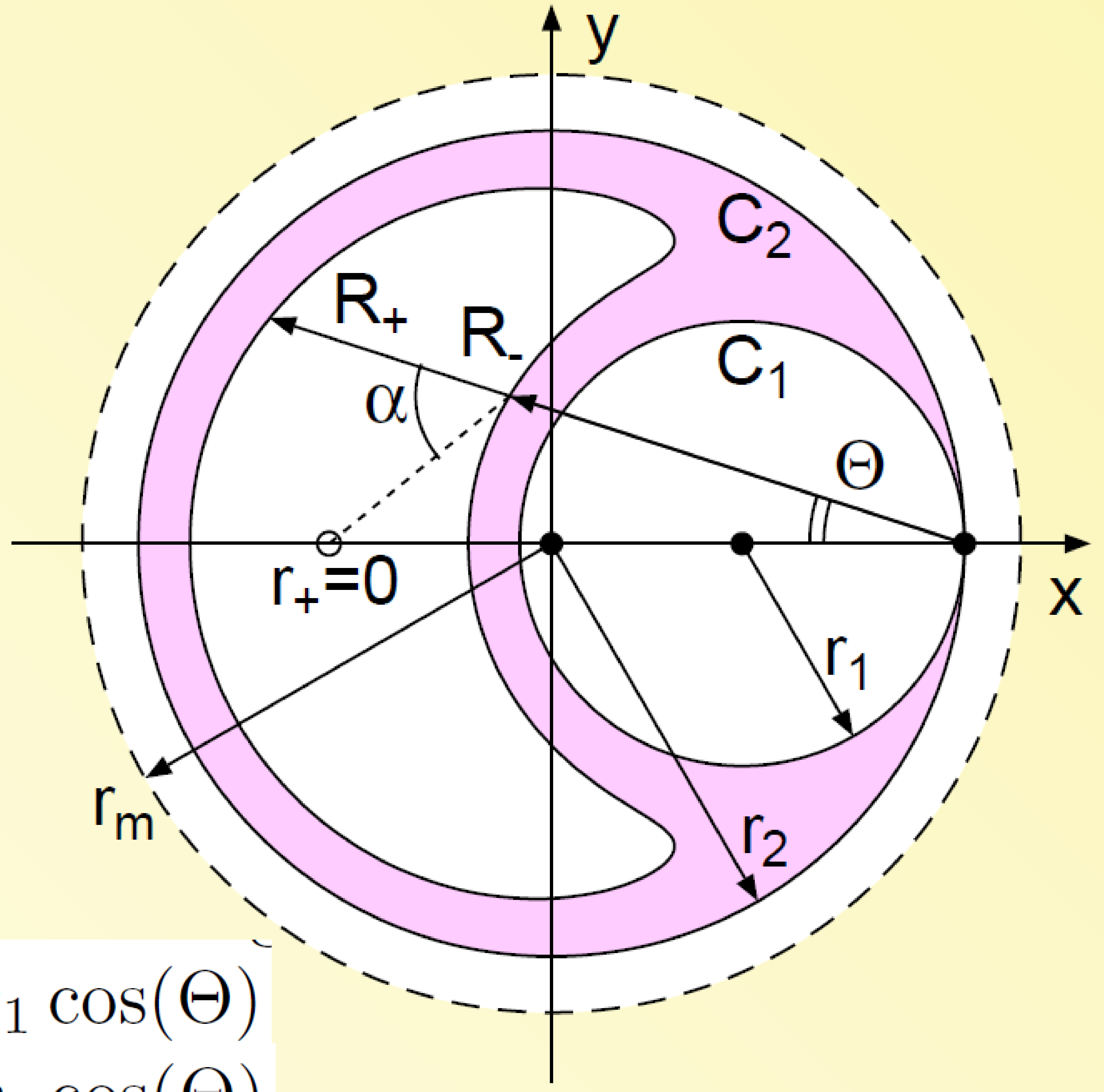

Free parameter κ determines the shift of the new magnetic axis.
Properties:

- The cross-section of each contour $r_+ =$ constant has area πr_+^2.
- $r = r_3$ at the circles C_1 and C_2, with $r_3(t) = \sqrt{r_2^2 - r_1^2}$ increasing from 0 to r_m.
- Allows for a continuous electric potential at C_1 and C_2.
- $\mathbf{B}$ is continuous at C_1, C_2 for one paramater value $\kappa = \kappa_c(r_1, r_2)$.

C_1 $\quad \tilde{R} = 2r_1\cos(\Theta)$

C_2 $\quad \tilde{R} = 2r_2\cos(\Theta)$

Defining the magnetic potential

$$\psi_* = \begin{cases} \psi_-\left(\sqrt{(\tilde{x}^2+\tilde{y}^2)}\right), & r > r_2 \rightarrow \text{unaffected area} \\ \psi_-\left(\sqrt{(\tilde{x}-\eta)^2+\tilde{y}^2}\right), & \zeta < r_1 \rightarrow \text{original core} \\ \psi_+(r_+), & \text{otherwise} \rightarrow \text{island} \end{cases}$$

$$r_+ = r_3\sqrt{\rho^2+\sin^2(\Theta)}.$$

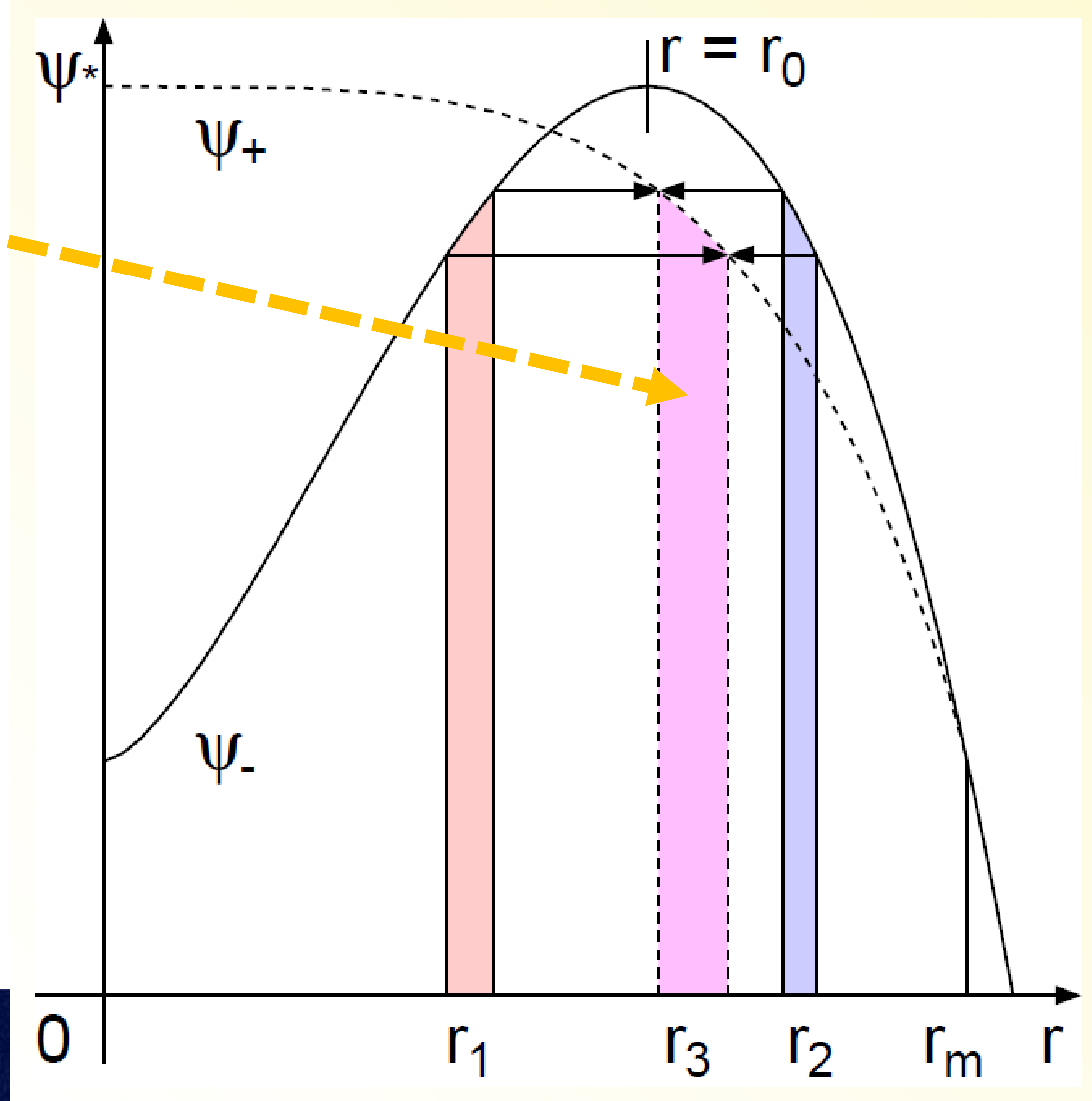

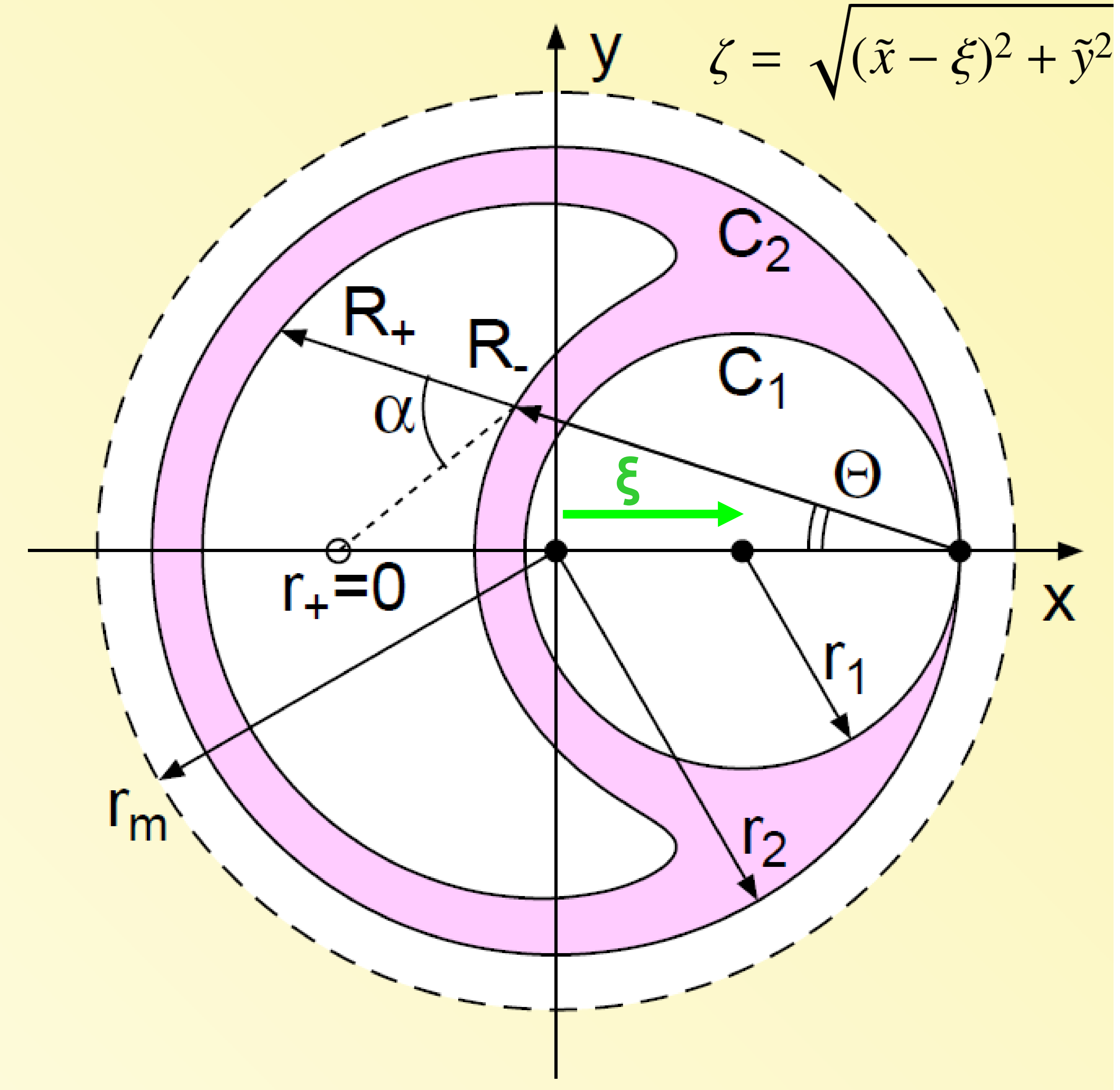

How to improve the Electric potential calculation?

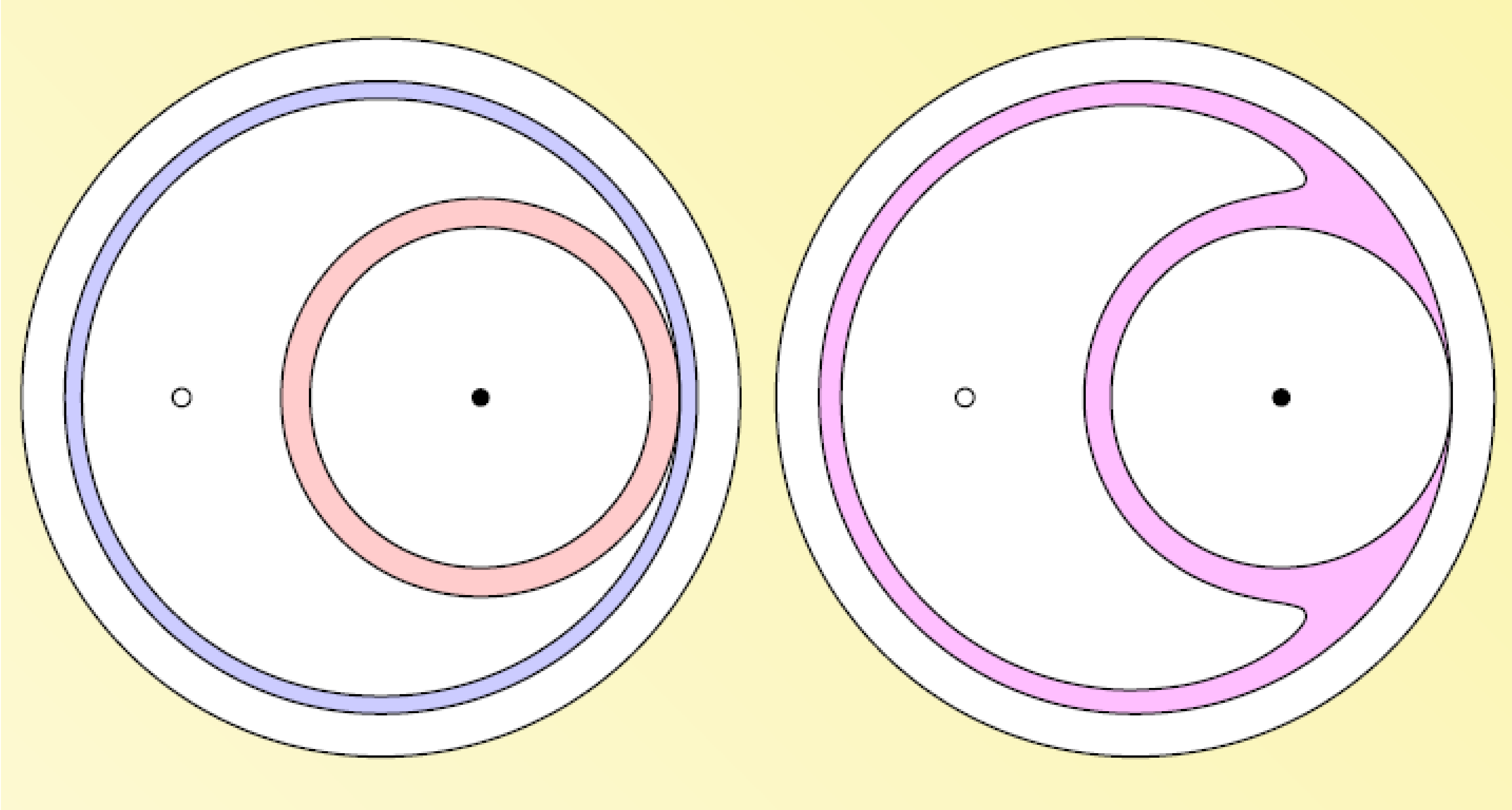

$$\Phi = \Phi_0(\psi_*) + \int_{\psi_*} \frac{\partial \psi_* / \partial t}{|\nabla \psi_*|} d\ell$$

This integral is the **area in the (x, y) plane swept out** by an arc of fixed ψ∗ while ψ∗(x, y, t) evolves.

How to improve the Electric potential calculation?

$$\Phi = \Phi_0(\psi_*) + \int_{\psi_*} \frac{\partial \psi_* / \partial t}{|\nabla \psi_*|} \, d\ell$$

$$\Phi(\mathbf{x}, t) = \Phi_0(r_+) - \int_{C(r_+)} \frac{\partial_t r_+}{|\nabla r_+|} \, d\ell.$$

$$\Phi = \dot{r}_2 \tilde{R} \sin(\Theta) - \frac{\partial}{\partial t} \int_{C(r_+)} \frac{1}{2} \tilde{R}^2 \mathrm{d}\Theta,$$

Inside the island

How to improve the Electric potential calculation?

$$\psi_* = \begin{cases} \psi_-\left(\sqrt{(\tilde{x}^2 + \tilde{y}^2})\right), & r > r_2 \rightarrow \text{unaffected area} \\ \psi_-\left(\sqrt{(\tilde{x} - \eta)^2 + \tilde{y}^2}\right), & \zeta < r_1 \rightarrow \text{original core} \\ \psi_+\left(r_+\right), & \text{otherwise} \rightarrow \text{island} \end{cases}$$

$$\Phi = \begin{cases} 0, & r > r_2 \\ \left(\dot{r_2} - \dot{r_1}\right)\tilde{R}\sin(\Theta), & \zeta < r_1 \\ \Theta\left[\frac{1}{2}\left(r_+^2 - r_3^2\right)\left(\dot{\kappa} - \dot{\kappa_r}\right) + \left(\kappa - \kappa_c\right) r_3 \dot{r_3}\right] & \\ +\sin(\Theta)\left[\dot{r_2}\tilde{R} - \left(r_1\dot{r_2} + r_2\dot{r_2}\right)\cos(\Theta) + \dot{r_3} r_3 \rho\right], & \text{otherwise} \end{cases}$$

COMPUTATIONALLY EFFICIENT POLOIDAL MAPPING OF THE RECONNECTING MAGNETIC FLUX

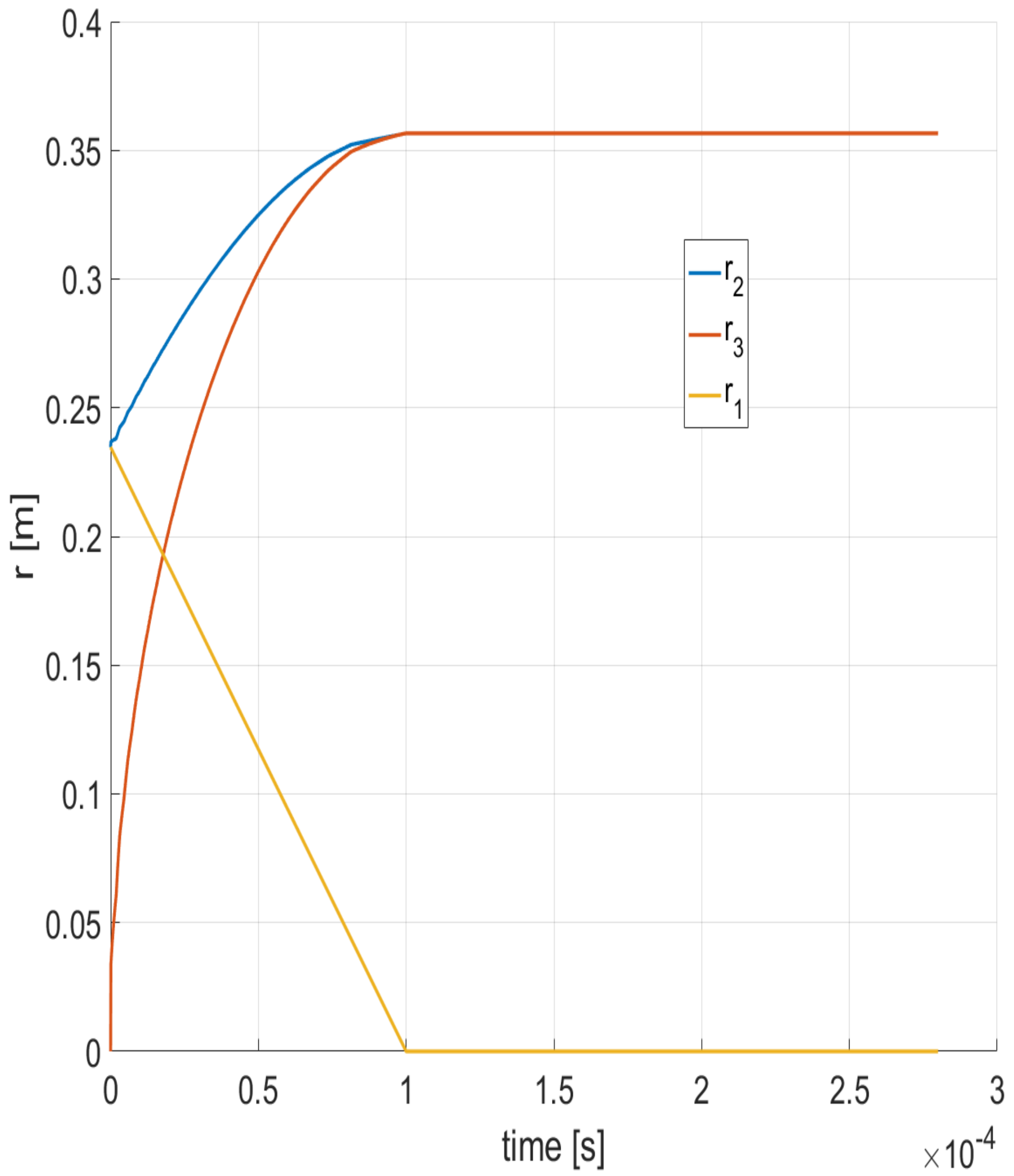

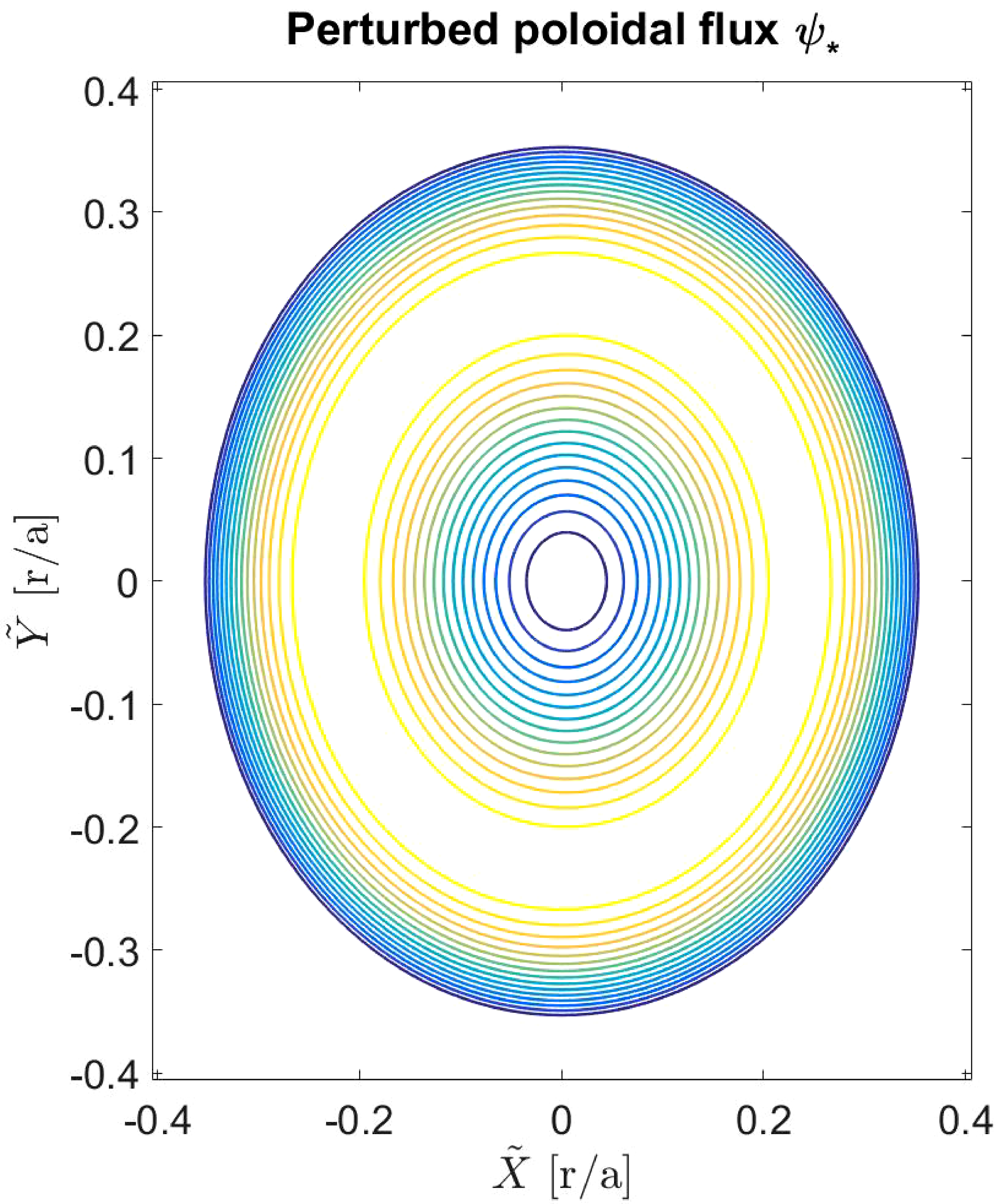

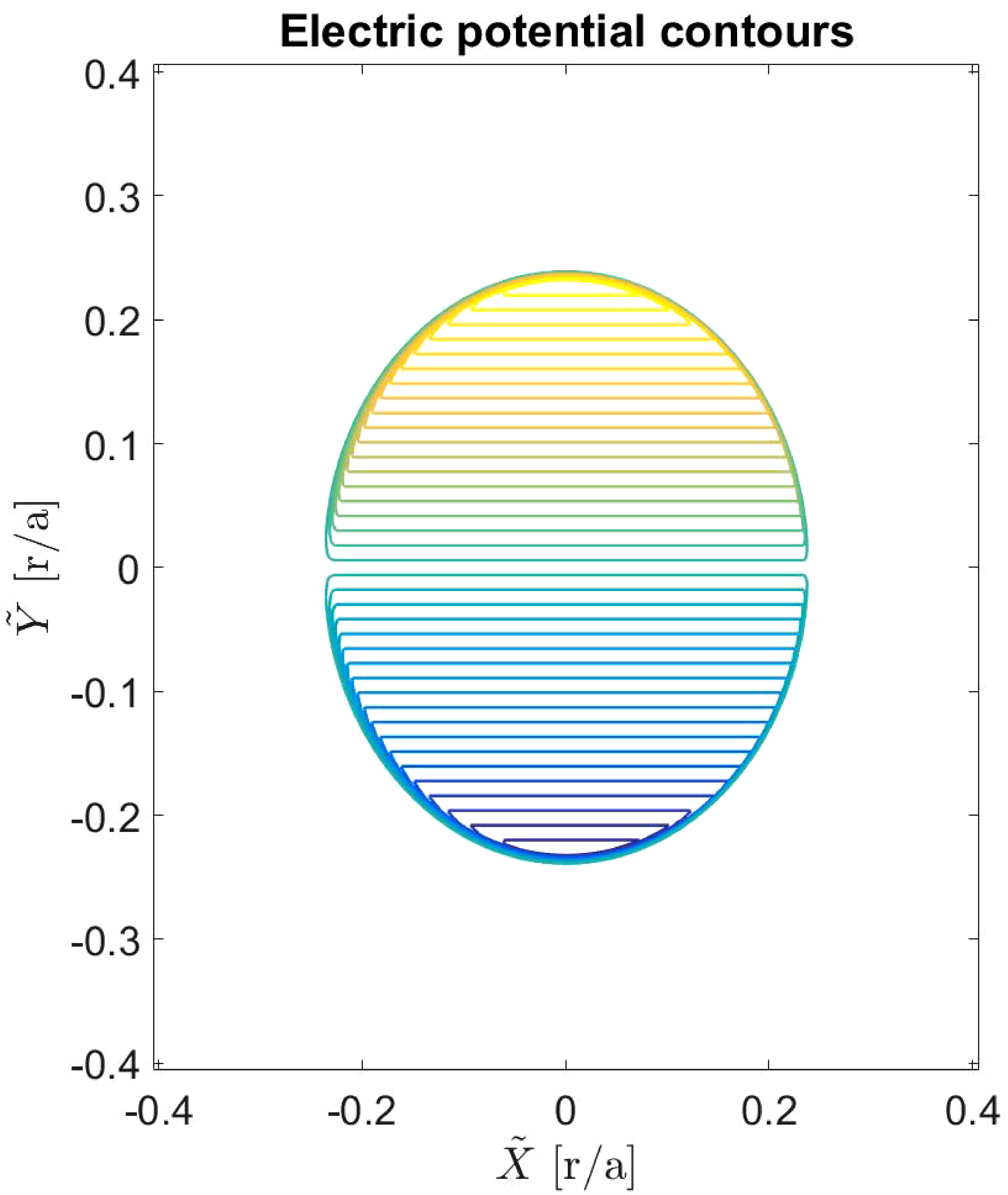

Illustration of ions motions in sawtooth crash

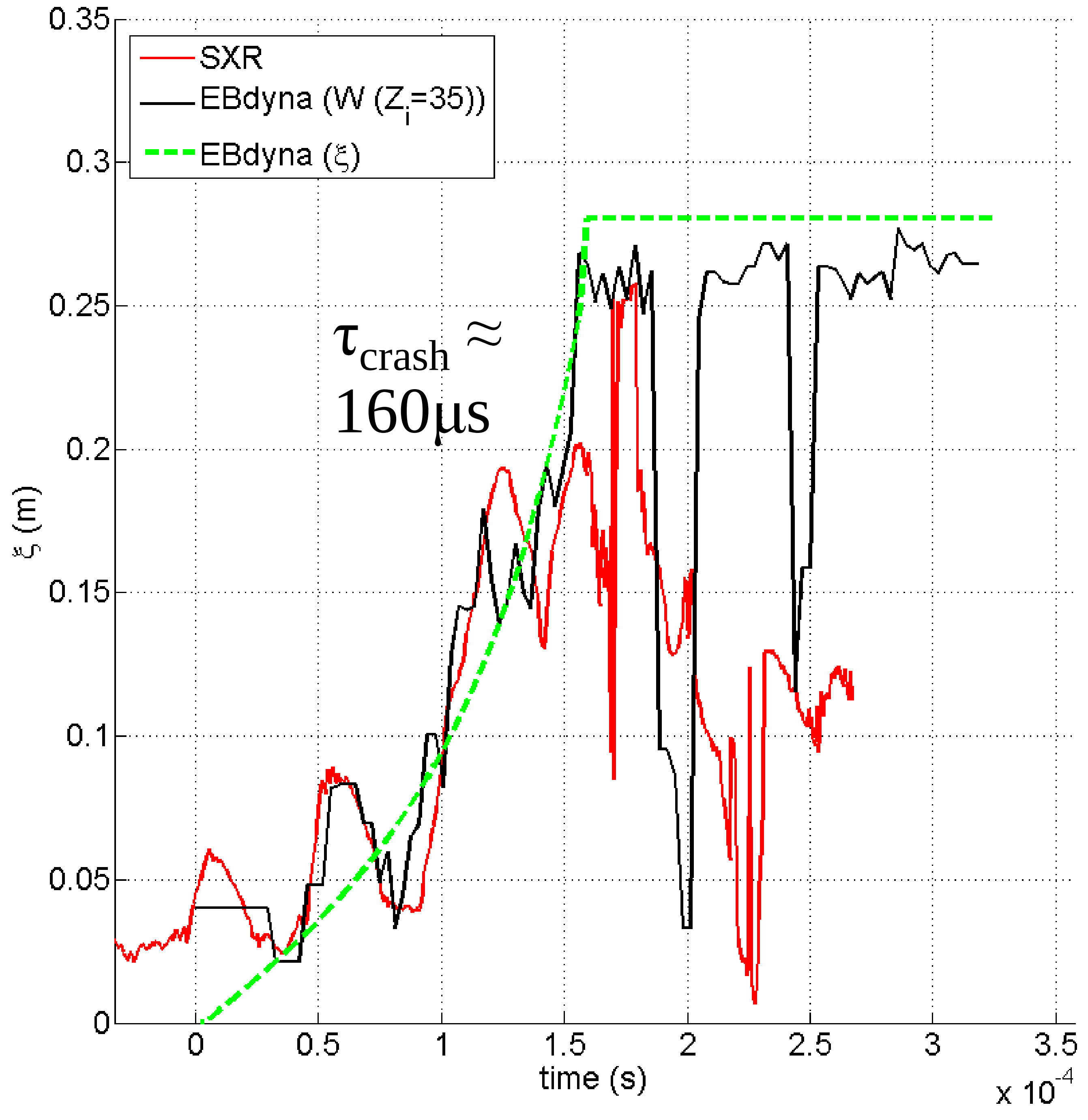

AUG30382 @ 2.5s

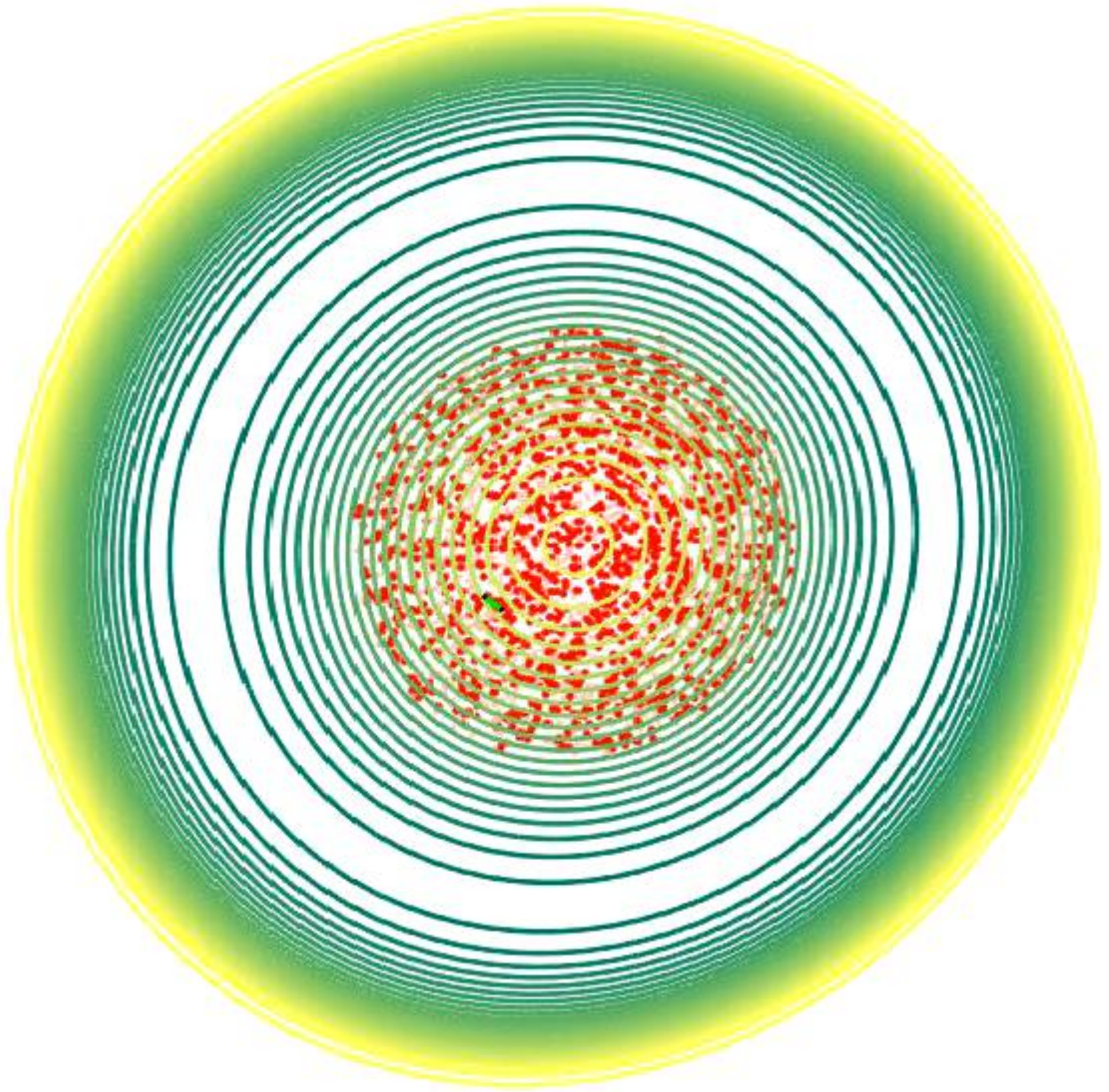

Thermal D (≈2 keV)

Simulation of sawtooth reconnection

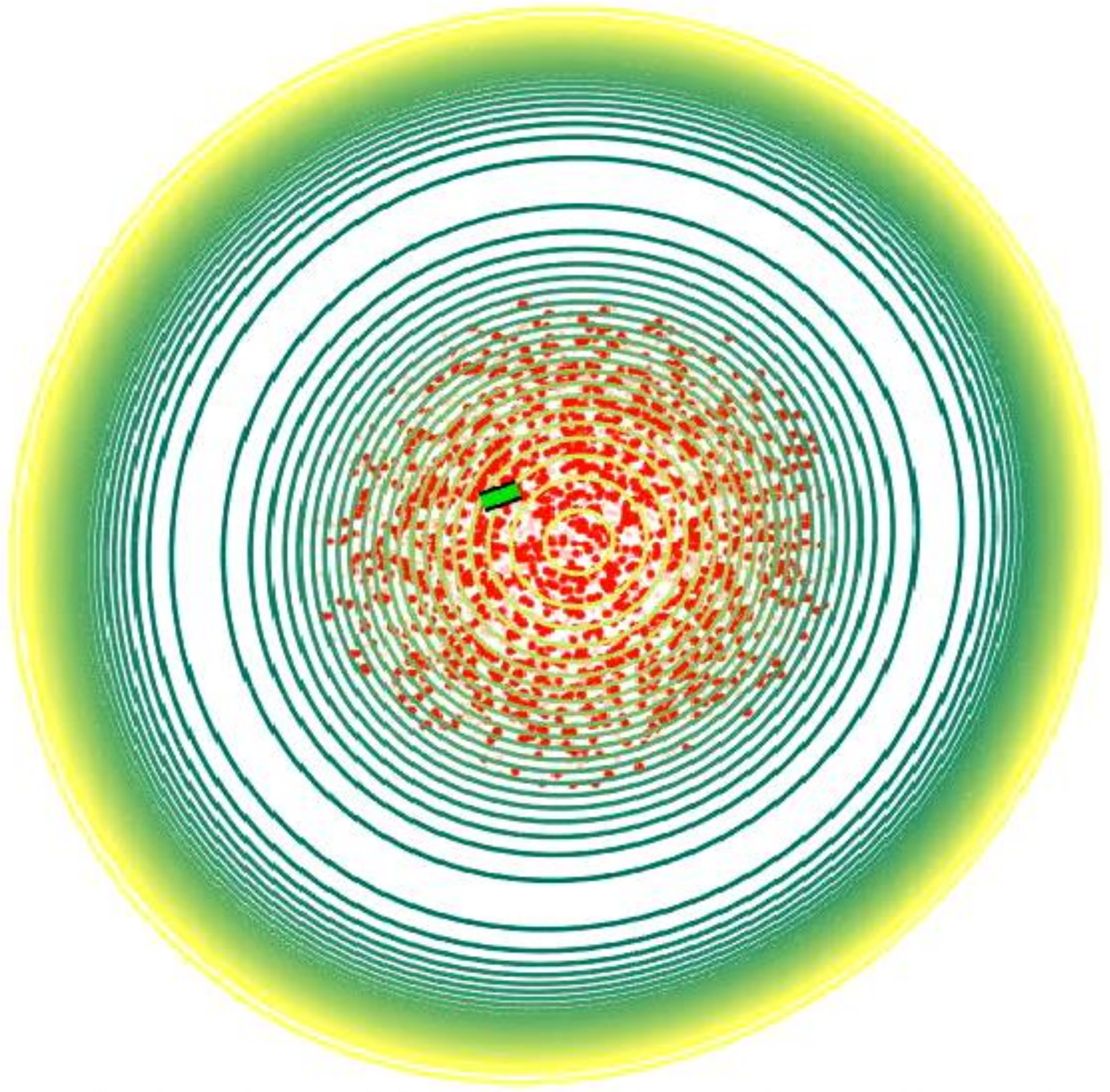

Fast D (≈50 keV)

Summary & outlook

- Safety factor is a critical parameter in order to derive stability of tokamak plasma
- The energy principle allows the derivation of the evolution of plasma in terms of linear stability for a given vector field. For a given test vector field, it is a simple matter of solving several volume integrals.
- Many MHD modes are driven by the local increase of the normalized plasma pressure (β)
- Ideal MHD and sophisticated geometric consideration allowed to derive a computationally efficient poloidal mapping of the reconnecting magnetic flux during a sawtooth crash

INSTITUTE OF PLASMA PHYSICS
OF THE CZECH ACADEMY OF SCIENCES

THANK YOU FOR YOUR ATTENTION

FABIEN JAULMES

MINISTRY OF EDUCATION,
YOUTH AND SPORTS

Thermonuclear plasma in a tokamak

Change of potential energy:

$$\delta W = \frac{1}{2}\int_{\mathcal{V}} \left[\frac{B_1^2}{\mu_0} + \frac{B^2}{\mu_0}|\boldsymbol{\nabla}\cdot\boldsymbol{\xi}_\perp + 2\boldsymbol{\xi}_\perp\cdot\boldsymbol{\kappa}|^2 - 2(\boldsymbol{\xi}_\perp\cdot\boldsymbol{\nabla}P)(\boldsymbol{\kappa}\cdot\boldsymbol{\xi}_\perp^*) - \mathbf{B_1}\cdot(\boldsymbol{\xi}_\perp\times\mathbf{b})j_\| + \gamma_{\text{thermo}}P(\boldsymbol{\nabla}\cdot\boldsymbol{\xi})^2\right]\mathrm{d}\mathcal{V}$$

$$\mathbf{B_1} = \nabla\times(\boldsymbol{\xi}_\perp\times\mathbf{B})$$

Conservation of the total energy of the plasma yields:

$$\delta W + \delta K = \delta W + \frac{1}{2}\int \rho_i|\dot{\boldsymbol{\xi}}|^2\mathrm{d}\mathcal{V} = 0$$

Considering an unstable displacement, growth rate γ_I:

$$\boldsymbol{\xi} = \boldsymbol{\xi}_0\exp(i\omega t) \qquad \omega^2 = \frac{2\delta W}{\int\rho_i|\boldsymbol{\xi}_0|^2\mathrm{d}\mathcal{V}} \qquad \gamma_I^2 = -\omega^2$$

$$\boldsymbol{\xi} = \sum_m \boldsymbol{\xi}_{\mathbf{m}}(\psi)\exp[i(m\theta-\varphi)]$$

Considering an approximate circular geometry (neglecting toroidal displacement):

$$\xi_\theta = (i/m)\partial(r\xi_r)/\partial r$$

Illustration of the energy principle to explain experimental effect of stabilization of kink by NBI particles

$$\delta W = \frac{1}{2}\int_{\mathcal{V}} \left[\frac{B_1^2}{\mu_0} + \frac{B^2}{\mu_0}\left|\boldsymbol{\nabla}\cdot\boldsymbol{\xi}_\perp + 2\boldsymbol{\xi}_\perp\cdot\boldsymbol{\kappa}\right|^2 - 2(\boldsymbol{\xi}_\perp\cdot\boldsymbol{\nabla}P)(\boldsymbol{\kappa}\cdot\boldsymbol{\xi}_\perp^*) - \mathbf{B_1}\cdot(\boldsymbol{\xi}_\perp\times\mathbf{b})j_\parallel + \gamma_{\mathrm{thermo}}P(\boldsymbol{\nabla}\cdot\boldsymbol{\xi})^2 \right] \mathrm{d}\mathcal{V}$$

$$\boldsymbol{\kappa_{pol}} = \frac{\mu_0}{B^2}\boldsymbol{\nabla}\left(P + \frac{B^2}{2\mu_0}\right) \; ; \qquad \kappa_\varphi = \left(\frac{(\mathbf{B}\times\boldsymbol{\nabla}B)\times\mathbf{B}}{B^3}\right)_\varphi \; .$$

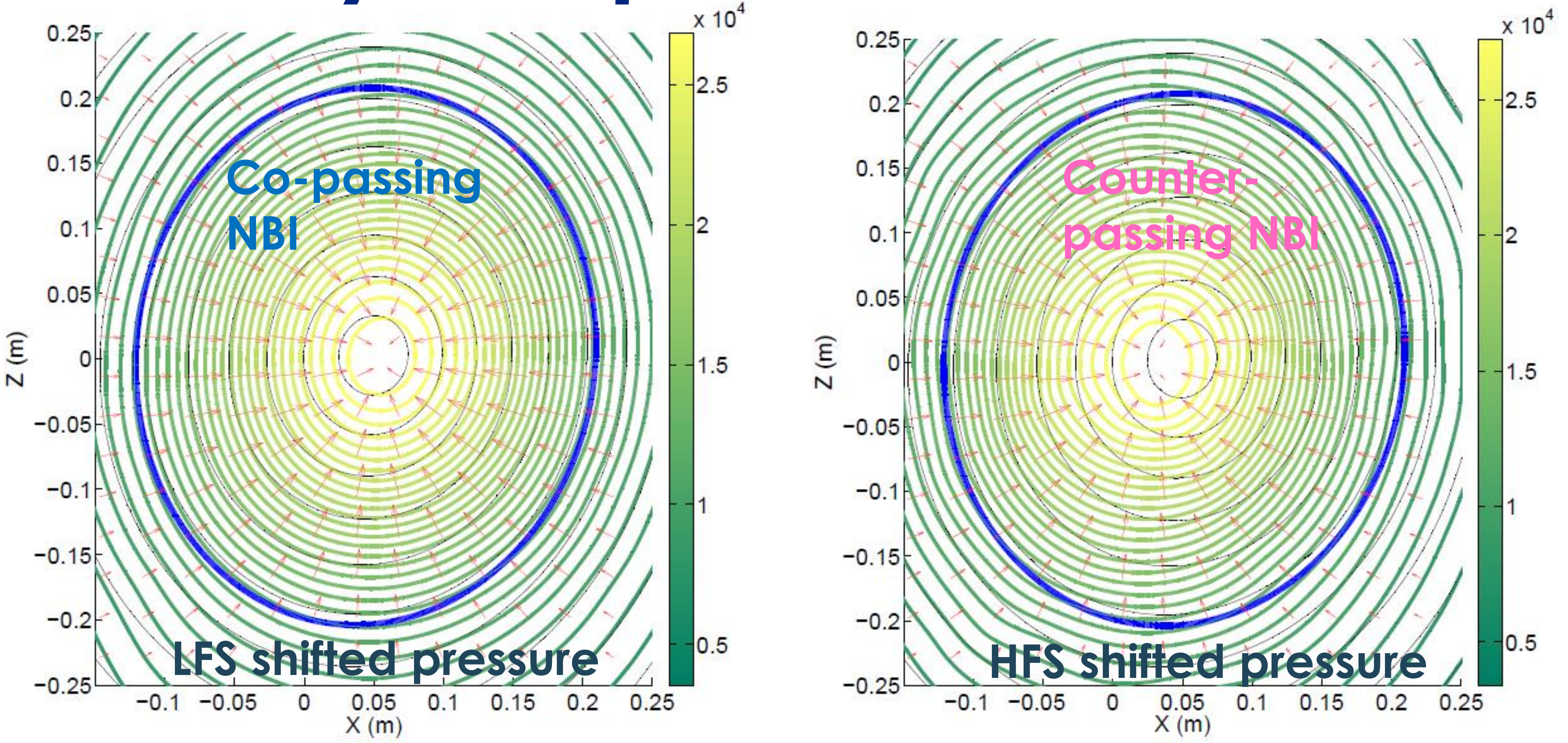

FIGURE 3.3: Compared pressure contours of the hot NBI population (in a sawtooth equilibrium in ASDEX Upgrade). The arrows indicate the direction of the hot pressure gradient of the NBI population. The left figure corresponds to the experimental case with on-axis co-passing NBI. The right figure corresponds to the same NBI with an opposite parallel velocity. The thick blue line underlines the position of the $q = 1$ surface.

NBI stabilization

$$\delta W = \frac{1}{2}\int_{\mathcal{V}} \Bigg[\frac{B_1^2}{\mu_0} + \frac{B^2}{\mu_0}|\boldsymbol{\nabla}\cdot\boldsymbol{\xi}_\perp + 2\boldsymbol{\xi}_\perp\cdot\boldsymbol{\kappa}|^2 - 2(\boldsymbol{\xi}_\perp\cdot\boldsymbol{\nabla}P)(\boldsymbol{\kappa}\cdot\boldsymbol{\xi}_\perp^*) - \mathbf{B_1}\cdot(\boldsymbol{\xi}_\perp\times\mathbf{b})j_{\|} + \gamma_{\text{thermo}}P(\boldsymbol{\nabla}\cdot\boldsymbol{\xi})^2\Bigg]\mathrm{d}\mathcal{V}$$

$$\boldsymbol{\kappa_{pol}} = \frac{\mu_0}{B^2}\boldsymbol{\nabla}\left(P + \frac{B^2}{2\mu_0}\right) \; ;$$

$$\kappa_\varphi = \left(\frac{(\mathbf{B}\times\boldsymbol{\nabla}B)\times\mathbf{B}}{B^3}\right)_\varphi \; .$$

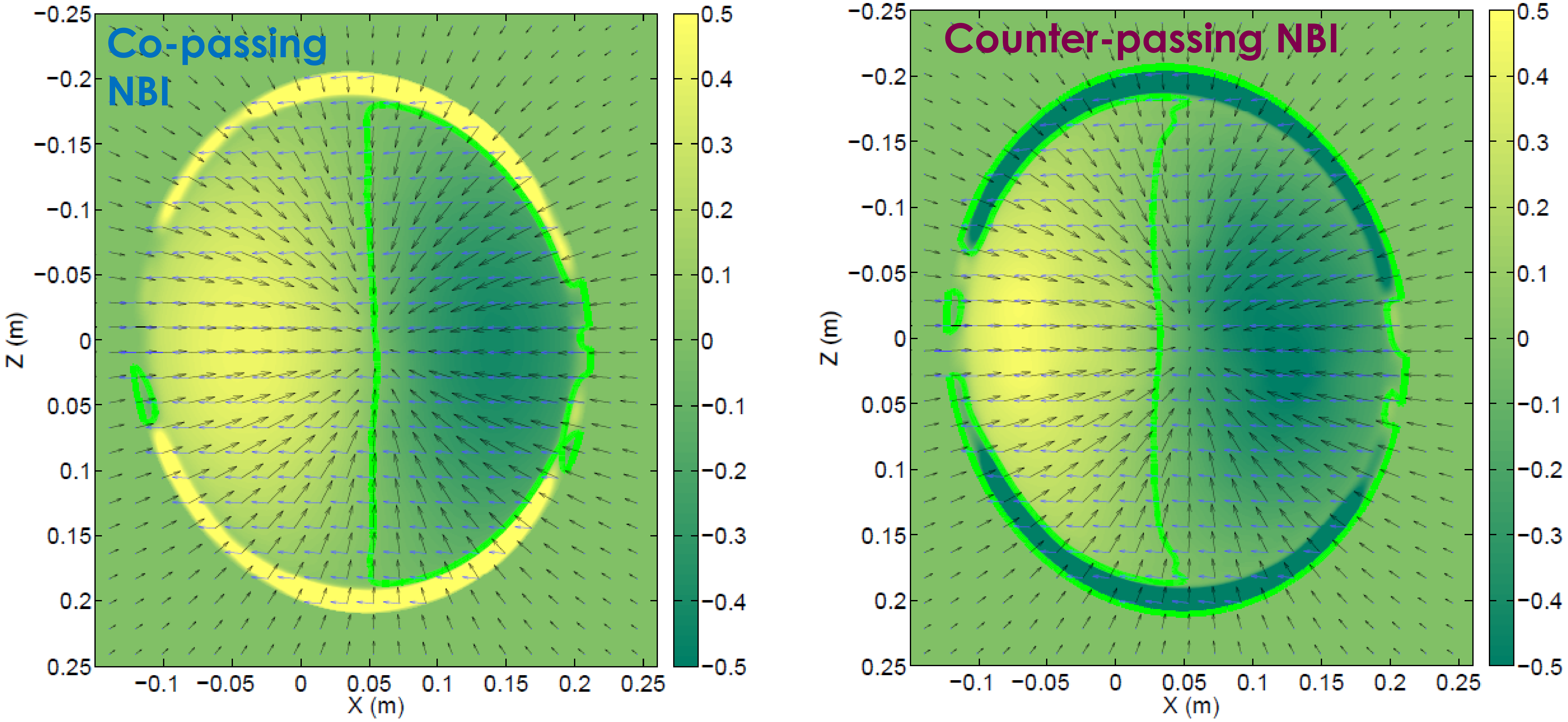

FIGURE 3.4: Compared values of the normalized potential energy density averaged over the toroidal direction. The left case if a stabilizing co-passing NBI (in a sawtooth equilibrium in ASDEX Upgrade) and the right one a destabilizing counter-passing situation. The quasi-horizontal blue arrows indicate the curvature $\boldsymbol{\kappa}$. The black arrows indicate the gradient of the hot NBI pressure. The thick green lines separates regions of stabilizing and destabilizing contributions. It is readily seen that the region around $q = 1$ plays an important role for the global stability, because of the large amplitude of the displacement vector there. Around $q = 1$, the stabilizing or destabilizing sign is induced by the reverse in sign of $\boldsymbol{\xi}\cdot\boldsymbol{\nabla}P_{hot}$: in both cases the backward poloidal flow in the $q = 1$ region is aligned with the equilibrium flux contours ; however the angle of the hot pressure gradient with the flux surface is different.

Reconnecting patterns of ψ*

$\psi_*(r,\omega)$

$\omega=\theta-\varphi$

$$\mathbf{B}_\mathbf{H} = \mathbf{B}_\varphi + q\mathbf{B}_\mathbf{pol}$$

$$\mathbf{B}_* = \frac{1}{R}(\mathbf{e}_\varphi \times \nabla\psi_*)$$

$$\mathbf{B} = \mathbf{B}_\mathbf{H} + \mathbf{B}_*$$

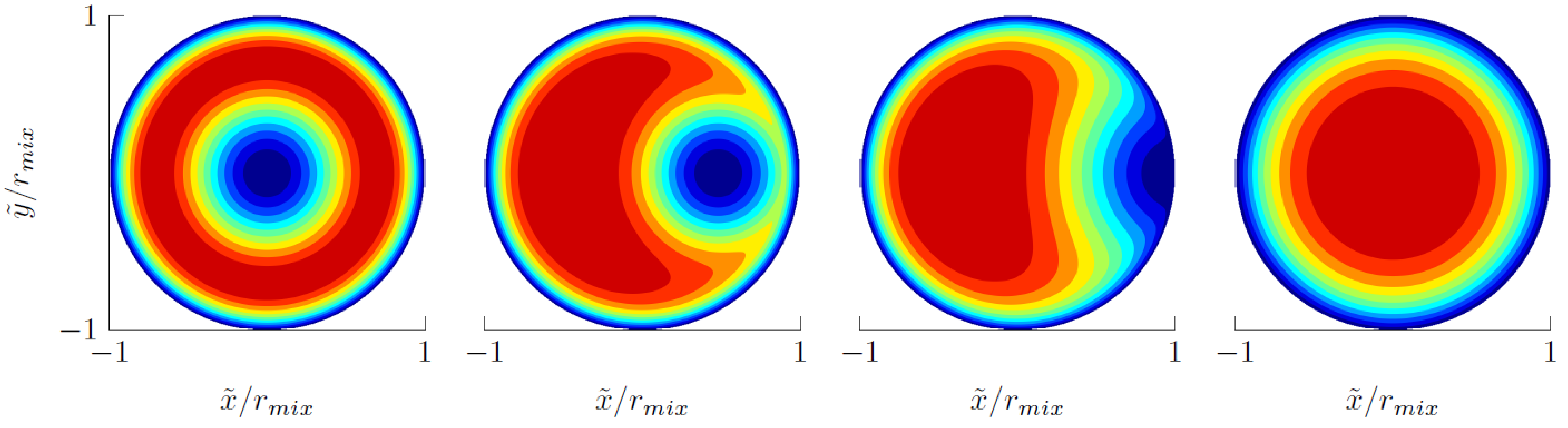

(a) initial situation (b) halfway through reconnection (c) start of recovery (d) final situation

Figure 2.19: Evolution of ψ_* profile in $\tilde{x},\tilde{y}$-space during collapse with two phases (colors range from 0 to $\max(\psi_*)$). Note that reconnection starts at the 'X'-points at $r = r_0$ on the $q = 1$ surface (red in figure 2.19(a)). The 'X'-point moves outwards till $r = r_{mix}$ (outer blue shell).

S. Cats, MSc thesis, 2017